

Impurity-induced states in conventional and unconventional superconductors

A. V. Balatsky*

Theoretical Division, Los Alamos National Laboratory, Los Alamos, New Mexico 87545

I. Vekhter†

Department of Physics and Astronomy, Louisiana State University, Baton Rouge, Louisiana 70803

Jian-Xin Zhu‡

Theoretical Division, Los Alamos National Laboratory, Los Alamos, New Mexico 87545

(Dated: October 18, 2005)

We review recent developments in understanding of how impurities influence the electronic states in the bulk of superconductors. Our focus is on the quasi-localized states in the vicinity of impurity sites in conventional and unconventional superconductors and our goal is to provide a unified framework for their description. The non-magnetic impurity resonances in unconventional superconductors are directly related to the Yu-Shiba-Rusinov states around magnetic impurities in conventional s -wave systems. We review the physics behind these states, including quantum phase transition between screened and unscreened impurity, and emphasize recent work on d -wave superconductors. The bound states are most spectacularly seen in scanning tunneling spectroscopy measurements on high- T_c cuprates, which we describe in detail. We discuss very recent progress on the states coupled to impurity sites which have their own dynamics. We also review inelastic electron tunneling spectroscopy (IETS) features as could be seen by scanning tunneling microscopy in real space and its Fourier-transformed images and impurity resonances in the presence of an order competing with superconductivity. Last part of the review is devoted to the influence of local deviations of the impurity concentration from its average value on the density of states in s -wave superconductors. We review how these fluctuations affect the density of states and show that s -wave superconductors are, strictly speaking, gapless in the presence of an arbitrarily small concentration of magnetic impurities.

Contents

I. Introduction	2	A. Potential scattering	13
A. Aim and scope of this article	2	B. Classical spins	14
B. Unconventional superconductivity	3	VII. Impurity-induced virtual bound states in d-wave superconductors	15
C. Outline	4	A. Single potential impurity problem	16
D. Other related work	5	B. Single magnetic impurity problem	18
II. A BCS theory primer	6	C. Self-consistent gap solution near impurity	18
A. Bogoliubov transformation	7	D. Spin-orbit scattering impurities	19
B. BCS variational wave function	7	E. Effect of doppler shift and magnetic field	19
C. Green's functions	8	F. Sensitivity of impurity state to details of band structure	19
III. Impurities in superconductors	9	VIII. Single impurity bound state in a pseudogap state of two-dimensional metals	21
A. Single impurity potential	9	A. General remarks on impurities in a pseudogap state	21
B. Scanning tunneling microscopy as a tool to measure local density of states	9	B. Impurity state in pseudogap models	23
C. Many impurities	10	IX. Scanning tunneling microscopy results	25
D. The self-energy and the T -matrix approximation	10	A. STM results around a single impurity	25
E. Static and dynamic impurities	11	B. Filter	27
IV. Non-magnetic impurities and Anderson's theorem	11	C. Spatial distribution of particle and hole components	29
V. Single impurity bound state in two-dimensional metals	12	D. Fourier-transformed STM maps	29
VI. Low-energy states in s-wave superconductors	13	X. Quantum phase transition in s-wave superconductors with magnetic impurity	31
		A. Introduction	31
		B. Quantum phase transition as a level crossing	31
		C. Particle and hole component of impurity bound state	33
		D. Intrinsic π phase shift for $J_0 > J_{crit}$ coupling	34
		XI. Kondo effect and quantum impurities	34
		A. Kondo effect in fully gapped superconductors	35
		1. Ferromagnetic exchange	35
		2. Antiferromagnetic coupling	35

*Electronic address: avb@lanl.gov, <http://theory.lanl.gov>

†Electronic address: vekhter@phys.lsu.edu

‡Electronic address: jxzhu@lanl.gov

3. Anisotropic exchange and orbital effects	36
B. Kondo effect in gapless superconductors	36
XII. Inelastic scattering in d-wave superconductor	39
A. Inelastic scattering: general remarks	39
B. Localized modes in d -wave superconductors	40
C. Interplay between collective modes and impurities in d -wave superconductors	42
XIII. Average density of states in superconductors with impurities	45
A. s -wave	46
1. Born approximation and the Abrikosov-Gor'kov theory	46
2. Shiba impurity bands	46
3. Quantum spins and density of states	48
B. d -wave	48
XIV. Optimal fluctuation	49
A. Introduction	49
B. Tail states in semiconductors and optimal fluctuation	50
C. s -wave superconductors	51
1. Magnetic and non-magnetic disorder	51
2. Diffusive limit, weak magnetic scattering	51
3. Diffusive limit, strong scattering	52
4. Ballistic limit, weak scattering	52
5. Ballistic regime, strong scattering	54
6. Summary	54
XV. Summary and outlook	54
Acknowledgments	55
List of Symbols	56
References	56

I. INTRODUCTION

A. Aim and scope of this article

Real materials are not pure. Often excessive impurities hinder observations of beautiful physics that exists in cleaner systems. For example, magnetic disorder destroys the coherence of the superconducting state. At the very least, in conventional metals, impurities lead to higher resistivity. It is therefore very tempting to treat impurities as unfortunate obstacles to understanding of the true underlying physics of the systems under consideration, to strive to make cleaner and better materials, and to ignore imperfections whenever possible.

Yet sometimes impurities directly lead to the desired physical properties. They are crucial in achieving functionality of doped semiconductors: undoped semiconductors are just band insulators and not useful for applications in electronics. The entire multi-billion dollar semiconducting electronics industry is based on the precise control and manipulation of electronic states due to dopant (impurity) states.

Consequently, sensitivity of a physical system to disorder can be a blessing in disguise. It can lead not only to achieving new applications but also to uncovering the nature of exotic ground states, elucidating details of electronic correlations, and producing electronic states that

are impossible in the bulk of a clean system. Until recently, this idea has not been emphasized in the study of correlated electron systems, but now more and more efforts are focused on understanding the changes produced by disorder in a wide variety of strongly interacting electronic matter. One of the most promising directions is the study of disorder near quantum critical points, where several types of ordering compete and exist in delicate balance that impurities have the power to tip in favor of one of the orders (Millis, 2003).

This is a review of the impurity effects on the electronic states in superconductors. The main purpose of our article is to give a reader an appreciation of recent developments, review the current understanding and outline further questions on how impurities affect conventional, and especially unconventional superconductors. Superconductors present probably the first example of a non-trivial many-electron system where consequences of disorder on the electronic states were studied experimentally and theoretically, and this review focuses on these effects.

The main classical results on impurity effects in superconductors, such as Abrikosov-Gor'kov theory of pair-breaking by magnetic impurities (Abrikosov and Gor'kov, 1960), and the Anderson theorem (Anderson, 1959), are well covered in textbooks and reviews (Abrikosov *et al.*, 1963; Annett, 1990; Fetter and Walecka, 1971; de Gennes, 1989; Schrieffer, 1964; Sigrist and Ueda, 1991; Tinkham, 1996). The need to review the subject arises since a) there are many new results; b) the analyses of the classical papers have been substantially modified in applications to novel materials; c) the emphasis of the study of the impurity effects shifted from macroscopic to atomic length scales.

From the early days, impurity doping was one of the most important tools to identify the nature of the pairing state and microscopic properties. A classical experimental study of the role of magnetic impurities in conventional superconductors was carried out by (Woolf and Reif, 1965), and followed by many detailed investigations, see e.g (Bauriedl *et al.*, 1981; Dumoulin *et al.*, 1975, 1977; Edelstein, 1967).

In the past two decades we have witnessed a tremendous growth of the number of novel superconductors. Many of them belong to the general class of strongly correlated electron systems, and, as a result of Coulomb interaction, the superconductivity is unconventional, see below. Both magnetic and nonmagnetic impurities are pairbreakers in unconventional superconductors, and often impurity suppression of superconductivity is a strong early hint of the unconventional pairing state. For example, rapid suppression of the transition temperature, T_c , in Al doped SrRuO₄ was the first indication that it is a p -wave superconductor (Mackenzie *et al.*, 1998; Mackenzie and Maeno, 2003). Study of the effect of impurities on unconventional superconductors is still a developing field, yet it is mature enough to warrant an overview.

Sometimes superconducting state emerges from competition between different phases, such as magnetically

ordered and paramagnetic in high-temperature cuprates, organic materials and heavy fermion systems. Experimentally, superconductivity often is the strongest when the two competing states are nearly degenerate, near quantum critical points, as in Ce based “115” heavy fermion materials (Sidorov *et al.*, 2002) and UGe_2 (Saxena *et al.*, 2000). Study of impurity effects allows (at least, in principle) to characterize the superconducting state and uncover competing electronic correlations.

The same reasoning has driven the study of impurity effects in high- T_c superconductors. Despite much progress, at present there is no complete microscopic description and certainly no consensus on the mechanism of superconductivity. Study of the impurity-induced states has the potential to reveal the nature and origin of the superconducting state. Much of recent experimental work focused on the high- T_c systems, and our comparison of theory and experiment inevitably emphasizes these materials. Nonetheless, this is emphatically not a comprehensive review of impurity effects in the cuprates. Their main properties are described in many excellent reviews, including those on scanning tunneling microscopy (STM) (Fischer *et al.*, 2005), angle-resolved photoemission spectroscopy (ARPES) (Campanozano *et al.*, 2004; Damascelli *et al.*, 2003) and on the pseudogap state (Timusk and Statt, 1999), to which we refer interested readers.

The new states and structures that appear due to disorder often are confined to micro- or mesoscopic length scales. They would remain in the realm of academic discussion were it not for the development of new techniques and probes of disorder. At the time of classical work, experimental interest was solely in macroscopic properties of materials: transition temperature, T_c , specific heat, and the average density of states (DOS) (deduced from measuring the tunneling conductance of planar junctions) were the experimentally measured quantities. With perfection of more local probes such as nuclear magnetic resonance (NMR), and especially with development of scanning tunneling microscopy and spectroscopy (STM/STS), it became possible to experimentally determine the structures on the atomic scales around the impurity sites. Therefore the emphasis of theoretical work also shifted to the study of local properties. It is therefore timely and useful to review new results and ideas about impurity-generated states in superconductors.

We had to be selective about the topics covered in this article. In the spirit of new approaches, our review primarily discusses the physics of the single impurity bound or quasi-bound states at the atomic scales, and the local electronic effects in the vicinity of defects. We also discuss mesoscopic effects, and the impurity effects in the presence of orders competing with superconductivity. The latter idea is applied to the pseudogap state of high- T_c materials.

We restricted ourselves to the study of the behavior of the density of states. A comprehensive review of all the effects that were studied experimentally and discussed

theoretically is a much more difficult task that would take substantially more space. We do not analyze here the behavior of transport coefficients: while this is a subject of intense current interest and many important results have been obtained, it is beyond the scope of this article.

To keep this review useful for people entering the field, we start with the Bardeen-Copper-Schrieffer (BCS) model for superconductivity, and use a modified version of this model throughout the article. In doing so we neglect the corrections due to strong coupling; in the known case of electron-phonon interaction these are quantitative rather than qualitative (Carbotte, 1990; Schachinger, 1982; Schachinger and Carbotte, 1984; Schachinger *et al.*, 1980). In many unconventional materials, such as cuprates, the dynamical glue in the self-consistent theory is not known. Yet most people agree that the superconducting state of cuprates not very anomalous, and has the superconducting gap of d -wave symmetry. We take a view that at low energies in cuprates and other compounds, *for the purposes of this article*, superconductivity is adequately described by the BCS theory with an anisotropic gap.

B. Unconventional superconductivity

Examples of exotic superconductors discovered in the last two decades include high- T_c , heavy fermion and organic superconductors, and SrRuO_4 . A common feature to all of them is that the superconductivity is unconventional, i.e., the pairing symmetry is non- s -wave (in contrast to conventional materials, such as lead).

Superconducting order parameter describes pairing of fermions with time-reversed momenta, \mathbf{k} and $-\mathbf{k}$,

$$\Psi(\mathbf{k})_{\alpha,\beta} = \langle \psi_{\mathbf{k},\alpha} \psi_{-\mathbf{k},\beta} \rangle, \quad (1.1)$$

where α, β are the spin indices. If the order parameter transforms according to a nontrivial (trivial) representation of the point group of the crystal, the superconductor is called unconventional (s -wave). We distinguish between the spin singlet pairing (total spin of the pair $S = 0$), for which $\Psi(\mathbf{k})_{\alpha,\beta} = \Psi(\mathbf{k})(i\sigma_y)_{\alpha\beta}$, where σ_y is the Pauli matrix in spin space, and spin triplet state ($S = 1$), when $\Psi_{\alpha\beta}$ is a symmetric spinor in α, β . Since the order parameter has to be antisymmetric under permutation of fermion operators in Eq. (1.1), the *spatial* part of $\Psi(\mathbf{k})_{\alpha,\beta}$ is even for spin singlet superconductors and odd in the spin-triplet case. Expanding in eigenfunctions of orbital momentum, it follows that spin singlet pairing corresponds to *even* orbital function of momentum \mathbf{k} and hence we call it s - (for $l = 0$), d -wave (for $l = 2$), etc., superconductor in analogy with the notation for the atomic states. For a spin triplet superconductor, the orbital part is an *odd* function of \mathbf{k} , and hence the spin triplet superconductor can be p -wave ($l = 1$), f -wave ($l = 3$) etc. More rigorously the pairing states are characterized by the irreducible representation of the symmetry

group of the crystal lattice, including the spin-orbit interaction (Blount, 1985; Sigrist and Ueda, 1991; Volovik and Gor'kov, 1984). Characterization in terms of orbital moment is an oversimplification, and we use this terminology with understanding that the correct symmetries are implied for a given crystal structure. This classification is given for BCS-like or *even frequency* superconductors. The classification is opposite for *odd-frequency* pairing, where, for example, spin singlet state has *odd* parity because pairing wave function is odd function of time (Balatsky and Abrahams, 1992; Berezinskii, 1974). We consider here only even-frequency superconductors.

We restrict ourselves to the most common examples of the unconventional pairing state, for which the order parameter averaged over the Fermi surface vanishes:

$$\sum_{\mathbf{k}} \Psi(\mathbf{k})_{\alpha\beta} = 0. \quad (1.2)$$

Hence superconductors with the constant or nearly constant order parameter on the Fermi surface are *s*-wave, while *p*-, *d*- or higher wave states, where Eq. (1.2) holds, are signatures of an unconventional superconductor. There are several excellent recent reviews that address the unconventional nature of superconducting pairing states in specific compounds, such as *p*-wave superconductivity in SrRuO₄ (Mackenzie and Maeno, 2003) and *d*-wave state in high-*T_c* materials (Annett, 1990; Harlingen, 1995; Tsuei and Kirtley, 2000).

C. Outline

We start with the general overview of BCS-like superconductivity. To review the effects of impurities we need to discuss the properties of superconductors in general. In cuprates, as well as in some heavy fermion systems and other novel superconductors, there is some evidence for the existence of an order competing with superconductivity on all or parts of the Fermi surface. The exact nature of the competing order parameter is only conjectured. A general feature of all such models is the enhancement of the competing order once superconductivity is destroyed, for example in the vicinity of a scattering center. It has been suggested that the reaction of the system to the introduction of impurities can be an important test of the order, or even growing correlations towards such an order, in the superconducting state.

The prerequisite for such a test is the detailed understanding of the behavior of “simple” superconductors with impurities. Work aimed at developing this understanding spans a period of more than 40 years, and some of the very recent results continue to be fresh and unexpected. Therefore we devote a large fraction of this review to the discussion of the properties of superconductors with impurities in the absence of any competing order. In this case, from a theoretical standpoint, before discussing the impurity effects we need to agree upon methods to describe the very phenomenon that makes the

impurity effects so interesting: superconductivity. Even in the most exotic compounds investigated so far the superconducting state itself is not anomalous, in that it results from pairing of fermionic quasiparticles, and in that these Cooper pairs may be broken by interaction with impurities or external fields.

Impurity effects in conventional superconductors were a subject of the very early studies by Anderson, who provided the so called “Anderson theorem” (Anderson, 1959), and by Abrikosov and Gor'kov (Abrikosov and Gorkov, 1960), hereafter AG. This pioneering work laid the foundation for our understanding of impurity effects in conventional and unconventional superconductors, described in terms of electron lifetime due to scattering on an ensemble of impurities. AG predicted the existence of the gapless superconductivity that was subsequently observed in experiments (Woolf and Reif, 1965). The brief summary of the AG theory and its extension to non-*s*-wave superconductivity are given in Table I, where effect of impurities on the superconducting state *on average*, or *globally* is listed.

	S-WAVE	P-WAVE	D-WAVE
POTENTIAL SCATTERING	–	+	+
MAGNETIC SCATTERING	+	+	+

TABLE I Effects of potential and magnetic impurity scattering on the *s*-, *p*- and *d*-wave superconductors are shown qualitatively. “+” indicate that impurity scattering is a pair-breaker and “–” is that impurity scattering is not a pair-breaker. There is a qualitative difference between the potential scattering in *s*-wave superconductors and any other case. Potential scattering impurities are not pairbreakers in *s*-wave case due to the Anderson theorem. This is an exceptional case. For any other case any impurity scattering will suppress superconductivity. Obviously the details depend on scattering strength and other details. At high enough concentrations both magnetic and nonmagnetic impurities will suppress superconductivity regardless of symmetry.

After intense interest in the early days of the BCS theory, the subject was considered “closed” in mid-60s, with most experimentally relevant problems solved. However, recently there has been a revival of the interest in the studies of “traditional” low-temperature *s*-wave superconductors with magnetic and non-magnetic impurities, with many new theoretical and experimental results changing our perspective on this classical problem.

A special place in this review is devoted to the study of impurity induced *local* bound states or resonances. This is an old subject, going back to the 60's when the bound states near magnetic impurities in *s*-wave superconductors were predicted in pioneering works of Yu (Yu, 1965), Shiba (Shiba, 1968), and Rusinov (Rusinov, 1969). They considered pairbreaking by a *single magnetic impurity* in a superconductor, and found that there are quasi-particle states inside the energy gap that are localized in the vicinity of the impurity atom. The corresponding gap suppression occurs locally and the concept of

lifetime broadening is inapplicable. In general, in this situation it is more useful to focus on local quantities, such as local density of states (LDOS), local gap etc., rather than on average impurity effects (which vanish for the single impurity in the thermodynamic limit). Yet it is clear that this local physics at some finite concentration of impurities suppresses superconductivity completely. This connection was discussed in (Rusinov, 1969; Shiba, 1968; Yu, 1965). In particular, the formation of intragap bound state and impurity bands due to magnetic impurities leads to filling of the superconducting gap, and therefore connects to the AG theory (Abrikosov and Gorkov, 1960).

At that time, there were no experimental techniques to directly observe single impurity states. As a result the entire subject was largely forgotten until the STM was applied to study the impurity states by Yazdani *et al.* (Yazdani *et al.*, 1997). This reinvigorated the field and led to a firm shift in the interest from global to local properties. Soon afterwards STM was used to observe local impurity states near vacancies and impurities in the high- T_c cuprates (Hudson *et al.*, 2001, 1999; Pan *et al.*, 2000b; Yazdani *et al.*, 1999). These discoveries opened a new field of research where impurities open a window into the study of electronic properties of exotic materials with atomic spatial resolution. As a first test of theories this allowed a direct comparison of the local electronic features in tunneling characteristics with the theoretical predictions for the density of states.

We start by briefly reviewing the BCS theory in Sec. II. Our main goal there is to review three approaches that will be used to analyze the impurity effects: direct diagonalization of the Hamiltonian via the Bogoliubov-Valatin transformation, the variational wave function of the original BCS paper, and the Green's function method which is well suited to the analysis of multiple impurity problems. Then we define different types of impurity scattering in Sec. III. We pay special attention to distinguishing between magnetic and non-magnetic impurities, and differentiating between static and dynamic scatterers. The basic features of non-magnetic scattering in s -wave superconductors are outlined in Sec. IV.

To keep in tune with our intention to make the review readable by graduate students and researchers entering the field, we begin the discussion of the localized states by considering an example of an impurity bound state in a two-dimensional (2D) metal in Sec. V. Then we discuss the low-energy bound state in s - and d -wave superconductors in Sec. VI and Sec. VII, respectively. We briefly touch upon possible existence of impurity resonances in different models of the pseudogap state of the cuprates in Sec. VIII. Recent STM measurements on both conventional and unconventional superconductors are discussed in Sec. IX. Changes in the ground state of a superconductor containing a classical spin as a function of the coupling strength between the spin and conduction electrons are discussed in Sec. X.

We proceed to consider the situations when the impu-

rities have their own dynamics, so that their effect on the electrons is complicated, see Secs. XI and XII, and we also study the combined influence of the collective modes and impurities in Sec. XII.C. The final two parts of our review are devoted to the discussion on the effects of impurities on meso- and macroscopic scale. For completeness, we briefly review the basic ideas of computing the average density of states for a macroscopic sample in Sec. XIII. For lack of space we cannot do justice to this very rich subject and use it largely to discuss new results on the impurity effect on the scales small compared to the sample size, but large relative to the superconducting coherence length. In that situation there are dramatic consequences of local impurity realizations that may be different from the average, and we overview the results for the density of states in Sec. XIV. We conclude with the summary in Sec. XV.

D. Other related work

In focusing largely on the properties of impurities on atomic or mesoscopic scales, we cannot give due attention within the confines of this review to several other questions that have been important in the studies of impurities. One of these is how exactly does the impurity band grow out of bound states on individual impurity sites, i.e. what is the effect of interference between such sites in real space. We briefly review some of recent work in Sec. XIII, but do not discuss the subject in depth, listing some of recent work that addresses the issue.

The usual finite lifetime diagrammatic approach, neglecting multiple impurity scattering (Gorkov and Kalugin, 1985; Hirschfeld *et al.*, 1986; Schmitt-Rink *et al.*, 1986; Ueda and Rice, 1985) yields a constant density of states at the Fermi level in a nodal superconductor with impurities. In three dimensional systems the neglected contributions are smaller by either a factor $(k_F l)^{-1} \ll 1$, where k_F is the Fermi wave vector, and l is the mean free path, or by additional power of impurity concentration, $n_{imp} \ll 1$. In two dimensions, and for d -wave superconductors, the neglected diagrams contain a low energy singularity, and therefore some of them contribute to the density of states at leading order (Nersesyan *et al.*, 1995). This result of Nersesyan *et al.* spawned a number of attempts to solve the problem of many impurities in a two-dimensional (2D) d -wave superconductor non-perturbatively. Some of the approaches and results are reviewed (from different standpoints) in Altland *et al.*, 2002; Hirschfeld and Atkinson, 2002.

Many of these non-perturbative solutions gave conflicting results for the residual density of states, including finite (Ziegler, 1996; Ziegler *et al.*, 1996), infinite (Pepin and Lee, 1998, 2001), and vanishing with different power laws in energy (Nersesyan and Tsvelik, 1997; Nersesyan *et al.*, 1995; Senthil and Fisher, 1999) (see also (Bhaseen *et al.*, 2001)). Further study demonstrated that the different results are due to subtle differences in the symme-

try of the model used (Altland *et al.*, 2000; Altland and Zirnbauer, 1997), and can be partly understood by analyzing the diffusion/cooperon mode of near nodal quasiparticles (Yashenkin *et al.*, 2001), in analogy to dirty metals (Altshuler, 1985; Lee and Ramakrishnan, 1985). Detailed self-consistent numerical studies confirm that the behavior of the DOS depends on the details of the impurity scattering and electronic structure (Atkinson *et al.*, 2000; Zhu *et al.*, 2000b). In particular, the divergence only occurs in perfectly particle-hole symmetric systems, and generically Atkinson *et al.* find that there is a non-universal suppression of the DOS over a small energy scale close to the Fermi level. Chamon and Mudry, 2001 conjectured that the residual DOS always diverges when the single impurity resonance is tuned to the Fermi level. This divergence was not found in numerical simulations of a model with large but finite on-site potential (Hirschfeld and Atkinson, 2002).

The interference between many impurities have been investigated recently (Atkinson *et al.*, 2003; Morr and Stavropoulos, 2002, 2003a; Zhu *et al.*, 2000c, 2003, 2004b) with the eye on the importance of these effects for the interpretation of the features in the STM data on the high- T_c cuprates collected over a large area of the sample. The interference is also responsible for the formation of the impurity bands and therefore is crucial for determining the transport properties, which we do not address in this review. Within the framework of the t -matrix approximation transport properties of unconventional superconductors in general (Arfi *et al.*, 1988; Graf *et al.*, 1996; Hirschfeld *et al.*, 1989, 1986, 1988; Pethick and Pines, 1986; Schmitt-Rink *et al.*, 1986), and high- T_c cuprates in particular (Duffy *et al.*, 2001; Graf *et al.*, 1995; Hirschfeld and Goldenfeld, 1993; Hirschfeld *et al.*, 1994, 1997; Quinlan *et al.*, 1996, 1994) have been extensively discussed, and the experiments on both microwave, optical, and thermal conductivity are used to extract properties of impurity scattering, see (Timusk and Statt, 1999) for a review as well as very recent results in both experiment (Carr *et al.*, 2000; Chiao *et al.*, 2000; Corson *et al.*, 2000; Hill *et al.*, 2004; Hosseini *et al.*, 1999; Lee *et al.*, 2004; Segre *et al.*, 2002; Tu *et al.*, 2002; Turner *et al.*, 2003) and theory (Berlinsky *et al.*, 2000; Chubukov *et al.*, 2003; Hettler and Hirschfeld, 1999; Howell *et al.*, 2004; Nicol and Carbotte, 2003). The question of localization in both s -wave (Ma and Lee, 1985) and d -wave (Atkinson and Hirschfeld, 2002; Lee, 1993; Senthil and Fisher, 2000; Senthil *et al.*, 1998; Vishveshwara *et al.*, 2000; Yashenkin *et al.*, 2001) continues to be investigated. Some of these results have been summarized in recent reviews on high- T_c systems (Timusk and Statt, 1999). We also do not touch upon the rich phenomena related to the surfaces playing the role of extended impurities that can also lead to the formation of the bound states (Aprili *et al.*, 1998; Blonder *et al.*, 1982; Buchholtz and Zwicknagl, 1981; Covington *et al.*, 1997; Fogelström *et al.*, 1997; Hu, 1994; Kashiwaya and Tanaka, 2000).

By now there are also few reviews available on the

subject of impurity states. Joynt (Joynt, 1997) reviewed early work on the impurity states within the t -matrix theory focusing on anomalous transport due to finite lifetime of the quasibound states around impurities. Byers, Flatté and Scalapino, were among the pioneers of the studies of the detailed electronic structure of the resonance state and interference patterns (Byers *et al.*, 1993; Flatté and Byers, 1997a,b; Flatté and Byers, 1998), and reviewed their and related work (Flatté and Byers, 1999). An excellent review of thermal and transport properties of low-energy quasiparticles in nodal superconductors was recently given by Hussey (Hussey, 2002).

The subject is so rich and well developed that it does not seem possible to do justice to addressing both local quasiparticle properties around a single impurity site and the questions of interference and transport within the confines of a single paper. Therefore in the following we overwhelmingly focus on the effect of impurities on the *local* density of states, rather than transport properties, and leave the discussion of the non-trivial effects of interference effects in low dimensions to future reviewers. With this in mind we now are ready for a main discussion.

II. A BCS THEORY PRIMER

We begin by reviewing the BCS theory. This section only briefly summarizes the results pertinent to our discussion; many textbooks provide an in-depth view of the theory (de Gennes, 1989; Ketterson and Song, 1999; Schrieffer, 1964; Tinkham, 1996). Consider a general Hamiltonian $\mathcal{H}_{BCS} = \hat{H}_0(\mathbf{r}) + H_{int}$, where

$$\hat{H}_0(\mathbf{r}) = \sum_{\alpha} \int d^d r \psi_{\alpha}^{\dagger}(\mathbf{r}) [\epsilon(-i\nabla_{\mathbf{r}}) - \mu] \psi_{\alpha}(\mathbf{r}) \quad (2.1)$$

is the band Hamiltonian of quasiparticles with dispersion $\epsilon(\mathbf{k})$, μ is the chemical potential, and the interaction part

$$H_{int} = -\frac{1}{2} \sum_{\substack{\alpha, \beta \\ \gamma, \delta}} \int d^d r d^d r' \psi_{\alpha}^{\dagger}(\mathbf{r}) \psi_{\beta}^{\dagger}(\mathbf{r}') V_{\alpha\beta\gamma\delta}(\mathbf{r}, \mathbf{r}') \psi_{\gamma}(\mathbf{r}') \psi_{\delta}(\mathbf{r}). \quad (2.2)$$

Here \mathbf{r} is the real space coordinate, α and β are the spin indices, and ψ^{\dagger} and ψ are the fermionic creation and annihilation operators, respectively. The mean field approximation consists of decoupling the four-fermion interaction into a sum of all possible bilinear terms, so that

$$H_{int} = \sum_{\alpha, \beta} \int d^d r d^d r' \left\{ \tilde{V}_{\alpha\beta}(\mathbf{r}, \mathbf{r}') \psi_{\alpha}^{\dagger}(\mathbf{r}) \psi_{\beta}(\mathbf{r}') + \Delta_{\alpha\beta}(\mathbf{r}, \mathbf{r}') \psi_{\alpha}^{\dagger}(\mathbf{r}) \psi_{\beta}^{\dagger}(\mathbf{r}') + \Delta_{\alpha\beta}^*(\mathbf{r}, \mathbf{r}') \psi_{\beta}(\mathbf{r}) \psi_{\alpha}(\mathbf{r}') \right\}. \quad (2.3)$$

The effective potential, $\tilde{V}_{\alpha\beta}(\mathbf{r}, \mathbf{r}')$ is the sum of the Hartree and Fock (exchange) terms, and the last two

terms account for superconducting pairing. The pairing field, Δ , is determined self-consistently from

$$\Delta_{\alpha\beta}(\mathbf{r}, \mathbf{r}') = -\frac{1}{2} \sum_{\gamma, \delta} V_{\alpha\beta\gamma\delta}(\mathbf{r}, \mathbf{r}') \langle \psi_{\gamma}(\mathbf{r}') \psi_{\delta}(\mathbf{r}) \rangle. \quad (2.4)$$

The pairing occurs only for positive $V_{\alpha\beta\gamma\delta}$, and only below the transition temperature, T_c ; above T_c $\Delta_{\alpha\beta} = 0$. In contrast, Hartree and Fock terms are finite at all temperatures, and can be incorporated in the quasiparticle dispersion, $\epsilon(\mathbf{k})$. These terms do change upon entering the superconducting state, but their relative change is of the order of the fraction of electrons participating in superconductivity, and therefore is small for weak coupling superconductors ($\sim \Delta/W \ll 1$, where W is the electron bandwidth). Therefore the effective potential, \tilde{V} , is not explicitly included in the following discussion except where specified.

Therefore we start with a reduced mean field BCS Hamiltonian,

$$\mathcal{H}_{BCS} = \sum_{\alpha} \int d^d r \psi_{\alpha}^{\dagger}(\mathbf{r}) \hat{H}_0(\mathbf{r}) \psi_{\alpha}(\mathbf{r}) + \sum_{\alpha, \beta} \int d^d r d^d r' \left\{ \Delta_{\alpha\beta}(\mathbf{r}, \mathbf{r}') \psi_{\alpha}^{\dagger}(\mathbf{r}) \psi_{\beta}^{\dagger}(\mathbf{r}') + h.c. \right\}. \quad (2.5)$$

The spatial and spin structure of $\Delta_{\alpha\beta}(\mathbf{r}, \mathbf{r}')$ determines the type of superconducting pairing. In most of this review we consider singlet pairing, $\Delta_{\alpha\beta}(\mathbf{r}, \mathbf{r}') = (i\sigma_y)_{\alpha\beta} \Delta(\mathbf{r}, \mathbf{r}')$, where Δ is a scalar function, see previous section.

In a uniform superconductor the interaction depends only on the relative position of the electrons, so that $V(\mathbf{r}, \mathbf{r}') = V(\boldsymbol{\rho})$ with $\boldsymbol{\rho} \equiv \mathbf{r} - \mathbf{r}'$. Therefore in the absence of impurities, the structure of the order parameter in real space depends on the symmetry properties of $V(\boldsymbol{\rho})$. These are easier to consider in momentum, rather than coordinate, space. In models with local attraction, when $V(\boldsymbol{\rho}) = V_0 \delta(\boldsymbol{\rho})$, the Fourier transform of the interaction is featureless, and $\Delta(\mathbf{k}) = \Delta_0$ — an example of an isotropic, or s -wave superconductor.

In the remainder of this section we overview the main methods solving the BCS Hamiltonian since the same methods are commonly applied to the studies of impurity effects in superconductors. The approaches that we consider are: a) direct diagonalization via the Bogoliubov-Valatin transformation; b) variational determination of the ground state energy from the trial wave function; and c) Green's function formalism.

A. Bogoliubov transformation

Since the effective Hamiltonian of Eq. (2.5) is bilinear in fermion operators, ψ and ψ^{\dagger} , it can be diagonalized by a canonical transformation of the form

$$\psi_{\alpha}(\mathbf{r}) = \sum_n \left[u_{n\alpha}(\mathbf{r}) \gamma_n - \alpha v_{n\alpha}^*(\mathbf{r}) \gamma_n^{\dagger} \right], \quad (2.6)$$

subject to condition $|u_{n\alpha}(\mathbf{r})|^2 + |v_{n\alpha}(\mathbf{r})|^2 = 1$. The coefficients u and v are determined by solving the Bogoliubov-de Gennes (BdG) equations (de Gennes, 1989):

$$E u_{\alpha}(\mathbf{r}) = H_0(\mathbf{r}) u_{\alpha}(\mathbf{r}) + \int d^d \mathbf{r}' \Delta_{\alpha\beta}(\mathbf{r}, \mathbf{r}') v_{\beta}(\mathbf{r}'), \quad (2.7)$$

$$E v_{\alpha}(\mathbf{r}) = -H_0^*(\mathbf{r}) v_{\alpha}(\mathbf{r}) + \int d^d \mathbf{r}' \Delta_{\alpha\beta}^*(\mathbf{r}, \mathbf{r}') u_{\beta}(\mathbf{r}'). \quad (2.8)$$

Here we suppressed the label n for brevity. Clearly, when $\Delta = 0$, coefficients u and v do not couple, and there is no particle-hole mixing.

For each n there are four functions, $u_{\uparrow}(\mathbf{r}), u_{\downarrow}(\mathbf{r}), v_{\uparrow}(\mathbf{r}), v_{\downarrow}(\mathbf{r})$ that need to be determined. However, for a singlet superconductor, the matrix $\Delta_{\alpha\beta}$ is off-diagonal in the spin indices, so that u_{\uparrow} (u_{\downarrow}) couples only to v_{\downarrow} (v_{\uparrow}), and hence only two of the equations are coupled. In the presence of the general impurity potential, however, all four components are interdependent.

Equations (2.7)-(2.8), are coupled integro-differential equations for the functions $u_{n\alpha}(\mathbf{r})$ and $v_{n\alpha}(\mathbf{r})$. They have to be complemented by the self-consistency equations on $\Delta_{\alpha\beta}$, which can be obtained directly from Eq. (2.4) to be

$$\Delta_{\alpha\beta}(\mathbf{r}, \mathbf{r}') = \frac{1}{2} V_{\alpha\beta\gamma\delta}(\mathbf{r}, \mathbf{r}') \sum_n \left[\delta u_{n\gamma}(\mathbf{r}') v_{n\delta}^*(\mathbf{r}) f(-E_n) + \gamma v_{n\gamma}^*(\mathbf{r}') u_{n\delta}(\mathbf{r}) f(E_n) \right]. \quad (2.9)$$

Here the Fermi function $f(E) = [\exp(E/T) + 1]^{-1}$.

In a uniform superconductor the Fourier transform of the BdG equations, Eqs. (2.7)-(2.8), into the momentum space gives

$$(\xi_{\mathbf{k}} - E_{\mathbf{k}}) u_{\mathbf{k}\alpha} + \Delta_{\alpha\beta}(\mathbf{k}) v_{\mathbf{k}\beta} = 0, \quad (2.10)$$

$$(\xi_{\mathbf{k}} + E_{\mathbf{k}}) v_{\mathbf{k}\alpha} + \Delta_{\alpha\beta}^*(-\mathbf{k}) u_{\mathbf{k}\beta} = 0, \quad (2.11)$$

where $\xi_{\mathbf{k}}$ is the bare quasiparticle energy, measured with respect to the chemical potential, $\xi_{\mathbf{k}} = \epsilon(\mathbf{k}) - \mu$. In a singlet superconductor

$$(\xi_{\mathbf{k}} - E_{\mathbf{k}}) u_{\mathbf{k}\uparrow} + \Delta(\mathbf{k}) v_{\mathbf{k}\downarrow} = 0, \quad (2.12)$$

$$(\xi_{\mathbf{k}} + E_{\mathbf{k}}) v_{\mathbf{k}\downarrow} + \Delta^*(\mathbf{k}) u_{\mathbf{k}\uparrow} = 0, \quad (2.13)$$

and we recover the familiar energy spectrum $E_{\mathbf{k}} = \sqrt{\xi_{\mathbf{k}}^2 + |\Delta(\mathbf{k})|^2}$, with the coefficients u and v given by

$$\begin{pmatrix} u_{\mathbf{k}} \\ v_{\mathbf{k}} \end{pmatrix} = \frac{1}{2} \begin{bmatrix} 1 \pm \frac{\xi_{\mathbf{k}}}{E_{\mathbf{k}}} \end{bmatrix}. \quad (2.14)$$

B. BCS variational wave function

Superconductivity originates from the instability of the Fermi sea towards pairing of time-reversed quasiparticle states. The variational wave function approach, originating with the BCS paper, is to restrict the trial wave

function to the subspace of either empty or doubly occupied states,

$$|\Psi_{BCS}(\mathbf{r})\rangle = \prod_n (a_n + b_n c_{n\uparrow}^\dagger c_{n\downarrow}^\dagger) |0\rangle, \quad (2.15)$$

and to minimize the energy, $E_{BCS} = \langle \Psi | H | \Psi \rangle$. This is an excellent approximation at low temperatures. In Eq. (2.15) the vacuum state $|0\rangle$ denotes the filled Fermi sea, and $c_{n\uparrow}^\dagger$ ($c_{n\downarrow}^\dagger$) creates a quasiparticle with spin up (down) and with the wave function $\phi_n(\mathbf{r})$ ($\phi_n^*(\mathbf{r})$) that is the eigenfunction of the single particle Hamiltonian. Normalization requires that $|a_n|^2 + |b_n|^2 = 1$.

In the absence of impurities the eigenfunctions, ϕ_n , can be labeled by the same indices, \mathbf{k} and α , as in the previous section. Consequently, the variational approach is equivalent to the Bogoliubov analysis with the choice $u_n(\mathbf{r}) = a_n \phi_n(\mathbf{r})$, and $v_n(\mathbf{r}) = b_n \phi_n(\mathbf{r})$. In general, however, interaction with impurities may lead to the appearance of the single particle states in the ground state wave function, see Sec. X. It is worth remembering that the energy of the BCS state is greater or equal to that of the exact ground state.

C. Green's functions

The third approach that we use is the Green's function method, which originates with the work of Gor'kov. Following Nambu we introduce a four-component vector that is a spinor representation of the particle and hole states,

$$\Psi^\dagger(\mathbf{r}) = (\psi_\uparrow^\dagger, \psi_\downarrow^\dagger, \psi_\uparrow, \psi_\downarrow). \quad (2.16)$$

The matrix Green's function is defined as the ordered average (hat denotes a matrix in Nambu space)

$$\hat{G}(x, x') = -\langle T_\tau \Psi(x) \Psi^\dagger(x') \rangle, \quad (2.17)$$

where the four-component vector $x = (\mathbf{r}, \tau)$ combines the real space coordinate, \mathbf{r} , and the imaginary time, τ . The time evolution of the operators in the Heisenberg approach is given by $\partial\psi/\partial\tau = [\mathcal{H}_{BCS}, \psi]$.

For a singlet homogeneous superconductor the Hamiltonian of Eq. (2.5) in the Nambu notation takes the form,

$$\mathcal{H}_{BCS} = \int d\mathbf{r} \Psi^\dagger(\mathbf{r}) \left[\xi(-i\nabla)\tau_3 + \Delta\tau_1\sigma_2 \right] \Psi(\mathbf{r}), \quad (2.18)$$

and we find (Maki, 1969)

$$\hat{G}_0^{-1}(\mathbf{k}, \omega) = i\omega_n - \xi(\mathbf{k})\tau_3 - \Delta(\mathbf{k})\sigma_2\tau_1. \quad (2.19)$$

Here $\omega_n = \pi T(2n + 1)$ is the Matsubara frequency, σ_i are the Pauli matrices acting in spin space, τ_i are the Pauli matrices in the particle-hole space, and $\tau_i\sigma_j$ denotes a direct product of the matrices operating in the

4-dimensional Nambu space. The Fourier transform in τ is defined as

$$\hat{G}(\mathbf{k}; \tau) = k_B T \sum_{\omega_n} \hat{G}(\mathbf{k}, \omega_n) e^{-i\omega_n \tau} \quad (2.20)$$

The self-consistency equation for a single superconductor takes the form

$$\Delta(\mathbf{k}) = -\frac{T}{4} \sum_{\omega_n} \int d\mathbf{k}' V(\mathbf{k}, \mathbf{k}') \text{Tr} [\tau_1 \sigma_2 G_0]. \quad (2.21)$$

In BCS the interaction is restricted to a thin shell of electrons near the Fermi surface, and therefore

$$\Delta(\hat{\Omega}) = -\frac{T}{4} N_0 \sum_{\omega_n} \int d\hat{\Omega}' V(\hat{\Omega}, \hat{\Omega}') \text{Tr} \left[\tau_1 \sigma_2 \int d\xi_{\mathbf{k}} G_0 \right], \quad (2.22)$$

where $\hat{\Omega}$ denotes a direction on the Fermi surface, and N_0 is the normal state density of states.

The off-diagonal component $(\hat{G}_0)_{12} = F$, is often called the Gor'kov's anomalous Green's function since it describes the pairing average

$$F_{\alpha\beta}(x, x') = -\langle T_\tau \psi_\alpha(x) \psi_\beta(x') \rangle. \quad (2.23)$$

In general $F_{\alpha\beta}(x, x') = g_{\alpha\beta} F(x, x')$, where the matrix g describes the spin structure of the superconducting order. For singlet pairing $g = i\sigma_y$, and in a spatially uniform superconductor

$$G(\omega_n, \mathbf{k}) = \frac{i\omega_n + \xi_{\mathbf{k}}}{(i\omega_n)^2 - \xi_{\mathbf{k}}^2 - |\Delta(\mathbf{k})|^2}, \quad (2.24)$$

$$F(\omega_n, \mathbf{k}) = \frac{\Delta(\mathbf{k})}{(i\omega_n)^2 - \xi_{\mathbf{k}}^2 - |\Delta(\mathbf{k})|^2}. \quad (2.25)$$

The connection with the Bogoliubov's transformation is provided by rewriting the Green's functions as

$$G(\omega_n, \mathbf{k}) = \frac{u_{\mathbf{k}}^2}{i\omega_n - E_{\mathbf{k}}} + \frac{v_{\mathbf{k}}^2}{i\omega_n + E_{\mathbf{k}}}, \quad (2.26)$$

$$F(\omega_n, \mathbf{k}) = u_{\mathbf{k}} v_{\mathbf{k}}^* \left(\frac{1}{i\omega_n - E_{\mathbf{k}}} - \frac{1}{i\omega_n + E_{\mathbf{k}}} \right), \quad (2.27)$$

where $u_{\mathbf{k}}$ and $v_{\mathbf{k}}$ are given by Eq. (2.14).

The three approaches discussed above are complementary and equivalent in the case of homogeneous superconductors. However, some of them are better suited for addressing specific questions in the presence of impurities. In particular, the Green's function method is advantageous for determining the thermodynamic properties of a material and averaging over many impurity configurations. For inhomogeneous problems, where we are interested in the spatial variations of the superconducting order and electron density, both the BdG equations and Green's functions are often used. The choice of method depends on the type of question asked, and we briefly describe the basic models and issues related to impurity scattering in superconductors below.

III. IMPURITIES IN SUPERCONDUCTORS

A. Single impurity potential

Grain and surface boundaries, twinning planes, and other structural inhomogeneities scatter conduction electrons and therefore affect the order parameters. Here we focus on only one type of imperfection: impurity atoms.

a. Potential scattering. First and foremost an impurity atom has a different electronic configuration than the host solid, and therefore interacts with the density of conduction electrons via a Coulomb potential.

$$H_{imp} = \sum_{\alpha} \int d\mathbf{r} \psi_{\alpha}^{\dagger}(\mathbf{r}) U_{pot}(\mathbf{r}) \psi_{\alpha}(\mathbf{r}). \quad (3.1)$$

In good metals the Coulomb interaction is screened at the length scales comparable to the lattice spacing, and therefore the scattering potential is often assumed to be completely local, $U_{pot}(\mathbf{r}) = U_0 \delta(\mathbf{r} - \mathbf{r}_0)$, with the impurity at \mathbf{r}_0 . The resulting scattering occurs only in the isotropic, *s*-wave, angular momentum channel. If finite range of the interaction is relevant, scattering in $l \neq 0$ channels needs to be considered. In that case the treatment is similar to that of magnetic scattering in conventional superconductors, see Sec. VI, and was applied to unconventional superconductors in, for example (Balatsky *et al.*, 1994; Kampf and Devereaux, 1997).

In the four-component vector notation of the previous section the potential scattering has the same matrix structure as the chemical potential, or $\xi(\mathbf{k})$ in Eq. (2.19), so that

$$H_{imp} = \int d\mathbf{r} \Psi^{\dagger}(\mathbf{r}) \widehat{U}_{pot}(\mathbf{r}) \Psi(\mathbf{r}), \quad (3.2)$$

$$\widehat{U}_{pot} = U_0 \tau_3 \delta(\mathbf{r} - \mathbf{r}_0) \quad (3.3)$$

b. Magnetic scattering. In addition to the electrostatic interactions, if the impurity atom has a magnetic moment, there is an exchange interaction between the local spin on the impurity site and the conduction electrons,

$$H_{imp} = \sum_{\alpha\beta} \int d\mathbf{r} J(\mathbf{r}) \psi_{\alpha}^{\dagger}(\mathbf{r}) \mathbf{S} \cdot \boldsymbol{\sigma}_{\alpha\beta} \psi_{\beta}(\mathbf{r}). \quad (3.4)$$

The range of interaction here is determined by the quantum mechanical structure of the electron cloud associated with the localized spin. Again, in reality we often consider a simplified exchange Hamiltonian with $J(\mathbf{r}) = J_0 \delta(\mathbf{r} - \mathbf{r}_0)$, which captures the essential physics of the problem. In the four-component vector notations of the previous section the electron spin operator becomes (Maki, 1969)

$$\boldsymbol{\alpha} = \frac{1}{2} \left[(1 + \tau_3) \boldsymbol{\sigma} + (1 - \tau_3) \sigma_3 \boldsymbol{\sigma} \sigma_3 \right]. \quad (3.5)$$

Therefore

$$H_{imp} = \int d\mathbf{r} \Psi^{\dagger}(\mathbf{r}) \widehat{U}_{mag}(\mathbf{r}) \Psi(\mathbf{r}), \quad (3.6)$$

$$\widehat{U}_{mag} = J(\mathbf{r}) \mathbf{S} \cdot \boldsymbol{\alpha}. \quad (3.7)$$

c. Anderson impurity. However, even if the ground state of an isolated atom has a spin, putting such an impurity into a host matrix may modify the spin configuration as the impurity electrons couple to the conduction band. Therefore a more realistic model for an impurity site is the Anderson model, with the Hamiltonian

$$H_A = \sum_{\alpha} E_0 d_{\alpha}^{\dagger} d_{\alpha} + U n_{d\uparrow} n_{d\downarrow} + H_{sd}, \quad (3.8)$$

$$H_{sd} = \sum_{\mathbf{k}, \alpha} V_{sd} c_{\mathbf{k}, \alpha}^{\dagger} d_{\alpha} + h.c. \quad (3.9)$$

Here E_0 is the position of the impurity level relative to the Fermi energy, d^{\dagger} and d operate on the impurity site, U is the Coulomb repulsion for the electrons localized on the impurity site, and $c_{\mathbf{k}}^{\dagger}, c_{\mathbf{k}}$ create and annihilate the conduction electrons. This Hamiltonian allows the electrons to hop on and off the impurity site, resulting in a finite width of the impurity level, $\Gamma = \pi |V_{sd}|^2 N_0$, see e.g. (Hewson, 1993) for a detailed analysis in a host normal metal. The model describes potential scattering, when $U \ll \Gamma$. On the other hand, when $E_0 \ll E_F$, $E_0 + U \gg E_F$, and $U \gg \Gamma$, the local levels remain split, so that the impurity state is singly occupied and has a local spin. Therefore the model allows a natural interpolation between potential and magnetic scattering. The price to pay for such a rich behavior is the difficulty of studying the model analytically, and in practice many results have been obtained in the simplified treatments of a) and b) above, although a number of very thorough numerical renormalization group (NRG) studies of Anderson impurities in superconductors exist. We review some of them, but do not focus on those extensively.

B. Scanning tunneling microscopy as a tool to measure local density of states

STM/STS is a powerful and versatile tool for studying electronic properties of solids. Its remarkable energy and spatial resolution is particularly well suited for characterization of materials at small energy and short length scales. STS measures the tunneling current between the metallic tip and the sample as a function of voltage bias, and the tip position is controlled with atomic resolution (Martnez-Samper *et al.*, 2003; Pan *et al.*, 1998; Suderow *et al.*, 2001; Yazdani *et al.*, 1997). From the tunneling Hamiltonian, the differential conductance – the derivative of the current with respect to the bias, is related to the electron spectral function of the sample, $A_{\sigma}(\lambda, \omega) = -(1/\pi) \text{Im} G_{\sigma}(\lambda, \omega + i\delta)$ with $\delta \rightarrow 0^+$, by

$$\frac{dI}{dV} \propto - \int d\omega \sum_{\lambda, \sigma} |T_{\lambda}|^2 A_{\sigma}(\lambda, \omega) f'_{FD}(\omega - eV). \quad (3.10)$$

Here f_{FD} is the Fermi distribution function, λ is the electronic eigenstate for states in the sample (for translationally invariant system λ is often chosen to be a

momentum index \mathbf{k}). The tunneling matrix element is $|T_\lambda|^2 = \sum_\rho |M_{\lambda\rho}|^2 A_{tip}(\rho, \omega)$, where $M_{\lambda\rho}$ is the matrix element for the overlap of the electronic states in the tip and sample. If the DOS of the tip is featureless around the Fermi energy, $|T_\lambda|^2$ is nearly energy independent. If we further assume a λ -independent tunneling matrix element, and consider low temperature ($T \rightarrow 0$), the tunneling conductance is proportional to the local density of state (LDOS) at the bias energy at the tip position, $dI/dV(\mathbf{r}) \propto \rho(eV, \mathbf{r}) = \sum_{\lambda, \sigma} \mathbf{A}_\sigma(\lambda, \omega = eV) |\langle \lambda | \mathbf{r} \rangle|^2$. This, in turn is related to the electronic Green's function via $\rho(\mathbf{r}, eV) = -\pi^{-1} \sum_\sigma \text{Im} G_\sigma(\mathbf{r}, \mathbf{r}; eV + i\delta)$. Therefore tunneling spectroscopy provides a real space image of the local density of states that is computed theoretically. For more details see also (Fischer *et al.*, 2005).

C. Many impurities

In all of our discussions we assume noninteracting impurities¹ so that the net impurity potential is

$$\hat{U}_{imp}(\mathbf{r}) = \sum_i \hat{U}_{imp}(\mathbf{r} - \mathbf{r}_i) \quad (3.11)$$

$$= \int d\mathbf{r}' \rho_i(\mathbf{r}') \hat{U}_{imp}(\mathbf{r} - \mathbf{r}'). \quad (3.12)$$

Here \hat{U} is a matrix in both spin and particle-hole space, and we introduced the impurity density,

$$\rho_i(\mathbf{r}) = \sum_i \delta(\mathbf{r} - \mathbf{r}_i). \quad (3.13)$$

We also work in the dilute limit, where the average impurity concentration $n_i = \int d\mathbf{r} \rho(\mathbf{r}) / \mathcal{V} \ll 1$ with \mathcal{V} being the system volume.

A local physical quantity, such as the LDOS at the position \mathbf{r} , measured by the STM, depends on the distance to nearby impurities, and therefore is different for different impurity distributions. In contrast, thermodynamic quantities, such as T_c or the density of states measured in planar junctions, are averaged over the sample and hence over many random local configurations of impurities. Therefore in computing their values we average over *all* impurity configurations (Abrikosov *et al.*, 1963), so that (bar denotes impurity average)

$$\bar{G}(\omega_n, \mathbf{k}) = \prod_{i=1}^{N_i} \left[\frac{1}{\mathcal{V}} \int d\mathbf{r}_i G(\omega_n, \mathbf{k}, \mathbf{r}_1, \dots, \mathbf{r}_{N_i}) \right]. \quad (3.14)$$

By definition $\bar{\rho}_{imp} = n_i$. We also assume an *uncorrelated*, or random, impurity distribution, which means

$$\overline{\rho(\mathbf{r})\rho(\mathbf{r}')} = n_i \delta(\mathbf{r} - \mathbf{r}') + n_i^2.$$

¹ For magnetic scatterers the effect of the RKKY interaction between impurities on the superconducting properties is small, (Galitskii and Larkin, 2002; Larkin *et al.*, 1971)

For dilute impurities $n_i^2 \ll n_i$, and we neglect the second term compared to the first. In Sec. XIII we implement this procedure to determine the impurity-averaged DOS.

D. The self-energy and the T -matrix approximation

To compute the Green's function in the presence of impurities we often employ the T -matrix approximation. This method is described elsewhere (Hirschfeld and Goldensfeld, 1993; Hirschfeld *et al.*, 1986, 1988; Hotta, 1993; Hussey, 2002; Mahan, 2000), and we only summarize it.

For a single impurity with the scattering potential $\hat{U}_{\mathbf{k}, \mathbf{k}'}$ in the momentum space, the T -matrix accounts exactly for multiple scattering off that impurity. In the language of Feynman diagrams, the corresponding process is shown in Fig. 1. Since the translational invariance is broken by the impurity, the Green's function depends on two momenta, \mathbf{k} and \mathbf{k}' ,

$$\hat{G}(\mathbf{k}, \mathbf{k}') = \hat{G}_0(\mathbf{k}) + \hat{G}_0(\mathbf{k}) \hat{U}_{\mathbf{k}, \mathbf{k}'} \hat{G}_0(\mathbf{k}') + \sum_{\mathbf{k}''} \hat{G}_0(\mathbf{k}) \hat{U}_{\mathbf{k}, \mathbf{k}''} \hat{G}_0(\mathbf{k}'') \hat{U}_{\mathbf{k}'', \mathbf{k}'} \hat{G}_0(\mathbf{k}') + \dots, \quad (3.15)$$

where \hat{G}_0 is given by Eq. (2.19). We suppressed the frequency index as the scattering is elastic. The series can be summed to write (see Fig. 1)

$$\hat{G}(\mathbf{k}, \mathbf{k}') = \hat{G}_0(\mathbf{k}) + \hat{G}_0(\mathbf{k}) \hat{T}_{\mathbf{k}, \mathbf{k}'} \hat{G}_0(\mathbf{k}'), \quad (3.16)$$

where the T -matrix is given by an infinite series

$$\hat{T}_{\mathbf{k}, \mathbf{k}'} = \hat{U}_{\mathbf{k}, \mathbf{k}'} + \sum_{\mathbf{k}''} \hat{U}_{\mathbf{k}, \mathbf{k}''} \hat{G}_0(\mathbf{k}'') \hat{U}_{\mathbf{k}'', \mathbf{k}'} + \dots \quad (3.17)$$

$$= \hat{U}_{\mathbf{k}, \mathbf{k}'} + \sum_{\mathbf{k}''} \hat{U}_{\mathbf{k}, \mathbf{k}''} \hat{G}_0(\mathbf{k}'') \hat{T}_{\mathbf{k}'', \mathbf{k}'}. \quad (3.18)$$

This equation needs to be solved for \hat{T} . If the impurity scattering is purely local, the scattering is isotropic, $\hat{U}_{\mathbf{k}, \mathbf{k}'} = \hat{U}$, greatly simplifying the equation, as \hat{T} depends only on energy, but not on the momentum.

Note that we can draw the set of diagrams in Fig. 1 in real space, and write the corresponding set of equations for the T -matrix and Green's function $\hat{G}(\mathbf{r}, \mathbf{r}')$

$$\hat{G}(\mathbf{r}, \mathbf{r}'; \omega) = \hat{G}_0(\mathbf{r}, \mathbf{r}'; \omega) + \hat{G}_0(\mathbf{r}, \mathbf{r}_0; \omega) \hat{T}(\omega) \hat{G}_0(\mathbf{r}_0, \mathbf{r}'; \omega) \quad (3.19)$$

The T -matrix lends itself easily to describe the effect of an ensemble of impurities. In the context of unconventional superconductors the first such treatment of transport properties is due to Pethick and Pines (Pethick and Pines, 1986). The so called self-consistent T -matrix approach (SCTM) considers multiple scattering on a single site of an electron that has already been scattered on all other impurity sites (Hirschfeld *et al.*, 1986, 1988; Schmitt-Rink *et al.*, 1986). This results in replacing

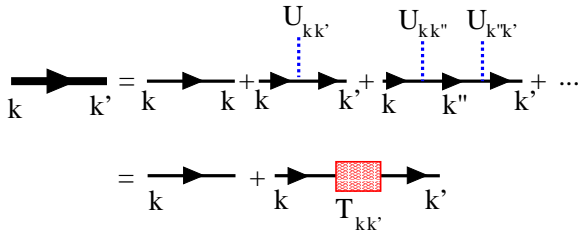


FIG. 1 Multiple scattering on a single impurity. Thick (thin) line denotes full (bare) Green's function, and the dashed line denotes scattering process. The second line defines the T -matrix according to Eq. (3.18).

the bare Green's function in Eq. (3.18) by its impurity-averaged counterpart, $\widehat{G}(\mathbf{k}, \omega)$. After averaging over the random impurity distribution the translational invariance is restored, and the Green's function depends on a single momentum \mathbf{k} . The combined effect of impurities is given by the self energy, $\widehat{\Sigma}(\mathbf{k}, \omega) = n_i \widehat{T}_{\mathbf{k}, \mathbf{k}}$, namely

$$\widehat{G}^{-1}(\mathbf{k}, \omega) = \widehat{G}_0^{-1}(\mathbf{k}, \omega) - \widehat{\Sigma}(\mathbf{k}, \omega). \quad (3.20)$$

In contrast to the single impurity case where Eq. (3.16) with the T -matrix given by Eq. (3.18) is the exact solution of the problem, the Green's function given above is an approximation, and much recent research is motivated by questions about how accurately it describes the properties of nodal superconductors with impurities.

E. Static and dynamic impurities

So far we only considered *static* impurities. However, for potential scattering it is possible that a vibrational mode modulates the charge on the impurity site, and U_{pot} acquires a characteristic frequency. Such a mode can be extended, as a phonon, or local. Influence of the dynamical impurity on the *local* properties of a superconductor is a relatively new subject discussed in Sec. XII, see however (Brandt, 1970).

For magnetic scattering the situation is more complex. Degeneracy between the spin-up and spin-down states on the impurity site and the non-trivial commutation relations between different spin components ensure that quantum dynamics of the impurity is relevant. The dynamics of the local spin flips leads to the screening of the impurity spin by the conduction electrons in a metal below the Kondo temperature, T_K , see (Hewson, 1993) for review. In Sec. XI we review the current status of the studies of Kondo effect in superconductors.

Impurity spin dynamics does not play a major role: a) for large spins, $S \gg 1$ (except in a magnetic field), or b) when the Kondo temperature is low, and measurements are done at $T \gg T_K$. In these limits the approximation of *classical* spin suffices, and the corresponding local and global density of states are analyzed in Sec. VI and Sec. XIII, respectively.

IV. NON-MAGNETIC IMPURITIES AND ANDERSON'S THEOREM

One of the most important early experimental results was the robustness of the conventional superconductivity to small concentrations of non-magnetic impurities. Theoretical underpinning of this result is known as Anderson's theorem (Anderson, 1959). Anderson noticed that, since superconductivity is due to the instability of the Fermi surface to pairing of time-reversed quasiparticle states, any perturbation that does not lift the Kramers degeneracy of these states does not affect the mean field superconducting transition temperature.

This is most clearly seen from the BCS analysis, which we carry out following Ma and Lee, 1985, for an isotropic pairing potential, $V_{\alpha\beta\gamma\delta}(\mathbf{r}, \mathbf{r}') = V\delta(\mathbf{r} - \mathbf{r}')\delta_{\alpha\delta}\delta_{\beta\gamma}$. In the absence of a magnetic field the coefficients $a_n = \sin\theta_n$ and $b_n = \cos\theta_n$ in Eq. (2.15) can be taken real without loss of generality, so that the self-consistency condition, Eq. (2.9) reads

$$\Delta_n = V \sum_{m \neq n} \frac{\Delta_m}{\sqrt{\epsilon_m^2 + \Delta_m^2}} \int d^d \mathbf{r} \phi_n^2(\mathbf{r}) \phi_m^2(\mathbf{r}). \quad (4.1)$$

Here ϵ_m are the energies of the eigenstates, and

$$\Delta_n = \int d^d \mathbf{r} \Delta(\mathbf{r}) \phi_n^2(\mathbf{r}). \quad (4.2)$$

As noted above, in the BCS approach ϕ 's are the eigenfunctions of the single particle Hamiltonian. In a pure system $\Delta(\mathbf{r}) = \Delta_n = \Delta_0$. The most important assumption underlying Anderson's theorem is that, in the presence of impurities, when $\phi_n(\mathbf{r})$ are rather complicated functions, the superconducting order parameter can still be taken to be uniform, $\Delta(\mathbf{r}) = \Delta_1$. Then the gap equation, Eq. (4.1), takes the form

$$\frac{1}{V} = \int d^d \mathbf{r} \epsilon \phi_n^2(\mathbf{r}) \frac{N(\epsilon, \mathbf{r})}{\sqrt{\epsilon^2 + \Delta_1^2}}. \quad (4.3)$$

If the density of states of the system with impurities,

$$N(\epsilon, \mathbf{r}) = \sum_m \phi_m^2(\mathbf{r}) \delta(\epsilon - \epsilon_m), \quad (4.4)$$

is unchanged compared to that of the pure metal, $N(\epsilon, \mathbf{r}) \approx \rho_0$, the solution of the gap equation Eq. (4.3), is $\Delta_1 = \Delta_0$. Therefore the transition temperature and the gap are insensitive to the impurity scattering at the mean field level.

The Anderson theorem explained why superconductivity was robust to disorder in early experiments. It is important to realize, however, that it is an *approximate* statement about the thermodynamic averages of the system. Beginning with the next section we analyze in more detail the changes that impurities create in superconductors. We will see that even purely potential scattering does induce changes in the local properties of

superconductors, albeit the corresponding change in the transition temperature remains minimal. The Anderson theorem brings to the need to separate the study of impurity effects on different length scales, from lattice spacing to the coherence length, to sample size.

Before proceeding we discuss the extensions of the Anderson's treatment of impurities. In weakly disordered systems $N(\epsilon, \mathbf{r}) \approx \rho_0$. Ma and Lee (Ma and Lee, 1985) argued that Anderson's theorem remains valid even in strongly disordered systems provided the localization length, $L \gg (\rho_0 \Delta_0)^{1/d}$. In that case a large number of states localized within energy Δ_0 of the Fermi surface form a local superconducting patch. Josephson interaction between the patches then leads to global phase coherence at $T = 0$. Ma and Lee argued that the theorem holds all the way to the limit of site localization.

At the same time the superfluid stiffness, i.e. the ability to carry supercurrent, is affected by disorder: when the quasiparticle lifetime, τ , becomes sufficiently short, $\Delta_0 \tau \ll 1$, the superfluid density $\rho_s \approx \Delta_0 \tau$. Consequently the local phase fluctuations of the order parameter are strong, and the experimentally observed transition temperature is severely suppressed compared to the mean field T_c . Studies of such granular superconductors are outside the scope of this review.

For dilute impurities Anderson's theorem is valid provided the superconducting order parameter is nearly uniform. Since the "healing length" of $\Delta(\mathbf{r})$ over which it can change appreciably is the coherence length, $\xi_0 \simeq \hbar v_F / \Delta_0$, where v_F is the Fermi velocity, while the Coulomb screening length for the charged impurities in metals is of the order of the lattice spacing, a , for $\xi_0 \gg a$ the order parameter remains essentially uniform, and Anderson's theorem holds. Recent studies considered impurity scattering in superconductors with ultrashort coherence, and found that, when the pairing range is of the order of the electron bandwidth, Anderson's theorem is violated (Ghosal *et al.*, 1998; Moradian *et al.*, 2001; Tanaka and Marsiglio, 2000).

Ghosal *et al.* (Ghosal *et al.*, 1998), and Xiang and Wheatley (Xiang and Wheatley, 1995) explored the difference between the single particle excitation gap and the superconducting order parameter as a function of disorder. When disorder depletes the density of states, both quantities at first decrease simultaneously. However, the spectral gap persists even when superconducting off-diagonal long range order vanishes: this may be related to formation of local pairs without phase coherence (Ma and Lee, 1985).

In most experimentally relevant situations, however, the corrections to the main statement of Anderson's theorem are quantitative rather than qualitative. Therefore it is very instructive and generally sufficient to consider the impurity effects in BCS-like superconductors.

V. SINGLE IMPURITY BOUND STATE IN TWO-DIMENSIONAL METALS

Before we proceed to superconductors, it is very instructive to review a simpler problem of an impurity in a metal. We show here a T -matrix calculation for finding the bound states due to a single impurity in d dimensions with an on-site attractive potential $U(\mathbf{r}) = U_0 \delta(\mathbf{r})$, where $U_0 \leq 0$. The Hamiltonian is

$$\mathcal{H} = \sum_{\mathbf{k}} [\epsilon(\mathbf{k}) - \mu] c_{\mathbf{k},\sigma}^\dagger c_{\mathbf{k},\sigma} + \sum_{\mathbf{k},\mathbf{k}'} U_0 c_{\mathbf{k},\sigma}^\dagger c_{\mathbf{k}',\sigma}, \quad (5.1)$$

We consider, for simplicity, the single particle case ($\mu = 0$), although the results for a normal metal follow by replacing $\epsilon(\mathbf{k}) \rightarrow \xi(\mathbf{k}) = \epsilon_{\mathbf{k}} - \mu$ below.

The bare Green's function for a free particle is

$$G_0(\omega, \mathbf{k}) = [\omega - \epsilon(\mathbf{k})]^{-1}. \quad (5.2)$$

Since the vertex of the impurity interaction, U_0 , is momentum independent, the equation for the T -matrix is particularly simple and follows from Eq. (3.18),

$$T(\omega) = U_0 + U_0 \sum_{\mathbf{k}} G_0(\omega, \mathbf{k}) T(\omega) \\ T(\omega) = \frac{U_0}{1 - U_0 \sum_{\mathbf{k}} G_0(\omega, \mathbf{k})} \quad (5.3)$$

Summation over \mathbf{k} is performed using the DOS

$$N(\epsilon) = \sum_{\mathbf{k}} \delta(\epsilon - \epsilon(\mathbf{k})) = \Gamma_d \epsilon^{\frac{d}{2}-1}, \quad (5.4)$$

where Γ_d is a constant dependent on dimension. Then

$$g_0(\omega) = \frac{1}{N} \sum_{\mathbf{k}} G_0(\omega, \mathbf{k}) = \int_0^W \frac{d\epsilon N(\epsilon)}{\omega - \epsilon} \simeq -\Gamma_d \omega^{\frac{d-2}{2}} \quad (5.5)$$

for $d \neq 2$, where W is the half bandwidth. Here N represents the system size. In two dimensions $g_0 \simeq -\Gamma_2 \ln(W/|\omega|)$. Consequently, the T -matrix for $d \neq 2$ is given by

$$T = \frac{U_0}{1 - g_d \omega^{\frac{d-2}{2}}} \quad (5.6)$$

where $g_d = -U_0 \Gamma_d > 0$ is the effective coupling constant, and by the same expression with the obvious substitution of $\ln(W/|\omega|)$ for $d = 2$.

Poles of the Green's function give the energy spectrum of single particle excitations. The poles of the Green's functions in the presence of impurity scattering, $G = G_0 + G_0 T G_0$, see Eq. (3.16), consist of the poles of the original \hat{G}_0 , and poles of the T -matrix. The latter signify the appearance of new states. We can find the energy of this state, ω_0 , from Eq. (5.6). The bound state ($\omega_0 < 0$, see Fig. 2) is formed for an arbitrarily small potential

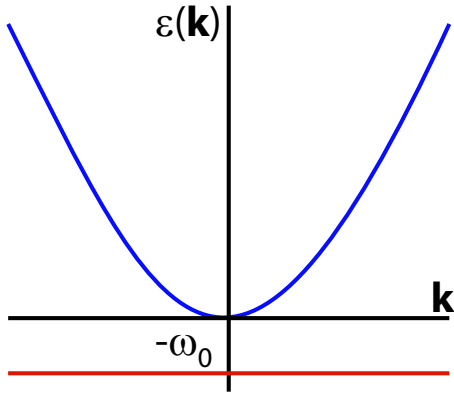


FIG. 2 Impurity bound state in a metal at energy ω_0 is formed as a result of a multiple scattering.

$|U_0|$ in $d = 1, 2$, but requires a critical coupling for $d = 3$. The energy of this state is given by

$$\omega_0 \sim (g_1)^2, \quad \text{if } d = 1; \quad (5.7)$$

$$\omega_0 = W \exp\left(-\frac{1}{g_2}\right), \quad \text{if } d = 2; \quad (5.8)$$

$$\omega_0 \sim [g_3^{\frac{1}{2}} - g_{3c}^{\frac{1}{2}}], \quad g_3 \geq g_{3c}, \quad \text{if } d = 3, \quad (5.9)$$

where the $d = 3$ critical coupling $g_{3c} \sim W^{-1/2}$.

We focus in more detail on the two-dimensional case, when $g_2 = \Gamma_2|U_0|$ and $\Gamma_2 = \frac{m}{2\pi}$ is the electron density of states. The bandwidth, $W \simeq \frac{\hbar^2}{2ma^2}$ is the ultraviolet cutoff corresponding to the lattice parameter a for free particle. This result can be compared to the solution of the Schrödinger's equation for the particle in the 2D attractive potential U_0 (Landau and Lifshitz, 2000), Ch. 45. For an arbitrary potential $U(\mathbf{r})$ the solution obtained using the T-matrix is asymptotically correct if the scattering length is greater than a . For shallow potential the bound state energy $-\omega_0$ is exponentially small, and the characteristic extent of the bound state wave function is $l_0 = (\frac{\hbar^2}{2m\omega_0})^{1/2} \gg a$. Therefore in this limit we can safely approximate $U(\mathbf{r}) = U_0\delta(\mathbf{r})$, where $U_0 = \int U(\mathbf{r})d\mathbf{r}$.

Finding the energy of the bound state, Eq. (5.8), is only one part to the solution. We also want to determine the corrections to the *local density of states* due to bound state. We write the equation for the Green's function in real space, Eq. (3.19),

$$G(\mathbf{r}, \mathbf{r}'; \omega) = G_0(\mathbf{r}, \mathbf{r}'; \omega) + G_0(\mathbf{r}, 0; \omega)T(\omega)G_0(0, \mathbf{r}'; \omega)$$

and read off the position dependent DOS

$$\begin{aligned} N(\mathbf{r}, \omega) &= -\frac{1}{\pi} \text{Im}G(\mathbf{r}, \mathbf{r}; \omega) \\ &= N_0(\mathbf{r}, \omega) + \delta N(\mathbf{r}, \omega). \end{aligned} \quad (5.10)$$

The first term is the DOS of a clean system, and the second is the correction due to the bound state. Consider $\omega \approx \omega_0$. Since the bound state is below the bottom of the

band, the unperturbed Green's function G^0 has no imaginary part in this range. Therefore the only contribution to $\text{Im}G(\mathbf{r}, \mathbf{r}; \omega)$ in Eq. (5.10) is from the T-matrix

$$\begin{aligned} \text{Im}T(\omega) &= \text{Im} \frac{1}{1/g_2 - \log[W/(-\omega)]} \\ &= \text{Im} \ln^{-1} \left[\frac{\omega + i\delta}{\omega_0} \right] \\ &= \pi \delta(\omega - \omega_0), \end{aligned} \quad (5.11)$$

and the correction to the DOS of a clean system is

$$\delta N(\mathbf{r}, \omega) = |G_0(\mathbf{r}, \omega_0)|^2 \delta(\omega - \omega_0) \quad (5.12)$$

with $G_0(\mathbf{r}, \omega) = N_0 J_0(k_F r) \ln[\frac{W}{\omega}]$ is the real part of Green's function in 2D systems. Equations (5.9) and (5.12) are the main results of this section. They establish the strategy to which we adhere in finding the impurity induced bound states: a) find the poles of the T matrix and the new poles of the full Green's function, b) compute the inhomogeneous DOS due to the impurity induced state. There are other approaches to search for scattering induced bound states. For example, the exact numerical solution for a finite system is the only approach available for calculations accounting for the self-consistent suppression of the superconducting order.

VI. LOW-ENERGY STATES IN *s*-WAVE SUPERCONDUCTORS

A. Potential scattering

Even though the potential scattering does not change the bulk properties of isotropic superconductors, it may affect the local density of states. The first analysis of the conditions for the existence of the bound state and the structure of the Friedel oscillations around a spherically symmetric impurity in an *s*-wave superconductor is due to Fetter (Fetter, 1965). Here we follow (Machida and Shibata, 1972; Shiba, 1973) and consider the Anderson impurity model, Eqs. (3.8)-(3.9) in the limit $U = 0$ (resonance scattering). As discussed above the localized state acquires a finite width, $\Gamma = \pi|V_{sd}|^2 N_0$, due to hybridization with the conduction band. Consequently the effective scattering potential varies significantly over the bandwidth energy, violating the provisions of Anderson's theorem. The T-matrix approach gives (Machida and Shibata, 1972; Shiba, 1973)

$$\hat{T}(\omega) = |V_{sd}|^2 \tau_3 \left[\omega - E_0 \tau_3 - |V_{sd}|^2 \tau_3 \sum_{\mathbf{k}} \hat{G}_0(\mathbf{k}, \omega) \tau_3 \right]^{-1} \tau_3. \quad (6.1)$$

The poles, ω_0 , of the T-matrix determine the location of the bound states

$$\omega^2 \left[1 + \frac{2\Gamma}{\sqrt{\Delta^2 - \omega^2}} \right] = E_0^2 + \Gamma^2. \quad (6.2)$$

In most physical situations $\Gamma \gg \Delta$, so that

$$\omega_0 = \pm \Delta(1 - 2\pi^2(\Delta N_d(0))^2), \quad (6.3)$$

where $N_d(0) = \pi^{-1}\Gamma/(\Gamma^2 + E_0^2)$ is the density of states of the resonant impurity level. Typically $\Delta N_d(0) \sim 10^{-3}$, so that the bound state lies essentially at the gap edge. Shiba considered a finite but small value of the Coulomb repulsion and allowed for the induced pairing on the impurity site (Shiba, 1973). He concluded that, even though the bound state may be shifted to lower energies, it still lies within $10^{-3}\Delta$ of the gap edge, and therefore can be neglected in the discussions of physical properties.

B. Classical spins

If the impurities are magnetic, the time-reversal symmetry is violated, and therefore superconductivity is suppressed. We consider a combination of the potential scattering, $\hat{U}_{pot}(\mathbf{r}) = V(\mathbf{r})\tau_3$, and the magnetic scattering, Eq. (3.6), written in the momentum space,

$$H_{ex} = \frac{1}{2N} \sum_{\substack{\mathbf{k}, \mathbf{k}' \\ \alpha\beta}} J(\mathbf{k} - \mathbf{k}') c_{\mathbf{k},\alpha}^\dagger \boldsymbol{\sigma}_{\alpha\beta} \cdot \mathbf{S}_{\mathbf{k}'\beta}. \quad (6.4)$$

As discussed in Sec. III.E, for $S \gg 1$ or $T \gg T_K$, we ignore Kondo screening, and consider scattering on *classical spins* first studied independently by Shiba, Rusinov, and Yu (Rusinov, 1968, 1969; Shiba, 1968; Yu, 1965). Technically this is achieved by taking $S \rightarrow \infty$, while simultaneously $J \rightarrow 0$ so that $JS = \text{const}$. In this limit the localized spin acts as a local magnetic field.

The impurity location is chosen at the origin for a BCS s -superconductor with the unperturbed Hamiltonian of the form

$$\mathcal{H}_0 = \sum_{\mathbf{k}\alpha} \varepsilon_{\mathbf{k}} c_{\mathbf{k},\alpha}^\dagger c_{\mathbf{k}\alpha} + \Delta_0 \sum_{\mathbf{k}} \{c_{\mathbf{k}\uparrow}^\dagger c_{-\mathbf{k}\downarrow}^\dagger + c_{-\mathbf{k}\downarrow} c_{\mathbf{k}\uparrow}\}. \quad (6.5)$$

This problem serves as a starting point for all subsequent analysis of the resonance states in superconductors.

To find a localized state with energy $0 < E < \Delta_0$ near a single paramagnetic impurity we perform a Bogoliubov transformation (Rusinov, 1968; Yu, 1965) to find

$$Eu_\alpha(\mathbf{r}) = \varepsilon(\mathbf{k})u_\alpha(\mathbf{r}) + i\Delta\sigma_{\alpha\beta}^y v_\beta(\mathbf{r}) + U_{\alpha\beta}(\mathbf{r})u_\beta(\mathbf{r}) \quad (6.6)$$

$$Ev_\alpha(\mathbf{r}) = -\varepsilon(\mathbf{k})v_\alpha(\mathbf{r}) - i\Delta\sigma_{\alpha\beta}^y u_\beta(\mathbf{r}) - U_{\alpha\beta}(\mathbf{r})v_\beta(\mathbf{r}) \quad (6.7)$$

This system is solved by Fourier transforming the equations and expanding the impurity potentials in spherical harmonics in \mathbf{k} -space, J_l and V_l , and has solutions at

$$\frac{E_l}{\Delta_0} = \frac{1 + (\pi N_0 V_l)^2 - (\pi N_0 J_l S/2)^2}{\sqrt{[1 + (\pi N_0 V_l)^2 - (\pi N_0 J_l S/2)^2]^2 + 4(\pi N_0 J_l S/2)^2}}, \quad (6.8)$$

where N_0 is the normal state DOS at the Fermi energy. This result can be written in a more elegant form using

the phase shifts, δ_l , of scattering for up (+) and down (-) electrons, in each angular channel,

$$\tan \delta_l^\pm = (\pi N_0)(V_l \pm J_l S/2). \quad (6.9)$$

Then the energies of the states in the gap become

$$\epsilon_l = \frac{E_l}{\Delta_0} = \cos(\delta_l^+ - \delta_l^-). \quad (6.10)$$

Clearly, for purely potential scattering ($\delta_l^+ = \delta_l^-$) the spectrum begins at the gap edge, and there are no intragap states. However, as the magnetic scattering increases, low-energy states appear below the gap edge. Purely magnetic scattering corresponds to $\delta_l^+ = -\delta_l^-$, and strong scattering (unitarity limit, $\delta \sim \pi/2$) yields a localized state deep in the gap, while weak scattering ($\delta \ll 1$) results in the bound state close to the gap edge.

The same result can be obtained using the Green's function formulation (Rusinov, 1969; Shiba, 1968) and solving the single impurity problem via the T -matrix. In the Nambu notations

$$\hat{G}(\mathbf{k}, \mathbf{k}'; \omega) = \hat{G}_0(\mathbf{k}, \omega)\delta(\mathbf{k} - \mathbf{k}') + \hat{G}_0(\mathbf{k}, \omega)\hat{T}(\mathbf{k}, \mathbf{k}')\hat{G}_0(\mathbf{k}', \omega). \quad (6.11)$$

Here the T -matrix is computed as in Sec. III.D for a matrix Hamiltonian of Sec. III.A, and we sum over the indices of the matrix $\boldsymbol{\alpha}$ in each vertex. The l -th angular component, \hat{T}_l , satisfies (for a spherical Fermi surface and isotropic gap)

$$\hat{T}_l(\omega) = \hat{U}_l + \hat{U}_l \int d\varepsilon \hat{G}_0(\mathbf{k}, \omega)\hat{T}_l(\omega). \quad (6.12)$$

The full expressions for T_l is straightforward to obtain (Rusinov, 1969) but is rather cumbersome, so that we do not give it here. Even for spherically symmetric scattering ($l = 0$ only) with both $V_0 \neq 0$ and $J \neq 0$ the T -matrix is simple yet lengthy (Okabe and Nagi, 1983). The bound state energy is, of course, still given by Eq. (6.10).

For purely magnetic spherically symmetric exchange, $J(\mathbf{k} - \mathbf{k}') = J$, the T -matrix has a particularly simple form (Shiba, 1968), with the diagonal, in spin indices, component

$$\hat{T}^{(1)}(\omega) = \frac{1}{N} \frac{(JS/2)^2 \hat{g}_0(\omega)}{I - (JS\hat{g}_0(\omega)/2)^2}. \quad (6.13)$$

Here \hat{g}_0 is the local matrix Green's function,

$$\hat{g}_0(\omega) = \frac{1}{N} \sum_{\mathbf{k}} \hat{G}_0(\mathbf{k}, \omega) = -\pi N_0 \frac{\omega + \Delta_0 \sigma_2 \tau_2}{\sqrt{\Delta_0^2 - \omega^2}}. \quad (6.14)$$

The bound state energy

$$\epsilon_0 = \frac{E_0}{\Delta_0} = \frac{1 - (JS\pi N_0/2)^2}{1 + (JS\pi N_0/2)^2}. \quad (6.15)$$

The wave functions of the bound states at E_l can be computed using the Bogoliubov equations above. In the

simplest case of isotropic scattering at distances $r \gg p_F^{-1}$, both $u(\mathbf{r})$ and $v(\mathbf{r})$ vary as (Fetter, 1965; Rusinov, 1969)

$$\frac{\sin(p_F r - \delta_0^\pm)}{p_F r} \exp(-r |\sin(\delta_0^+ - \delta_0^-)| / \xi_0), \quad (6.16)$$

that is, the state is localized near the impurity site at distances

$$r_0 \sim \frac{\xi_0}{|\sin(\delta_0^+ - \delta_0^-)|} = \frac{\xi_0}{\sqrt{1 - \epsilon_0^2}}. \quad (6.17)$$

The square of these coefficients gives the spatial dependence of the amplitude of the particle and hole components of the density of states at a given position \mathbf{r} (Yazdani *et al.*, 1997).

The analysis above was carried out under the assumption that the variation of the order parameter, Δ , around the impurity site does not change the position of the resonance state. There are several characteristic length scales for this variation, $\delta\Delta(\mathbf{r})$. Far away from the impurity, $r \gg \xi_0$, at temperatures close to T_c , where this variation can be determined perturbatively, $\delta\Delta(\mathbf{r})/\Delta_0 \simeq 1/(p_F r)$ (Heinrichs, 1968; Rusinov, 1968). This power law is insensitive to the phase shifts of scattering on the impurity. At low temperatures a fully self-consistent treatment is required, which leads to $\delta\Delta(\mathbf{r})$ decaying as $(p_F r)^{-3}$ and oscillating on the scale of $\xi_0 \Delta_0 / \omega_D$, where the Debye temperature ω_D sets the scale for the interaction between electrons (Schlottmann, 1976).

In the immediate vicinity of impurity, $v_F / \omega_D \ll r \ll \xi_0$, the variation of the order parameter is $\delta\Delta(\mathbf{r})/\Delta_0 \simeq 1/(p_F r)^2$ in the linear response approximation (Rusinov, 1968). In the fully self-consistent treatment at distances $r \ll \xi_0 \omega_D / E_F$, this dependence was found to acquire an oscillating factor $\sin^2 p_F r$ (Schlottmann, 1976).

In the Anderson model the local change $\Delta(\mathbf{r})$ is related to the impurity T -matrix (Kim and Muzikar, 1993), and can be determined if a reliable approximation for the T -matrix exists for the given parameter range. In principle, the method of Kim and Muzikar covers both Kondo and mixed-valence regimes, and is useful in determining the local structures of the order parameter.

In all these cases, the suppression of the order parameter is determined by the Fermi wavelength, and does not affect the position of the bound state.

VII. IMPURITY-INDUCED VIRTUAL BOUND STATES IN d -WAVE SUPERCONDUCTORS

We now extend our discussion to impurity induced states in d -wave superconductors. Scalar (non-magnetic) impurities are pair-breakers for ‘‘higher-orbital-momentum’’ states, such as d -wave: The change of the quasiparticle momentum upon scattering disrupts the phase assignment for particular directions of the momenta in a nontrivial pairing state (Anderson, 1959; Markowitz and Kadanoff, 1963; Tsuneto, 1962). This

also follows from the analysis of the self-energy in the Abrikosov-Gorkov theory (Abrikosov *et al.*, 1963). An early argument about pairbreaking effects of potential scattering is due to Larkin (Larkin, 1965).

As we have emphasized, for pairbreaking impurities the local properties of the superconductor near the impurity site, such as the LDOS and the gap amplitude, are modified dramatically. To capture these modifications, we use a variation of the Yu-Shiba-Rusinov approach (Rusinov, 1968; Shiba, 1968; Yu, 1965), see Sec. VI. We restrict our consideration to the s -wave scatterers ($l = 0$) close to the unitarity limit, $\delta_0 \simeq \pi/2$, when the bound state energy is far from the gap edge. In contrast to the s -wave superconductors, in d -wave systems the density of states below the gap maximum, Δ_0 , is non-zero, and varies linearly with energy in a pure system, $N(\omega)/N_0 \simeq \omega/\Delta_0$. Consequently, the overlap with the particle-hole continuum only allows the formation of resonance, or *virtual bound* states, with a finite lifetime.

We focus on point-like defects, and use the T -matrix approach. A closely related method uses quasiclassical approximation and ideas of Andreev scattering to reproduce the same results (Chen *et al.*, 1999; Choi and Muzikar, 1990; Shnirman *et al.*, 1999). Interesting extensions are obtained within the quasiclassical formalism for extended defects: for example, index theorem dictates the existence of a low energy quasi-bound state in unconventional superconductors (Adagideli *et al.*, 1999).

High- T_c cuprates with Zn substitution for in-plane Cu is a well studied example of impurity system. Zn ions have a full d shell, and are nominally non-magnetic. High stability of this configuration, and rapid suppression of T_c by Zn doping (Hotta, 1993; Ishida *et al.*, 1991) support the view that Zn ions are strong non-magnetic scatterers. Another point of view, that Zn induces localized moment on neighboring Cu sites (Bobroff *et al.*, 2001; Polkovnikov *et al.*, 2001), leads naturally to Kondo problem in gapless superconductors, and we discuss it in Sec. XI.

Based on strong anisotropy of electronic transport, we model cuprates as a 2D d -wave superconductor, and analyze virtual impurity-induced bound states, closely following (Balatsky *et al.*, 1995; Buchholtz and Zwicky, 1981; Salkola *et al.*, 1996, 1997; Stamp, 1987). Our results are easily extended to any nontrivial pairing state and to higher dimension, and are relevant, for example, for heavy-fermion superconductors with impurities.

Main results of this section are as follows: (i) A strongly-scattering scalar impurity produces a localized, virtual or virtually bound state (or resonance) in a d -wave superconductor. It is intuitively obvious that any strong enough pair-breaking impurity — magnetic or non-magnetic — will induce such a state. Indeed, the low-lying quasiparticle states close to the nodes in the energy gap will be strongly influenced even by a non-magnetic impurity potential, resulting in a virtual bound state in the unitarity limit. (ii) This should be compared to the fact that, in s -wave superconductors, magnetic impurities produce bound states inside the energy

gap (Machida and Shibata, 1972). The energy Ω' and the decay rate Ω'' of this state are given by

$$\Omega \equiv \Omega' + i\Omega'' = -\Delta_0 \frac{\pi c/2}{\log(8/\pi c)} \left[1 + \frac{i\pi}{2} \frac{1}{\log(8/\pi c)} \right] \quad (7.1)$$

where $c = \cot \delta_0$. These results are valid provided $\log(8/\pi c) \gg 1$, and assuming band particle-hole symmetry. The impurity breaks local particle-hole symmetry, however, since Ω' has a definite sign. In the unitary limit, $c \rightarrow 0$, the virtual bound state is a sharp resonance at $\Omega \rightarrow 0$ with $\Omega''/\Omega' \rightarrow 0$. In the opposite case of weak scattering, $c \lesssim 1$, the energy of the state formally approaches $\Omega' \sim \Delta_0$ and the state is ill-defined since $\Omega'' \sim \Omega'$ (see Fig. 10 in Sec. VIII). The wave function of the bound state decays as a power law, $\Psi(r) \sim 1/r$, and is not normalizable. The wave function is localized along the directions where gap vanishes (nodal directions).

A. Single potential impurity problem

Consider a potential impurity at $\mathbf{r} = 0$ described by

$$H_{\text{int}} = \sum_{\mathbf{k}\mathbf{k}'\sigma} U_0 c_{\mathbf{k}\sigma}^\dagger c_{\mathbf{k}'\sigma} \quad (7.2)$$

where U_0 is the strength of the isotropic scattering, resulting in phase shift δ_0 . The T -matrix is independent of wavevector, and the Green's function is

$$\widehat{G}(\mathbf{k}, \mathbf{k}'; \omega) = \widehat{G}_0(\mathbf{k}, \omega) \delta_{\mathbf{k}\mathbf{k}'} + \widehat{G}_0(\mathbf{k}, \omega) \widehat{T}(\omega) \widehat{G}_0(\mathbf{k}', \omega) \quad (7.3)$$

where in \widehat{G}_0 we chose the $d_{x^2-y^2}$ gap $\Delta_{\mathbf{k}} = \Delta_0 \cos 2\varphi$.

For s -wave scattering the matrix $\widehat{T} = T_0 \widehat{\tau}_0 + T_3 \widehat{\tau}_3$ (Balatsky *et al.*, 1994; Hirschfeld and Goldenfeld, 1993; Hirschfeld *et al.*, 1988; Lee, 1993; Loktev and Pogorelov, 2002; Pethick and Pines, 1986; Pogorelov, 1994; Schmitt-Rink *et al.*, 1986; Shiba, 1968; Stamp, 1987), and its diagonal element is

$$T(\omega)_{11} = 1/[c - g_{11}(\omega)], \quad (7.4)$$

where $g_{11}(\omega) = \frac{1}{2\pi N_0} \sum_{\mathbf{k}} [\widehat{G}^{(0)}(\mathbf{k}, \omega) (\widehat{\tau}_0 + \widehat{\tau}_3)]_{11}$. The quasi-bound states are given by the poles of the T -matrix,

$$c = g_{11}(\Omega), \quad (7.5)$$

which is an implicit equation for the energy of the impurity resonance Ω_0 as a function of $c = \cot \delta_0$.

For particle-hole symmetric case $g_{11} = g_0(\omega) = \langle \omega / \sqrt{\Delta(\varphi)^2 - \omega^2} \rangle_{FS}$, where the angular brackets denote an average over the Fermi surface; for simplicity, we take $\langle \bullet \rangle_{FS} = \int \bullet d\varphi / 2\pi$.² For $|\omega| \ll \Delta_0$, we find

$$g_0(\omega) = -\frac{2\omega}{\pi\Delta_0} \left(\log \frac{4\Delta_0}{\omega} - \frac{i\pi}{2} \right). \quad (7.6)$$

² We assume that the energy gap has line nodes in three dimensions with weak quasiparticle dispersion along the z axis; an extension to a general three-dimensional case is straightforward.

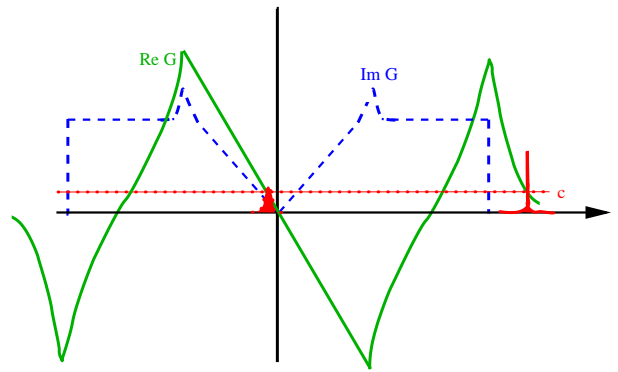


FIG. 3 Graphic solution of Eq. (7.5) for $U_0 > 0$. We show physically relevant solution with $\Omega''_0 \ll \Omega'_0$. If $\text{Im}g_0(\Omega_0) \gg \text{Re}g_0(\Omega_0)$, the resonance is broadened and merges with continuum. Resonances below (or above, for $U_0 < 0$) the band are sharp, with most of spectral weight. The virtual bound state inside the gap is well resolved for large U_0 (small c).

Substituting in Eq.(7.5) the solution, Eq.(7.1), follows immediately. In Fig. 3 we illustrate a solution of the Eq. (7.5) for fermions with a finite bandwidth.

The solution of Eq. (7.5) is complex, indicating a resonant nature of the quasiparticle state, better described as a virtual state. This is easily seen from Eq. (7.1), which solves Eq. (7.5) to logarithmic accuracy. However, as $c \rightarrow 0$, the resonance can be made arbitrarily sharp. For $c = 0$, the virtual state becomes a sharp resonance state bound to the impurity (Balatsky *et al.*, 1995). As $c \rightarrow 1^-$, Ω' and Ω'' increase without bound so that $\Omega''/\Omega' \rightarrow 1^-$, and the solution becomes unphysical. For $c > 1$, no solution has been found for Ω .³

To solve the single impurity problem one has to retain both T_0 and T_3 components of the T -matrix,

$$T_0 = \frac{g_0(\omega)}{c^2 - g_0^2(\omega)}, \quad T_3 = \frac{c}{c^2 - g_0^2(\omega)}. \quad (7.7)$$

Each of them has *two* poles at $c = \pm g_0(\omega)$, however, $T_{11} = T_0 + T_3$ has only one pole, see Eq. (7.4). Sign of the resonance energy reflects a particle-hole asymmetry introduced by the on-site impurity potential U_0 .

Now we turn to the physical implications of these virtual bound states in a d -wave superconductor, and consider the most interesting case of unitary impurities in the dilute limit, separated by a distance $l \gg \xi_0$. These bound states are *nearly localized* close to the impurity sites (see below), and substantially modify the local characteristics of the superconductor, such as density of tunneling

³ A related model of the Anderson impurity in an unconventional superconductor was considered by L. Borkowski and P. Hirschfeld, Phys. Rev. B **46**, 9274 (1992). The results found here for pure potential scattering require the generalization of the Anderson model to include the impurity potential phase shift, independent of the Kondo temperature. This aspect of impurity scattering has not been addressed previously.

states, observed in STM, and the local NMR relaxation rate close to the impurity site.

Consider a local density of electronic states,

$$N(\mathbf{r}, \omega) = -\frac{1}{\pi} \text{Im} g_{11}(\mathbf{r}, \mathbf{r}; \omega + i0^+) \quad (7.8)$$

with the Green's function in real space

$$\widehat{G}(\mathbf{r}, \mathbf{r}'; \omega) = \widehat{G}_0(\mathbf{r} - \mathbf{r}', \omega) + \widehat{G}_0(\mathbf{r}, \omega) \widehat{T}(\omega) \widehat{G}_0(\mathbf{r}', \omega).$$

The local density of states, $N(\mathbf{r}, \omega) = N(\omega) + N_{\text{imp}}(\mathbf{r}, \omega)$, has two contributions. The first, position-independent, is due to bulk delocalized quasiparticles with $E_{\mathbf{k}} = \sqrt{\xi_{\mathbf{k}}^2 + \Delta_{\mathbf{k}}^2}$. Using $g^{(0)}(0, \omega) = \sum_{\mathbf{k}} [u_{\mathbf{k}}^2/(\omega - E_{\mathbf{k}}) + v_{\mathbf{k}}^2/(\omega + E_{\mathbf{k}})]$, where $u_{\mathbf{k}}$ and $v_{\mathbf{k}}$ are the Bogoliubov factors, we find for a superconductor with line nodes, $N(\omega)/N_0 = \omega/\Delta_0$, at $\omega \ll \Delta_0$. The second term,

$$N_{\text{imp}}(\mathbf{r}, \omega) = -\frac{1}{\pi} \text{Im} [\widehat{G}_0(\mathbf{r}, \omega) \widehat{T}(\omega) \widehat{G}_0(\mathbf{r}, \omega)]_{11} \quad (7.9)$$

describes a local change in the DOS due to the virtual bound state created around the impurity site.

In 2D d -wave SC this impurity state is cross-shaped in real space, with long tails extending along the gap nodes as shown in Fig. 4. Consider unitary scattering, for which the resonance is at $E_{\text{imp},n} \equiv \Omega \rightarrow 0$; see Sec. V. As $\text{Im} G^{(0)}(\mathbf{r}, \omega = 0) = -\pi N(\omega = 0) = 0$ for bulk quasiparticles, only the imaginary part of the T-matrix contributes to N_{imp} . The probability density for the bound-state decays quadratically in the distance from the impurity. Along the gap nodes,

$$N_{\text{imp}}(\mathbf{r}, \omega = 0) = \text{Re} [\widehat{G}^{(0)}(\mathbf{r}, \omega = 0)]^2 \propto r^{-2}, \quad (7.10)$$

while in the direction of the maximal gap

$$N_{\text{imp}}(\vec{r}, \omega = 0) \propto \frac{\Delta_0^2}{E_F^2} r^{-2}. \quad (7.11)$$

In addition to the power law asymptotic decay at large distances, there is an additional contribution that decays exponentially with the angle-dependent coherence length of the superconductor $\xi(\varphi) = \hbar v_F / |\Delta(\varphi)|$. This contribution is important for the detailed comparison of the induced LDOS to that measured by STM near the impurity site, since the intensity near impurity is mapped out only within few lattice spacings. For resonance energy away from the Fermi energy the wave functions of the resonance decay exponentially with the characteristic length scale $\hbar v_F / |\Omega_0|$. Detailed discussion of this decay and the particle-hole asymmetry due to impurity potential is given in (Aristov and Yashenkin, 1998; Balatsky and Salkola, 1998).

Gap nodes lead to the power law decay of the wave function along all directions at large distances $r \gg \xi$. This follows from the power counting of the d -wave propagator: $G(\mathbf{r}, \omega \rightarrow 0) \sim \int d^2k \exp(i\mathbf{k} \cdot \mathbf{r}) G(\mathbf{k}, \omega \rightarrow 0) \sim \int k dk \exp(i\mathbf{k} \cdot \mathbf{r}) \frac{v_F k}{k^2} \sim 1/r$. The logarithmically divergent

normalization reflects the fact that the impurity state is virtually bound. At finite impurity concentration the divergence is cut off at the average distance between impurities. For an arbitrary position of the resonance, taking into account that only one state has been produced with $E_{\text{imp},n} = \Omega' + i\Omega''$, we find

$$N_{\text{imp}}(\mathbf{r}, \omega) = \frac{\Omega_i''}{\pi} \sum_i \left[\frac{|u(\mathbf{r} - \mathbf{r}_i)|^2}{(\omega - \Omega_i')^2 + \Omega_i''^2} - \frac{|v(\mathbf{r} - \mathbf{r}_i)|^2}{(\omega + \Omega_i')^2 + \Omega_i''^2} \right]. \quad (7.12)$$

Here the sum is over impurity positions, \mathbf{r}_i , and $u(\mathbf{r} - \mathbf{r}_i)$, $v(\mathbf{r} - \mathbf{r}_i)$ are the eigenfunction of the Bogoliubov-de Gennes equation with an impurity.

Local effects of impurities are best revealed by local probes. NMR experiments on Cu in Zn-doped cuprates are quite useful in this regard. From Eq. (7.10) and below, one concludes immediately that the NMR signal shows two distinct relaxation rates (or even a hierarchy of rates) depending on the distance of the Cu sites from the impurity location. The Cu sites near the impurities couple to the higher LDOS and have a faster relaxation rate at low T . At finite impurity concentration ($\sim 2\%$), the volume-averaged density of states is finite as $\omega \rightarrow 0$, and therefore the relaxation rate of Cu atoms close to and away from an impurity have the same temperature dependence, $(T_1 T)^{-1} = \text{const}$, but are of a different magnitude. Precisely this behavior has been observed experimentally: Ishida *et al.* (Ishida *et al.*, 1991) measured two NMR relaxation rates for Cu in Zn-doped $\text{YBa}_2\text{Cu}_3\text{O}_{7-\delta}$. The second NMR signal with faster relaxation was inferred to arise from the sites near the impurities. Alloul and collaborators pointed out that the NMR signal from the sites close to impurities shows a distribution of relaxation rate, which reflects local electronic and magnetic distortions produced by the impurity in the host system, see (Bobroff *et al.*, 2001) and references therein.

More direct evidence for the impurity induced resonances in high- T_c came from scanning-tunneling microscopy. These experiments were crucial in establishing the existence of the impurity induced resonances in cuprates and their anisotropic nature (Hudson *et al.*, 1999; Pan *et al.*, 2000b), and are discussed in section IX.

We contrast our picture of the dilute limit of strongly scattering centers with the usual approach of averaging over a finite concentration of impurities. In the latter approach the two distinct NMR relaxation rates, arising from inequivalent sites, cannot be resolved. Similarly the inhomogeneous LDOS due to localized states is lost after averaging over impurity positions.

The distinction between the a true bound states and continuum in nodal superconductors is not as well defined as in s -wave systems. Any finite temperature leads to a finite lifetime for the bound states, and they hybridize with the continuum of low-energy extended quasiparticles since the two are not separated by an energy gap.

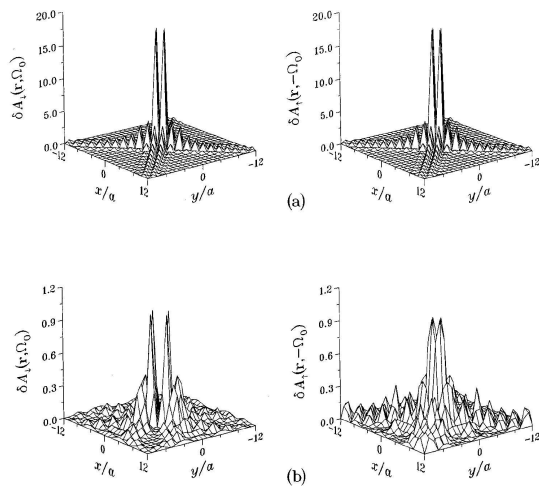


FIG. 4 Illustration of the cross shaped nature of the impurity state. Shown is the spectral density $A_x(\mathbf{r}, \pm\Omega_0)$ as a function of position and spin in units of $N_0\Delta_0$ for a) $\mu = 0$ and b) $\mu = -W$, $2W$ is the bandwidth, in a two-dimensional d-wave superconductor as a function of position around a classical magnetic moment ($N_0J_0 = 10$ and $U_0 = 0$) located at $\mathbf{r} = 0$; a is the lattice spacing. These results are computed self-consistently with $\xi = 10a$. At half filling, the spectral density obeys particle-hole symmetry: $A_\uparrow(\mathbf{r}, \Omega_0) = A_\downarrow(\mathbf{r}, -\Omega_0)$. The energies of the shown virtual-bound states are a) $\Omega_0 = 0.05\Delta_0$ and b) $\Omega_0 = 0.5\Delta_0$. From (Salkola *et al.*, 1997)

B. Single magnetic impurity problem

Full analysis for a magnetic impurity is more involved. For a quantum spin one needs to address the Kondo effect, which is discussed in Sec. XI. In the simplified treatment of a “classical” spin ($S \gg 1$ or $T \gg T_K$) the mean field analysis is similar to that in previous section (Salkola *et al.*, 1997). In that case the main effect of the exchange coupling between the local moment S and electron spin is the renormalization of the effective scattering potential for electrons of two different spin orientations: they see net impurity potential $U_0 \pm J$, where U_0 is the potential scattering strength and J is the exchange coupling to the impurity spin. There are two virtual bound states, one for each electron spin orientation, with the energies,

$$\Omega_{1,2} = -\frac{\Delta_0}{2N_0(U_0 \pm J) \ln |8N_0(U_0 \pm J)|} \quad (7.13)$$

STM data on Ni-doped high- T_c cuprate $\text{Bi}_2\text{Sr}_2\text{CaCu}_2\text{O}_{8+\delta}$ are fit well using this simple formula, see Sec. IX. Even in the classical limit the spin S may have its own dynamics, that was omitted in the mean field approach of Ref. (Salkola *et al.*, 1997). Further studies are certainly desirable.

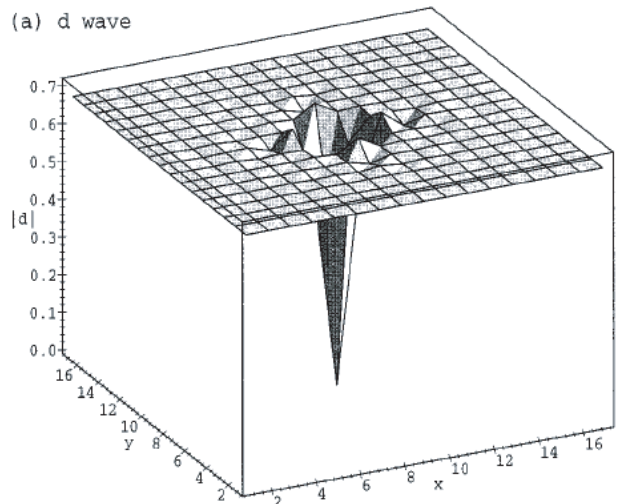


FIG. 5 Self-consistently determined gap function near scalar impurity in a 2D d -wave superconductor. Gap suppression is strongly localized near impurity site aside from weak oscillating tails. From (Franz *et al.*, 1996)

C. Self-consistent gap solution near impurity

Impurity scattering locally modifies the order parameter, and we discuss the self-consistent gap in 2D d -wave systems. To address these effects one has to use the (numerically determined) exact electron spectra near the impurity, and solve the self-consistent equation on the d -wave gap, defined on the bonds of a square lattice,

$$\Delta(i, i + \delta) = \frac{V_{i, i+\delta}}{2} \sum_n [u_n(i + \delta)v_n^*(i) + u_n^*(i)v_n(i + \delta)] \times \tanh\left(\frac{E_n}{2k_B T}\right). \quad (7.14)$$

Such numerical solutions were presented in (Franz *et al.*, 1996; Salkola *et al.*, 1997; Tsuchiura *et al.*, 2000; Zhu *et al.*, 2000a). Impurity scattering clearly suppresses the gap magnitude, and the suppression is the strongest at the impurity site. The gap quickly recovers to a bulk value, although there are oscillating tails at long distances due to $2k_F$ oscillations, as shown in Fig. 5.

Realistically the difference between the self-consistent and the non self-consistent solutions is not important beyond few lattice spacings from the impurity site. Near such a site local gap suppression is clearly seen in the STM data, see Sec. IX.

For superconducting order parameters with complex internal structure there is a possibility that impurity couples to a soft mode other than the amplitude mode (Rainer and Vuorio, 1977). This was investigated for the non-unitary A-phase superconductor by Choi and Muzikar (Choi and Muzikar, 1990), who concluded that an *indirect* coupling to the rotational mode may produce a local magnetic moment around the impurity site.

D. Spin-orbit scattering impurities

Spin-orbit coupling in impurity scattering in superconductors is much less thoroughly investigated than purely magnetic or potential scattering. The standard form of the spin orbit scattering is due to Elliott and Yafet:

$$H_{SOimp} = \sum_{\mathbf{k}, \mathbf{k}'} \lambda_{SO} c_{\mathbf{k}, \alpha}^\dagger \vec{\sigma}_{\alpha\beta} \cdot (\mathbf{k} \times \mathbf{k}') c_{\mathbf{k}'\beta}, \quad (7.15)$$

where λ_{SO} is the scattering strength. This coupling is present even for nonmagnetic impurities, is pairbreaking, and produces additional quasi-bound states inside the gap. The structure of these additional resonances and their response to a Zeeman magnetic field were studied by Grimaldi (Grimaldi, 1999, 2002), who concluded that in the limit of strong SO scattering the local DOS exhibits off-site particle-hole symmetric resonance (in contrast to potential scatterers), which is not split by the field.

In a different type of SO scattering from a magnetic impurity, the impurity spin is coupled to the orbital motion of the conduction electrons. For 2D d -wave systems this was motivated by experiments on Ni doped Bi2212 (Movshovich *et al.*, 1998; Neils and Harlingen, 2002) and studied in (Balatsky, 1998; Barash *et al.*, 1997; Graf *et al.*, 2000). We write the Hamiltonian, $H_{SO,imp} = \gamma_{SO} \hat{\mathbf{L}} \cdot \mathbf{S}$, in second quantized notation:

$$H_{SO,imp} = \sum_{\mathbf{k}, \mathbf{k}'} \gamma_{SO} c_{\mathbf{k}, \sigma}^\dagger \mathbf{S} \cdot (\mathbf{k} \times \mathbf{k}') c_{\mathbf{k}'\sigma}, \quad (7.16)$$

where γ_{SO} is the strength of coupling and \mathbf{S} is the impurity spin. Predominantly in plane motion of electrons (as is the case in Bi2212) couples the angular momentum L_z with respect to the impurity site $\hat{\mathbf{L}}_z = i\hbar\partial_\phi$ to S_z . The net effect of this term is twofold. First, it is pairbreaking, so that the gap is locally suppressed, and a resonance is formed. Even more interesting and nontrivial is the distortion of the $d_{x^2-y^2}$ -wave order parameter in the vicinity of impurity, which results from the nontrivial orbital structure of the d -wave order. This state is a linear combination of the state with $l_z = 2$ and $l_z = -2$, $\Delta(\phi) = \Delta_0 \cos(2\phi) \propto \exp(2i\phi) + \exp(-2i\phi) \sim x^2 - y^2$. The two orbital components are affected differently by scattering. Treating H_{SOimp} perturbatively, one generates in the *first order* the correction to the order parameter $\Delta' = i\Delta_0\gamma_{SO} \sin(2\phi) \sim xy$. There is a finite amplitude for incoming d -wave pair $|in\rangle \propto |x^2 - y^2\rangle$ to scatter into $|out\rangle \propto i|xy\rangle$ channel:

$$|out\rangle = i\gamma_{SO}\Delta_0\hat{\mathbf{L}} \cdot \mathbf{S}|in\rangle = i\hbar\gamma_{SO}\Delta_0 \sin(2\phi), \quad (7.17)$$

generating an out of phase component of the order parameter near an SO impurity, coexisting with and induced by the original $d_{x^2-y^2}$ symmetry.

This illustrated one of the more non-trivial effects of the impurity scattering in superconductors with orbital structure to the Cooper pair wave function. For more details, see (Balatsky, 1998; Graf *et al.*, 2000; Zhu and

Balatsky, 2002). An applied magnetic field (which couples to L_z similarly to the S_z term in Eq. (7.17)), not only suppresses the d -wave order parameter but also produces the secondary d_{xy} component, see (Balatsky, 2000; Franz and Tešanović, 1998; Kuboki and Sigrist, 1998; Laughlin, 1998; Tanuma *et al.*, 1998).

E. Effect of doppler shift and magnetic field

The main effect of the Zeeman field is to split the impurity induced resonances (Grimaldi, 1999, 2002). The orbital effect of magnetic field can be analyzed by considering the Doppler shift of the quasiparticle energy.

In the simplest approach, due to Galilean invariance, in the presence of a superflow with velocity $\mathbf{v}_S(\mathbf{r})$ the electron propagators are modified: $G(\mathbf{k}, \omega) \rightarrow G(\mathbf{k}, \omega - \mathbf{k} \cdot \mathbf{v}_S)$ for a planar wave state at \mathbf{k} . The rest of the calculation for the impurity state follows exactly the previous analysis. The local scattering potential of the impurity means summing over all momenta to obtain local Green's function $G_0(\omega)$, and only this local propagator enters the solution for the resonance, Eq. (7.1). Therefore all the changes in the resonance state are due to the increase in the density of states arising from the Doppler shift.

The effect of the superflow produced by the screening currents on the impurity resonance was studied by Samokhin and Walker, 2001, who pointed out that Doppler shift leads to the broadening of the resonance. The scale of the effect is set by the ratio of the typical Doppler shift $v_S k_F$ at the impurity site to the resonance energy, Ω' . If the Doppler shift is small, the effect is negligible, while in the opposite limit of $v_S k_f \gg \Omega'$ the superflow broadens the resonance significantly. The superflow does not shift the resonance energy.

Tsai and Hirschfeld (Tsai and Hirschfeld, 2002) analysed the effect of an isolated impurity on the penetration depth of a d -wave superconductor, and concluded that it leads to a divergent $1/T$ contribution at finite temperatures, in close analogy to the Andreev bound states (Barash *et al.*, 2000; Walter *et al.*, 1998).

F. Sensitivity of impurity state to details of band structure

Above we used a single band model with particle-hole symmetry to prove the existence and explore the basic features of the impurity induced resonance. Real bands are asymmetric, and the effect of asymmetry was considered by Joynt (Joynt, 1997), who modeled it by a constant DOS with different energy cutoffs at the upper and lower limit. To make a quantitative comparison with the experimental data on impurity resonances, see Sec. IX, we have to understand the details of the band structure. For example, in the cuprates, the in-plane Cu $d_{x^2-y^2}$ and O $p_{x,y}$ bands are relevant. Above we *assumed* that upon the reduction of the complicated band structure of high- T_c (or another material) to a single band model, one can

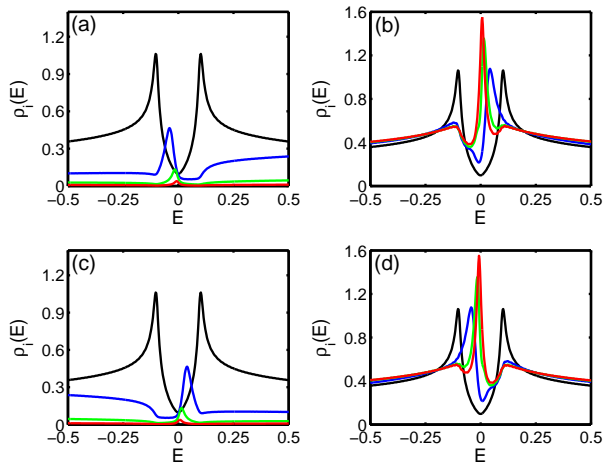


FIG. 6 The LDOS as a function of energy at the impurity site (left panels) and at one of its nearest neighbors (right panels) in a 2D lattice. The upper panels are for repulsive potential, $U_0 = 0$ (black line), 2 (blue line), 5 (green line), and 10 (red line) while the lower panels are for attractive potential, $U_0 = 0$ (black line), -2 (blue line), -5 (green line), and -10 (red line). The band structure parameters are $t = 1$, $t' = 0$, and the chemical potential $\mu = 0$.

still describe nonmagnetic impurity by a single parameter, the on-site potential U_0 . Reality is more complex.

Even within the one band approach one can still explore the change in the position of the impurity-induced resonance beyond the simplest assumptions. The resonance position depends on the sign of the impurity potential, the electron occupation numbers, and the band structure. To illustrate sensitivity to the latter we performed an exact diagonalization for the t - t' - V model with nearest-neighbor hopping t , next nearest neighbor hopping t' , and a negative V that describes the nearest neighbor attraction and produces d -wave pairing. The single particle energy dispersion in the normal state is

$$\xi_k = -2t(\cos k_x + \cos k_y) - 4t' \cos k_x \cos k_y - \mu, \quad (7.18)$$

and μ is the chemical potential. Impurity was modeled by an on-site potential U_0 . We considered three possibilities: (i) $t = 1, t' = 0, \mu = 0$ (the filling factor $n = 1.0$), with band particle-hole symmetry present, Fig. 6; (ii) $t = 1, t' = -0.2, \mu = -0.784$ ($n = 0.84$), with no band particle-hole symmetry, Fig. 7; (iii) $t = 1, t' = -0.3, \mu = -1.0$ ($n = 0.85$), again with band particle-hole symmetry absent, Fig. 8. We refer to the band particle-hole symmetry because the local particle-hole symmetry is broken by the potential U_0 .

As shown in these figures, for the cases (i) and (ii), the band DOS has two coherent peaks. Also for the case (ii), the DOS is asymmetric with respect to the zero energy. In these two situations, a repulsive potential $U_0 > 0$ leads to an impurity state at $\Omega'_0 < 0$, manifested by a peak in the LDOS below the Fermi energy at the impurity site. In contrast, the peaks are above the Fermi energy at the four nearest neighbor sites. Correspondingly, an

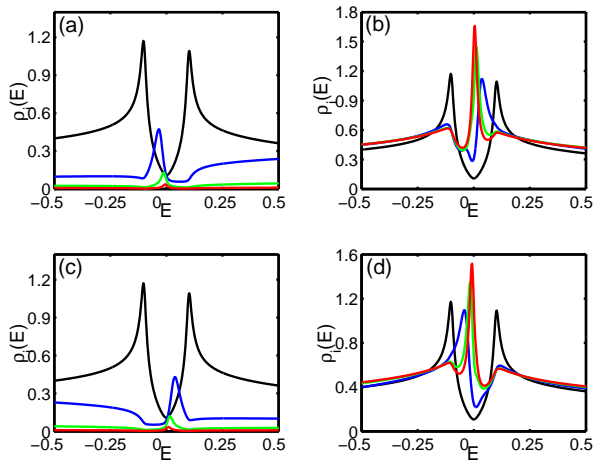


FIG. 7 Same as Fig. 6 for $t = 1$, $t' = -0.2$, and $\mu = -0.784$.

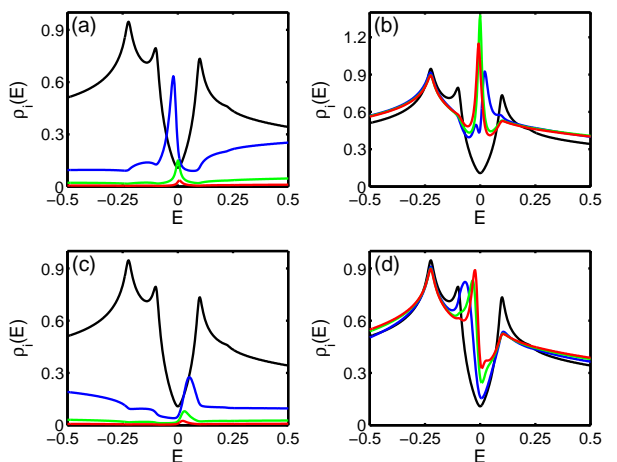


FIG. 8 Same as Fig. 6 for $t = 1$, $t' = -0.3$ and $\mu = -1.0$.

attractive impurity potential $U_0 < 0$ induces a state at $\Omega'_0 > 0$ at the impurity site, but below the Fermi energy at its nearest neighbors.

For the case (iii), in addition to the two coherent peaks, there are also two van Hove singularity peaks (more pronounced on the negative energy side and faint at the positive side). Now for a repulsive impurity, the on-site resonance peak does shift from the negative energy side slightly above the zero energy. This phenomenon is absent for the cases of (i) and (ii). For $U_0 < 0$, the result is similar to the cases (i) and (ii). Here we the optimal doping consider regime for (ii) and (iii). At other dopings all possibilities discussed above could occur depending on band structure.

The sign of the impurity potential for Zn and Ni atoms in cuprates is still an unsettled issue. It is believed that these atoms substitute Cu in the Cu-O plane, and do not change the hole doping. Then Zn^{++} is in d^{10} configuration, and the third ionization energy is a rough measure of the impurity potential, U_0 (even though the

Cu d -orbitals form a band). By comparing the energies of Cu atom $E_{Cu^{++}} = -36.83$ eV, and Zn atom $E_{Zn^{++}} = -39.722$ eV, we estimate $U_0 \simeq -2.89$ eV. Therefore, Zn atom plays the role of a strong attractive potential in Cu-O lattice. Location of the level at negative energy is consistent with the d^{10} configuration.

Ni^{++} has a $3d^8$ shell, and a spin $S = 1$ ground state. Therefore, to describe the effect of Ni impurity we need to account for both potential (U_0) and magnetic (J) scattering. We again estimate the energy U_0 by taking the difference between atomic energies using $E_{Ni^{++}} = -35.17$ eV to find $U_0 \simeq 1.66$ eV for Ni. Compared to Zn, its potential is weaker and repulsive. Similar conclusions about the sign and strength of Zn and Ni impurities were reached recently in a more sophisticated three-band model (Xiang *et al.*, 2002).

For detailed comparison of the results from model calculations with the experimental data, the band structure effects need to be well understood. Ultimately we need a realistic band structure calculations with impurities for these complex materials.

VIII. SINGLE IMPURITY BOUND STATE IN A PSEUDOGAP STATE OF TWO-DIMENSIONAL METALS

A. General remarks on impurities in a pseudogap state

A natural question to address is whether superconductivity, or even any off-diagonal long range order are required for a resonance state, and we address this in the experimentally relevant context of the cuprates. Many experiments (Loram *et al.*, 2000; Norman *et al.*, 1998; Renner *et al.*, 1998) show that in high- T_c systems the electronic density of states near the Fermi surface is suppressed above the superconducting transition temperature T_c , but below a characteristic temperature T^* . The energy range of this suppression, Δ_{PG} , is known as the pseudogap (PG), and its origin is hotly debated, see (Timusk, 2003; Timusk and Statt, 1999). Scenarios for this anomalous phenomenon include precursors to superconductivity, such as pre-formed pair with phase-fluctuations (Emery and Kivelson, 1995), Bose-Einstein condensation of Cooper pairs (Chen *et al.*, 1998), as well as various competing orders not related to superconductivity, such as the time-reversal-symmetry-breaking circulating current (Varma, 1999), and unconventional d -density-wave (DDW) (Chakravarty *et al.*, 2001). The latter is a variant of the staggered flux state (Affleck and Marston, 1988; Hsu *et al.*, 1991; Marston and Affleck, 1989). In the first scenario, the “normal” state contains preformed Cooper pairs, but the phase fluctuations of the pairing field destroy the long range order, that is, the bulk superconductivity. Since at the onset the pairing field has d -wave symmetry in the momentum space, a d -wave pseudogap follows.

Here, instead of discussing the origin of the PG, we model it phenomenologically in some of these scenarios,

and study the electronic properties around a single impurity. If an STM measurement is done at different temperatures, there are two possibilities for the evolution of impurity resonance at $T > T_c$: a) it gradually broadens and disappears when the superconductivity vanishes, as in conventional superconductor; and b) the resonance broadens but survives above in the PG state. It was argued experimentally (Krasnov *et al.*, 2000; Loram *et al.*, 2000) that in the underdoped cuprates the superconducting gap and PG are separate phenomena, and we show below that in this case the resonance survives above T_c . We find that its position and width of the depend on both the impurity scattering strength and the PG energy scale.

Our simplest model of the (unrelated to superconductivity) pseudogap is a metallic state with linearly vanishing DOS around the Fermi energy, but no off-diagonal order, see Fig. 9. This simplification allows analytical calculations, and provides a “reference point” for the impurity state in the PG regime. Once again we focus on the Zn substitution for Cu, and use the T -matrix approach. We find that the depletion of the DOS alone is sufficient to produce a resonance near a nonmagnetic impurity.

The analysis is quite general, and is similar to that of Sec.V and (Balatsky *et al.*, 1995). The states generated by the impurity are given by the poles, Ω , of the T matrix:

$$g_0(\Omega) = \frac{1}{U_0}. \quad (8.1)$$

This is an implicit equation for $\Omega(U_0)$, and complex solutions indicate the resonant nature of the state. To solve it, we need the unperturbed local Green’s function on the impurity site, $g_0(E) = g'_0 + ig''_0$, where the imaginary part, $g''_0(\omega) = -\pi N_0(\omega)$, and $N_0(\omega)$ is the bulk DOS.

Measurements of the electronic specific heat by Loram *et al.* (Loram *et al.*, 2000) show that the pseudo gap opens below hole doping $p_{crit} \sim 0.19$ holes/CuO₂, and has a V-shape energy profile. Guided by these data, we assume that the low energy electronic states are partially depleted, so that $N_0(\omega) = N_0|\omega|/\Delta_{PG}$ for $|\omega| \leq \Delta_{PG}$, and $N_0(\omega) = N_0$ for $\Delta_{PG} < |\omega| < W/2$ with W the bandwidth, see Fig. 10(a). We use this DOS to generate solutions of Eq. (8.1). Clearly, the precise position and the width of the resonance depend on the specific form chosen for $N(\omega)$ (in our case linear). Results for other forms of $N(\omega)$ are very similar.⁴

Using this DOS for g''_0 and invoking the Kramers-

⁴ We argue that the appearance of the intragap impurity state is a robust feature of any depleted DOS around the Fermi surface. We considered a model with $N_0(\omega) = N_0[a + (1-a)\omega^2/\Delta_{PG}^2]$, which to a similar resonant state at $\Omega = -\Delta_{PG}(1 + i\pi a N_0 U_0)/(4N_0 U_0(1-a - \Delta_{PG}/W)) \approx -\Delta_{PG}(1 + i\pi a N_0 U_0)/(4N_0 U_0(1-a))$ when $\Delta_{PG}/W \ll 1$. For a fully gapped DOS, $N(\omega) = N_0$ for $|\omega| \in [\Delta_{PG}, W/2]$ and zero otherwise, the resonant state is at $\Omega = -\Delta_{PG}/(2U_0 N_0)$.

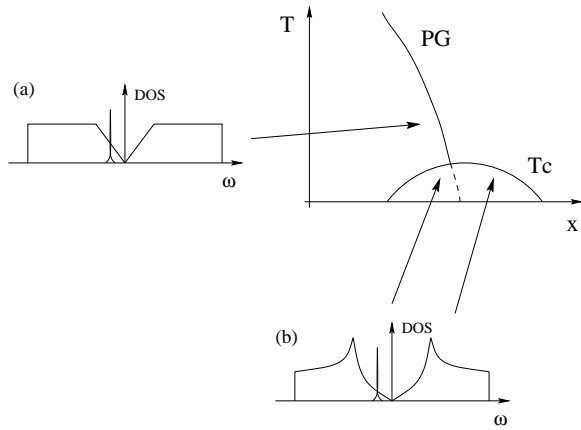


FIG. 9 An impurity state in a high T_c superconductor: (a) The DOS in the pseudogap regime used in this article (see also [11]) and (b) the DOS in the superconducting state as was used in [1]. In both phases there is a resonant state.

Kronig relation, see e.g. (Mahan, 2000),

$$g'_0(\omega) = \frac{1}{\pi} \int_{-\infty}^{\infty} d\omega' g''_0(\omega') P \left(\frac{1}{\omega' - \omega} \right), \quad (8.2)$$

with P the Cauchy's principal value, we find

$$g'_0(\omega) = -N_0 \ln \left| \frac{\frac{W}{2} - \omega}{\frac{W}{2} + \omega} \right| + N_0 \ln \left| \frac{\Delta_{PG} - \omega}{\Delta_{PG} + \omega} \right| - N_0 \frac{\omega}{\Delta_{PG}} \ln \left| \frac{\Delta_{PG}^2 - \omega^2}{\omega^2} \right|. \quad (8.3)$$

Fig. 10(b) shows $g'_0(\omega)$ together with $1/U_0$ to obtain a graphical solution as in Fig.3. For $2U_0N_0 > 1$, Eq. (8.1) has four solutions. Since the width of the resonance is proportional to $|\Omega|$, only the solutions with $|\Omega|$ close to zero are sharp. Expanding in ω in Eq. (8.3) we find

$$g_0(\Omega) = -\frac{2\Omega N_0}{\Delta_{PG}} \left[\ln \left| \frac{\Delta_{PG}}{\Omega} \right| + 1 - \frac{i\pi \operatorname{sgn}(U_0)}{2} \right] = \frac{1}{U_0}, \quad (8.4)$$

This equation can be solved exactly in terms of Lambert's W functions,⁵ which, to logarithmic accuracy in

$\ln |2U_0N_0| > 1$, gives $\Omega = \Omega' + i\Omega''$ with⁶

$$\Omega' = -\frac{\Delta_{PG}}{2U_0N_0} \frac{1}{\ln |2U_0N_0|} \left[1 - \frac{1}{\ln |2U_0N_0|} \right], \quad (8.5)$$

$$\Omega'' = -\frac{\pi \Delta_{PG} \operatorname{sgn}(U_0)}{4U_0N_0 \ln^2 |2U_0N_0|}. \quad (8.6)$$

Here Ω' is the energy position and Ω'' the decay rate.

Using Eq.(8.5) for Zn doping in the cuprates, and taking $N_0 = 1$ state/eV, $\Delta_{PG} \sim 300\text{K} \sim 30\text{meV}$ and the scattering potential $U_0 \approx \pm 2\text{eV}$, we estimate $\Omega \sim \pm 2\text{meV} \sim \pm 20\text{K}$ as was found by Loram *et al.* (Loram *et al.*, 2000). This value is close to the Zn resonance energy $\omega_0 = -16\text{K}$, seen in the superconducting state (Pan *et al.*, 2000b). By combining these results with the band-structure arguments (Martin *et al.*, 2002), we conclude that the Zn impurity in Bi2212 is strongly attractive, with $U_0 \sim -2\text{eV}$. This value, as we see below, is modified due to the particle-hole asymmetry expected in the doped cuprates.

A similar calculation can be done in the absence of particle-hole symmetry. The simplest way to introduce the asymmetry is by making the upper and lower cut-offs in the DOS different, i.e. keep the bare density of states featureless, but move the chemical potential, μ , away from the middle of the band. The pseudogap is still centered at the chemical potential. Therefore the calculation proceeds as above with sole change in the first logarithmic term of Eq. (8.3):

$$-N_0 \ln \left| \frac{\frac{W}{2} - \mu - \omega}{\frac{W}{2} + \mu + \omega} \right| \quad (8.7)$$

Neglecting the frequency ω relative to chemical potential μ and assuming that μ is small relative to the bandwidth, we find that the asymmetric case can be mapped onto the symmetric situation by the substitution

$$\frac{1}{U_0} \rightarrow \frac{1}{U_0} - \frac{4N_0\mu}{W}. \quad (8.8)$$

The effect of the asymmetry can be estimated. In cuprates, for 20% hole doping, $\mu \sim -(1/5)W/2 = -W/10$. Hence, the modified value for the Zn impurity strength in Bi2212 can be obtained from the symmetric result, $1/U^* = 1/U_0 + 4N_0\mu/W$. The new value is $U^* \sim -1$ eV, which is a strongly attractive potential, as is expected from the band structure arguments.

The solution for the resonance state involves determining the energy position and the width of the resonance, as well as the real space shape of the impurity state. The energy of the resonance for a local impurity potential,

⁵ The exact solution in terms of a Lambert's W function, $Lw(-1, x)$, defined from $Lw(x) \exp[Lw(x)] = x$, is $\Omega = -\Delta_{PG} \operatorname{sgn}(U_0) \exp\{Lw(-1, -\operatorname{sgn}(U_0) \exp(i\pi/2 - 1)/(2N_0U_0)) + 1 - i\pi/2\}$.

⁶ The simplest model for thermal broadening is to assign the temperature dependent width: Thermal broadening at high temperatures $T > T_c$ substantially broadens the impurity resonance peak $\Omega''(T) = \sqrt{(\Omega''(T=0))^2 + T^2}$.

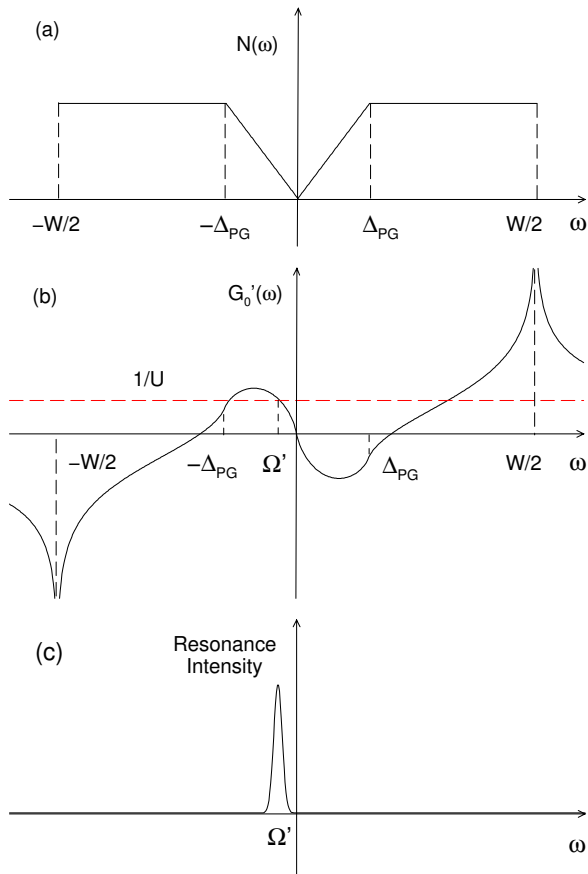


FIG. 10 (a) The density of states $N(\omega) = -g_0''(\omega)/\pi$ for the model discussed in text. (b) The real part $g_0'(\omega)$ of Green's function together with $1/U_0$ and U_0 positive. Ω' is the real part of the solution of the equation $g_0(\Omega) = 1/U_0$. (c) The impurity induced resonance at $\Omega' = -\Delta_{PG}/2U_0N_0 \ln(2U_0N_0)$. The other three solutions of Eq. (8.1) are much broader, and are not depicted. All the plots are at the impurity site. From Kruis, Martin and Balatsky (Kruis *et al.*, 2001)

U_0 , depends only on the local propagator $g_0(\omega)$. Hence the knowledge of the DOS (related to the imaginary part of the on-site propagator) is sufficient to determine (via Kramers-Kronig relations) the real part of g_0 , and find the energy of the impurity state. On the other hand, to determine the real space image of the resonance, one requires a more detailed knowledge of the state and its the Green's function. Quite generally, for a d -wave-like PG with nearly nodal points along the $(\pm\pi/2, \pm\pi/2)$ directions, the impurity resonance is four-fold symmetric, similar to superconducting solutions (Balatsky *et al.*, 1995). However, any detailed calculation requires a more specific model for the PG state. Some of these are considered below.

B. Impurity state in pseudogap models

a. D-density wave (DDW). This model postulates the mean field Hamiltonian (Chakravarty *et al.*, 2001)

$$H_0 = \sum_{ij,\sigma} [-t_{ij} + (-1)^i i W_{ij}] c_{i\sigma}^\dagger c_{j\sigma} - \mu \sum_{i,\sigma} c_{i\sigma}^\dagger c_{i\sigma}. \quad (8.9)$$

with the order parameter W_{ij} defined at the bonds of a square lattice, $W_{i,i\pm\hat{x}} = W_{\pm\hat{x}} = \frac{W_0}{4}$ and $W_{i,i\pm\hat{y}} = W_{\pm\hat{y}} = -\frac{W_0}{4}$, and zero otherwise. The prefactor $i = \sqrt{-1}$ indicates that the DDW state breaks the time reversal symmetry. In the momentum space,

$$H_0 = \sum_{k,\sigma} \xi_k c_{k\sigma}^\dagger c_{k\sigma} + \sum_{k,\sigma} i W_k [c_{k\sigma}^\dagger c_{k+Q,\sigma} - c_{k+Q,\sigma}^\dagger c_{k\sigma}]. \quad (8.10)$$

We take the single particle energy ξ_k from Eq. (7.18) with $t' = 0$ for simplicity. For k_x and k_y in the first Brillouin zone, the DDW gap is d -wave-like,

$$W_k = \frac{W_0}{2} (\cos k_x - \cos k_y). \quad (8.11)$$

DDW order breaks the symmetry with respect to translations by a lattice constant, a , along x or y , but preserves translations by $\sqrt{2}a$ along the diagonals of the square lattice. Therefore it is convenient to rewrite the Hamiltonian in the reduced Brillouin zone. Introducing a two-component operator $\Psi_{k\sigma}^\dagger = (c_{k\sigma}^\dagger, c_{k+Q,\sigma}^\dagger)$ with $Q = (\pi, \pi)$, we find

$$H_0 = \sum_{k \in rBZ, \sigma} \Psi_{k\sigma}^\dagger \begin{pmatrix} \xi_k & i2W_k \\ -2iW_k & \xi_{k+Q} \end{pmatrix} \Psi_{k\sigma}, \quad (8.12)$$

where rBZ denotes the reduced Brillouin zone.

In analogy to the Gor'kov-Nambu notation, we introduce the matrix Green functions (cf. Sec.II.C)

$$\hat{\mathcal{G}}^{(0)}(k; \tau) = \begin{pmatrix} \mathcal{G}_{11}^{(0)} & \mathcal{G}_{12}^{(0)} \\ \mathcal{G}_{21}^{(0)} & \mathcal{G}_{22}^{(0)} \end{pmatrix}, \quad (8.13)$$

where

$$\mathcal{G}_{11}^{(0)}(k; \tau) = -\langle T_\tau [c_{k\sigma}(\tau) c_{k\sigma}^\dagger(0)] \rangle, \quad (8.14a)$$

$$\mathcal{G}_{12}^{(0)}(k; \tau) = -\langle T_\tau [c_{k\sigma}(\tau) c_{k+Q,\sigma}^\dagger(0)] \rangle, \quad (8.14b)$$

$$\mathcal{G}_{21}^{(0)}(k; \tau) = -\langle T_\tau [c_{k+Q,\sigma}(\tau) c_{k\sigma}^\dagger(0)] \rangle, \quad (8.14c)$$

$$\mathcal{G}_{22}^{(0)}(k; \tau) = -\langle T_\tau [c_{k+Q,\sigma}(\tau) c_{k+Q,\sigma}^\dagger(0)] \rangle. \quad (8.14d)$$

From the Hamiltonian Eq. (8.12), using equation of motion for the operators $c_{k\sigma}$ and $c_{k\sigma}^\dagger$, and by performing a Fourier transform with respect to τ , we find

$$\hat{\mathcal{G}}^{(0)}(k; i\omega_n) = \begin{pmatrix} i\omega_n - \xi_k & -2iW_k \\ 2iW_k & i\omega_n - \xi_{k+Q} \end{pmatrix}^{-1}. \quad (8.15)$$

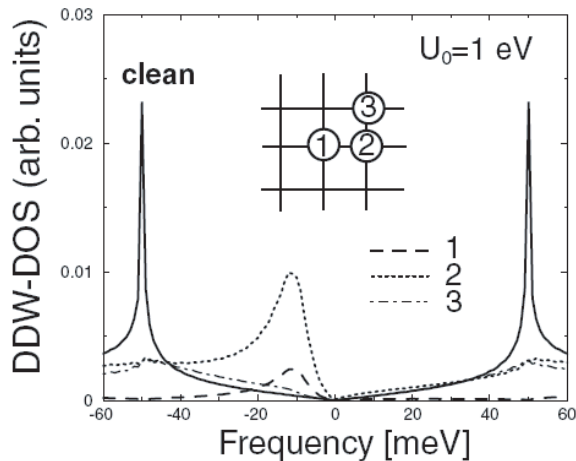


FIG. 11 DDW-DOS for the clean case (solid line) and in the presence of a non-magnetic impurity with $U_0 = 1$ eV: (1) DOS on the impurity site, (2) DOS on the nearest-neighbor site, and (3) DOS on the next-nearest-neighbor site. The other parameter values are: $t = 300$ meV, $W_0 = 25$ meV, $t' = 0$, and $\mu = 0$. From Morr (Morr, 2002).

To solve for the bound state we need the Green's function in real space,

$$\mathcal{G}^{(0)}(i, j; i\omega_n) = \frac{1}{N} \sum_{k \in rBZ} e^{i\mathbf{k} \cdot \mathbf{R}_{ij}} [\mathcal{G}_{11}^{(0)}(k; i\omega_n) + \mathcal{G}_{22}^{(0)}(k; i\omega_n) + e^{-i\mathbf{Q} \cdot \mathbf{R}_j} \mathcal{G}_{12}^{(0)}(k; i\omega_n) + e^{i\mathbf{Q} \cdot \mathbf{R}_i} \mathcal{G}_{21}^{(0)}(k; i\omega_n)]$$

where \mathbf{R}_i are the lattice vectors and $\mathbf{R}_{ij} = \mathbf{R}_i - \mathbf{R}_j$. From Eqs. (8.15)-(8.16), the local Green's function is

$$\mathcal{G}^{(0)} = \frac{1}{N} \sum_{k \in rBZ} \frac{2i\omega_n - \xi_{k+Q} - \xi_k}{(i\omega_n - \xi_k)(i\omega_n - \xi_{k+Q}) - 4W_k^2}. \quad (8.17)$$

We analyze now the scattering on a single non-magnetic impurity in the DDW state. Without loss of generality, hereafter we assume that the impurity is located at the origin. The poles of the T -matrix give the energy of resonance state, i.e. once again

$$\mathcal{G}^{(0)}(0, 0; \omega + i0^+) = \frac{1}{U_0}. \quad (8.18)$$

The real space map of the resonant states is manifested in the local density of states:

$$N_i(\omega) = -\frac{2}{\pi} \text{Im} \mathcal{G}(i, i; \omega + i\delta). \quad (8.19)$$

The numerical results are displayed in Figs. 11 and 12. As shown in these figures, the electronic excitation spectrum around the impurity in the DDW state is very sensitive to the band structure. For $t' = 0$ and at the half filling ($\mu = 0$), the electron density of states of a pure DDW system vanishes at the Fermi energy. Therefore in

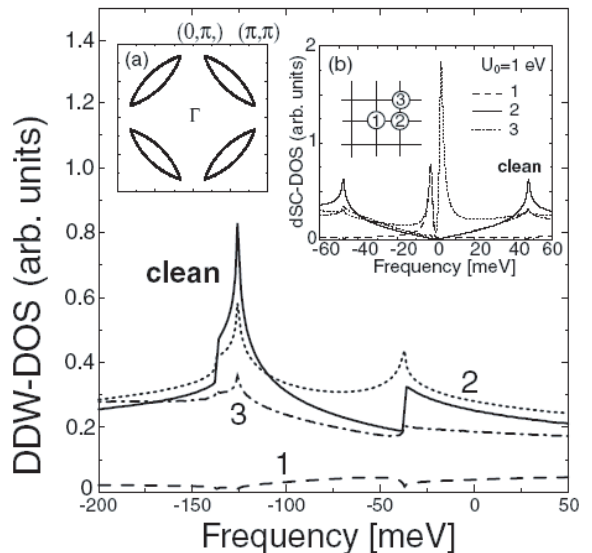


FIG. 12 (a) Fermi surface in the DDW state with $t' = -0.3t$, $\mu = -0.91t$ (hole-doping of 10%) and $W_0 = 25$ meV. The hole pockets are centered around $(\pm\pi/2, \pm\pi/2)$. (b) DOS in the DDW state with the same band parameters as in (a), for the clean case (solid line) and in the presence of a non-magnetic impurity with $U_0 = 1$ eV: (1) DOS on the impurity site, (2) DOS on the nearest-neighbor site, and (3) DOS on the next-nearest-neighbor site. Inset: SC DOS for the same band parameters as in (a). From Morr (Morr, 2002)

the presence of an impurity, resonance states appear at low energies. With $t' = 0$ but the system doped away from the half filling, the resonant peak in the LDOS is shifted away from the Fermi energy. This is because the energy at which the band DOS vanishes no longer coincides with the Fermi energy. For more realistic parameter values, the density of states in the clean limit shows essentially no reduction at low energies, and the LDOS near the impurity does not exhibit any signature of a resonance state. These results were independently obtained by Zhu *et al.* (Zhu *et al.*, 2001), Wang (Wang, 2002), and Morr (Morr, 2002). The quasiparticle states in the DDW state with a finite concentration of non-magnetic impurities were investigated by Ghosal and Kee (Ghosal and Kee, 2004).

b. Phase-fluctuation scenario: We now discuss the impurity state in a phase-fluctuating superconductor, see (Wang, 2002) for details. The mean field Hamiltonian for a d -wave superconductor on a square lattice is

$$H = \sum_{ij} \Psi_i^\dagger \begin{pmatrix} -t_{ij} - \mu\delta_{ij} & -\Delta_{ij} \\ -\Delta_{ij}^* & -(t_{ji} - \mu\delta_{ij}) \end{pmatrix} \Psi_j, \quad (8.20)$$

where $\Psi_i^\dagger = (c_{i\uparrow}^\dagger, c_{i\downarrow})$ is the Nambu spinor, Δ_{ij} is defined on the bonds in analogy to Sec. VII.C, and its phase is allowed to fluctuate, while its amplitude is fixed,

$$\Delta_{ij} = \frac{\Delta_0 \eta_{ij}}{4} e^{i\varphi_{ij}} = \tilde{\Delta}_{ij} e^{i\varphi_{ij}}. \quad (8.21)$$

For d -wave pairing $\eta_{ij} = 1$ (-1) for x (y) direction bonds and the phase $\varphi_{ij} = (\varphi_i + \varphi_j)/2$. Spatial variation of the phase gives rise to the superfluid flow of the Cooper pairs. By performing a gauge transformation,

$$\tilde{\Psi}_i = e^{-i\varphi_i\sigma_3/2}\Psi_i \quad (8.22)$$

where σ_3 is the Pauli matrix, we transfer the phase from the pairing field to the hopping, t , so that

$$\tilde{H} = \sum_{ij} \tilde{\Psi}_i^\dagger \begin{pmatrix} -\tilde{t}_{ij} - \mu\delta_{ij} & -\tilde{\Delta}_{ij} \\ -\tilde{\Delta}_{ij}^* & -(-\tilde{t}_{ji} - \mu\delta_{ij}) \end{pmatrix} \tilde{\Psi}_j, \quad (8.23)$$

where $\tilde{t}_{ij} = t_{ij}e^{-i(\varphi_i - \varphi_j)/2}$. Assuming that the length scale of the phase variation (the London penetration depth) is much greater than the Fermi wavelength, we can define the phase for the Cooper pair, $\varphi_i = 2\mathbf{q}_s \cdot \mathbf{R}_i$, where \mathbf{q}_s is the average momentum per electron in the superfluid state. This ansatz gives the Green function

$$\hat{\mathcal{G}}^{(0)}(\mathbf{k}; q_s; i\omega_n) = \begin{pmatrix} i\omega_n - \xi_{\mathbf{k}+q_s} & -\Delta_{\mathbf{k}} \\ -\Delta_{\mathbf{k}}^* & i\omega_n + \xi_{\mathbf{k}-q_s} \end{pmatrix}^{-1}, \quad (8.24)$$

for a pure systems, where $\Delta_{\mathbf{k}} = \frac{\Delta_0}{2}(\cos k_x - \cos k_y)$ and the $\xi_{\mathbf{k}}$ is still given by Eq. (7.18).

In the presence of a non-magnetic impurity at site $i = (0, 0)$, the Green function becomes

$$\hat{\mathcal{G}}(i, j; q_s; i\omega_n) = \hat{\mathcal{G}}^{(0)}(i, j; q_s; i\omega_n) + \hat{\mathcal{G}}^{(0)}(i, 0; q_s; i\omega_n) \times \hat{T}(q_s; i\omega_n) \hat{\mathcal{G}}^{(0)}(0, j; q_s; i\omega_n), \quad (8.25)$$

$$\hat{T}^{-1}(i\omega_n; \mathbf{q}_s) = \hat{\tau}_3/U_0 - \hat{\mathcal{G}}^{(0)}(0, 0; q_s; i\omega_n). \quad (8.26)$$

For a fixed \mathbf{q}_s , the LDOS at site i is given by

$$N(i; q_s; \omega) = -(2/\pi)\text{Im}\mathcal{G}_{11}(i, i; q_s; \omega + i0^+). \quad (8.27)$$

Averaging over the fluctuating phases in Δ_{ij} is equivalent to taking an average over \mathbf{q}_s . If the fluctuations are thermal, the statistical distribution of \mathbf{q}_s is Gaussian, as in the Kosterlitz-Thouless (KT) theory (Kosterlitz and Thouless, 1973, 1974; Sheehy *et al.*, 2001), $\rho(q_s) = e^{-q_s^2/2n_v} / \sum_{q_s} e^{-q_s^2/2n_v}$, where $n_v = \exp[-\sqrt{aT_c}/(T - T_c)]$ is the vortex concentration. In the continuum limit, $\sqrt{\langle q_s^2 \rangle} = \sqrt{n_v}$. The averaged LDOS is calculated as $N(i; \omega) = \langle N(i; q_s; \omega) \rangle$.

The results are shown in Fig. 13. For small n_v , the resonance peak is sharp and similar to that in the superconducting state ($n_v = 0$). As n_v is increased, the peak is broadened and its height is reduced until the spectrum at low energies becomes featureless.

We can therefore compare the predictions of different models. In the phase fluctuation scenario, the electron excitation spectrum around the impurity is very sensitive to how far the temperature is from the actual T_c . In contrast, in the normal-state ordering scenario, the resonance states are not sensitive to the temperature up

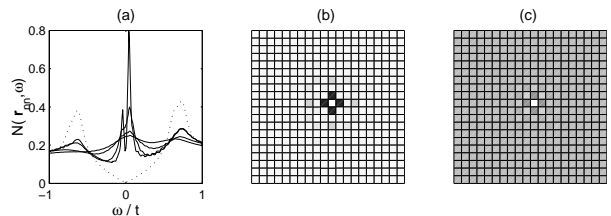


FIG. 13 Local density of states with $\Delta_0 = 0.68t$, $\mu = -0.3t$, $t' = 0$ and $U_0 = 100t$. (a) $N(\mathbf{r}_{nn}, \omega)$ versus ω . Solid lines: $n_v = 10^{-6}, 10^{-4}, 10^{-3}$, and 5×10^{-3} with decreasing peaks. The dotted line is the LDOS at $n_v = 0$ and $U_0 = 0$ for comparison. (b) $N(\mathbf{r}, 0.05t)$ at $n_v = 0$. The impurity is at the center. (c) The same as (b) for $n_v = 5 \times 10^{-3}$. The gray scale is the same in (b) and (c). From Wang (Wang, 2002).

to the closing of the pseudogap. Notice that the energy of the resonance state in the phase fluctuation scenario is not sensitive to the doping while in the state with a normal (particle-hole) ordering it shifts with the doping. Generally, if superconducting fluctuations are present, a satellite peak appears at the opposite bias due to the particle-hole nature of the Bogoliubov quasiparticles. The relative magnitude of the particle and the hole parts of the impurity spectrum can be used to determine the extent to which the PG is governed by the superconducting fluctuations. For fully non-superconducting PG (e.g., the DDW state), there is no counterpart state. Combined with other proposals (Janko *et al.*, 1999; Martin and Balatsky, 2000), study of the impurity resonances can help to better understand the mysterious PG state.

IX. SCANNING TUNNELING MICROSCOPY RESULTS

A. STM results around a single impurity

Experimental attempts to detect and accurately resolve the sub-gap features in the density of states in superconductors with impurities have a long history. Their signatures were found early on in the planar junctions doped with magnetic impurities (Dumoulin *et al.*, 1975, 1977), but a direct observation using scanning tunneling spectroscopy (STS) only became possible in late 1990's. Yazdani and co-workers (Yazdani *et al.*, 1997) deposited adatoms, Mn, Gd and Ag, on the (110)-oriented surface of a superconducting Nb sample, and examined the electronic structure around them. Figure 14 shows the tunneling spectra. The main findings are: (1) The local density of states is essentially identical in the vicinity of Ag impurity atoms and far away from them. This is consistent with the belief that Ag is non-magnetic; (2) Near magnetic Mn and Gd atoms the LDOS is enhanced at the length scale of 10\AA , at energies below the Nb superconducting gap, indicating that the impurity states are bound; (3) The LDOS spectra are asymmetric about the Fermi energy. Within the BdG theory, the authors used a two-parameter magnetic impurity model, where the elec-

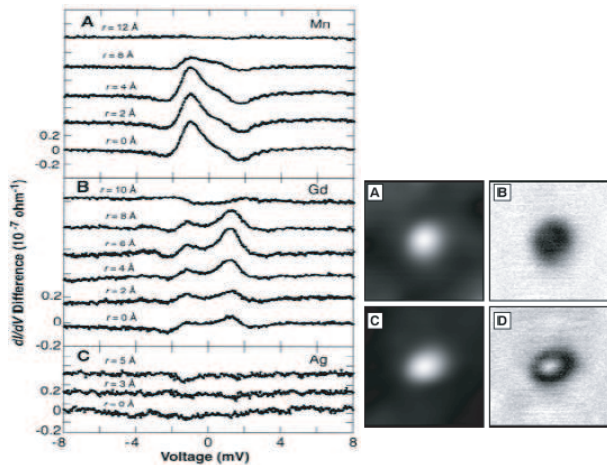


FIG. 14 Left panel: The dI/dV spectra measured near (A) Mn, (B) Gd, and (C) Ag atoms and far away from the impurity. Right panel: Constant-current topographs and simultaneously acquired dI/dV images show the spatial extent of the bound state near Mn and Gd adatoms. (A) Constant-current (32 \AA by 32 \AA) topograph of a Mn adatom. (B) Image of dI/dV near the Mn adatom, acquired simultaneously with the topograph in (A). Reduced dI/dV (dark areas) marks the bound state. The contrast is reversed because dc bias voltage was chosen well above the energy of the bound state, and the resonance affects dI/dV only indirectly. (C) Constant-current (32 \AA by 32 \AA) topograph of a Gd adatom. (D) Image of dI/dV near the Gd adatom, acquired simultaneously with the topograph in (C). From Yazdani (Yazdani *et al.*, 1997).

trons are coupled with the impurity both through a magnetic exchange interaction J and a nonmagnetic potential scattering U . The obtained results were consistent with the Yu-Shiba-Rusinov prediction and more recent theories (Yazdani *et al.*, 1997), and fit the experimental data. However, the model calculation required the value of J of the order of 4 eV, in the strong coupling limit, and failed to capture the detailed spatial dependence of the spectra around Gd site.

Byers, Flatte, and Scalapino (Byers *et al.*, 1993) were the first to suggest the use of STM to study the local effects of impurities in the superconducting state. Balatsky and co-workers predicted (Balatsky *et al.*, 1995; Salkola *et al.*, 1996) that quasiparticle resonance states are induced around a nonmagnetic impurity in a d -wave superconductor, in striking contrast to s -wave systems. The pioneering STM experiments to test these predictions were carried out in the nominally pure samples of the high- T_c cuprate $\text{Bi}_2\text{Sr}_2\text{CaCu}_2\text{O}_{8+\delta}$ (BSCCO) by the groups of Eigler (Yazdani *et al.*, 1999) and Davis (Hudson *et al.*, 1999). The STM spectra clearly showed the enhancement of the local density of states near the zero bias near the chemically induced defects. These experiments provided strong evidence for the existence of low-energy quasiparticle resonance states around single nonmagnetic impurities, as predicted theoretically. The asymmetry or splitting of the measured resonance was conjectured

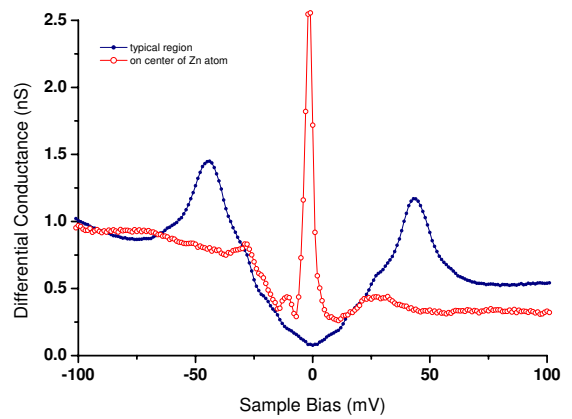


FIG. 15 Differential tunneling spectra taken at the Zn-atom site (open circles) and a location far away from the impurity (filled circles). Note that even on the impurity site one has peaks at both positive and negative bias albeit of very different magnitude that are reflection of the particle hole character of the impurity resonance. To fit the data one can use a simple potential scattering model with essentially unitary scattering phase shift $\theta = 0.48\pi$. Phase shift is related to a impurity potential U_0 via simple formula: $\cot \theta = \frac{1}{\pi N_F U_0}$. From Pan *et al.* (Pan *et al.*, 2000b).

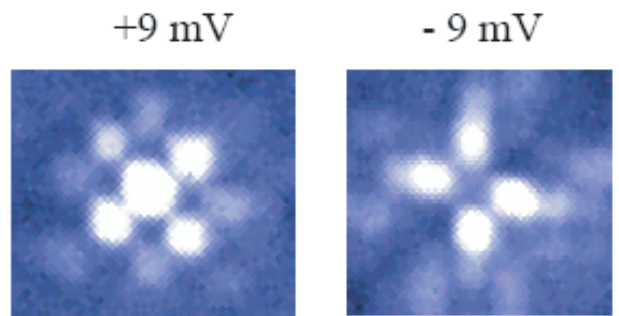


FIG. 16 Differential conductance spectra above the Ni atom and at several nearby locations. Differential conductance spectra obtained at four positions near the Ni atom showing the maxima at $eV = \pm\Omega_1$. Intensity as a function of position relative to impurity site reverses upon change of the bias sign. This effect is explained as a result of particle and hole components of the impurity state. From Hudson *et al.* (Hudson *et al.*, 2001).

to result from breaking of the particle-hole symmetry by the defects locally or from the asymmetry of the underlying realistic band structure of BSCCO (Flatte and Byers, 1998; Zhu *et al.*, 2000a). However, in these experiments, the location in the crystal and the identity of these scattering centers were unknown. Moreover, since the enhancement of the LDOS at these scattering centers is not large, and since the coherence of high- T_c superconductors is short, it was difficult to investigate in detail the LDOS at the atomic scale.

STM studies on the $\text{Bi}_2\text{Sr}_2\text{Ca}(\text{Cu}_{1-x}\text{Zn}_x)_2\text{O}_{8+\delta}$ single crystals intentionally doped with $x = 0.6\%$ Zn were re-

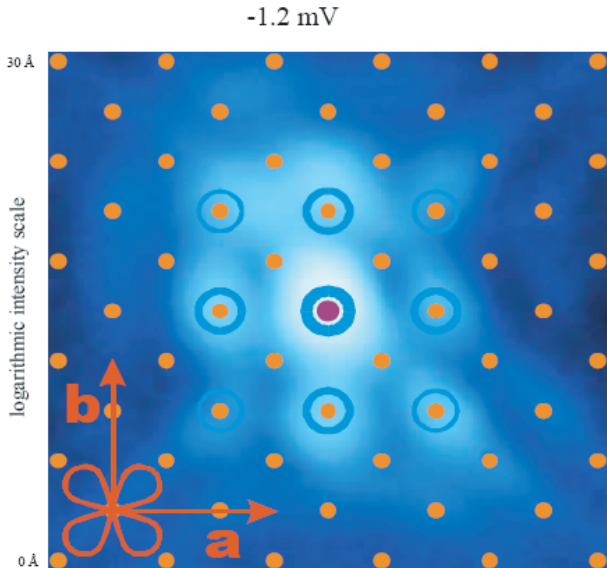


FIG. 17 High-spatial-resolution image of the differential tunneling conductance at a negative tip voltage bias $eV = -1.2$ meV at a $60 \times 60 \text{Å}^2$ square. Also shown d -wave gap nodes orientation and lattice sites to indicate that impurity state is registered to lattice. From Pan *et al.* (Pan *et al.*, 2000b).

ported by the Davis' group (Pan *et al.*, 2000b). Zn^{2+} has a filled d -shell, and hence acts as a strong potential scatterer for holes in the CuO_2 plane. Therefore, according to the predictions of Balatsky *et al.*, the quasiparticle resonance is expected close to the Fermi energy. To search for it, Pan *et al.* mapped the differential tunneling conductance at zero bias over a large area, and found randomly distributed sites corresponding to high LDOS, which they associated with Zn dopants. Typical tunneling spectrum at the center of such a site is shown in Fig. 15: it exhibits a very strong peak (up to six times greater than the normal-state conductance) at the energy $\Omega = -1.5 \pm 0.5$ meV. At the same location, the intensity of the superconducting coherence peak is strongly suppressed, indicating almost complete local destruction of superconductivity. Both features are in agreement with the predictions for quasiparticle scattering off of a strong nonmagnetic impurity in a d -wave superconductor.

High intensity of the intra-gap peak allowed close inspection of the electronic structure around the Zn impurity. As shown in Fig. 17, the differential conductance map at $\Omega = -1.5$ meV exhibits two novel features. First, the intensity is the strongest directly at the impurity site, and local maxima and minima occur at the sites belonging to the different sublattices with respect to the impurity. Second, the intensity decays much faster along the nodal direction than along the bond direction. These features are at variance with the theory based on a purely potential scattering, which predicts vanishingly small intensity at the impurity near unitarity limit. The discrepancy motivated additional studies. One approach focused

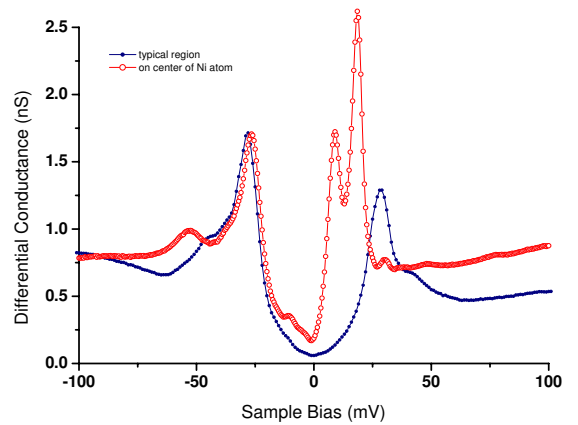


FIG. 18 Tunneling DOS for tunneling on Ni impurity site. Note that there are always states at opposite bias as well. The peak intensity is largest on either positive or negative bias depending on the position. To fit the data one needs to use both U_0 and J . From Hudson *et al.* (Hudson *et al.*, 2001).

on the Kondo resonance as a contribution to the zero-bias peak (Polkovnikov *et al.*, 2001; Zhang *et al.*, 2001; Zhu and Ting, 2001a); this is discussed in Sec. XI. An alternative explanation considers the tunneling path via the BiO layer which is exposed when the sample is cleaved (Martin *et al.*, 2002; Zhu and Ting, 2001b; Zhu *et al.*, 2000c); this physics is outlined later in this section.

When Ni atom is substituted for the plane Cu in BSCCO, it is in the $3d^8$ state, and therefore has spin $S = 1$. The potential part of scattering is also present, but is much weaker than for Zn. The experimental study of Ni-doped samples was reported in (Hudson *et al.*, 2001), where two resonance states were found, as shown in Fig. 18. Observation of two distinct resonance energies is in agreement with theoretical models that include both nonmagnetic and magnetic scattering (Salkola *et al.*, 1997; Tsuchiura *et al.*, 2000), and predict spin-resolved states at the energies $\pm\Omega_{1,2}$ given by Eq. (7.13) (Salkola *et al.*, 1997). In experiment $\Omega_1 = 9.2 \pm 1.1$ meV and $\Omega_2 = 18.6 \pm 0.7$ meV. Using the value for the superconducting energy gap $\Delta_0 = 28$ meV, one finds $N_F U = -0.67$ and $N_F J = 0.14$. This implies that the scattering on Ni atoms is dominated by potential interactions, even though the impurity has a magnetic moment. The experiment also showed that the intensity at the gap edge in the tunneling conductance directly at the Ni impurity site is almost unaffected.

B. Filter

As mentioned above, for strong potential scattering it is difficult, if not impossible, to produce large intensity on the impurity site. Indeed, independently of the model, scattering in the near-unitarity limit produces a node in the wave function. Yet, experimentally, in the STM im-

ages the Zn-impurity site is bright (Pan *et al.*, 2000b), indicating an enhanced low-energy DOS. One possible explanation of this discrepancy is that the image seen by STM is not simply the local intensity of the impurity state directly underneath the tip. The sample is cleaved, and the conduction plane where resonance resides is buried below the exposed layer, so that the tunneling occurs predominantly via a particular combination of the atomic orbitals that allow electron transfer from the STM tip to the conduction plane. This provides a “filter” that emphasizes or hides certain features of the bare LDOS. Martin *et al.* (Martin *et al.*, 2002) proposed that intensity seen by STM is a convolution of initial intensity due to impurity scattering and filter function that accounts for the matrix element of hopping between CuO planes, $t_k \propto |\cos k_x - \cos k_y|^2$.

In the simplified form this idea is based on the essential role of Copper s -orbitals for interplane tunneling (Andersen *et al.*, 1995; Xiang and Wheatley, 1995). The DOS near the Fermi surface is dominated by the $d_{x^2-y^2}$ orbitals of Cu (for simplicity we treat hybridization with oxygen p -orbitals perturbatively), while the s -orbitals are far from the chemical potential. However, interplane tunneling between the $d_{x^2-y^2}$ orbitals in different planes via the apical oxygen p_z shell is prohibited by symmetry, and therefore must occur via virtual hopping on the s -orbitals. Locally, $d_{x^2-y^2}$ and s orbitals are orthogonal on a given site, and the next available s -orbitals are on the four nearest copper atoms. Therefore electron hops virtually on to p_x or p_y orbitals of nearest O and then onto Cu s -orbital, as shown in Fig. 19.

It is clear from this figure that the sign of the hopping amplitude Cu $d_{x^2-y^2} \rightarrow$ O $p_{x,y} \rightarrow$ Cu s is different for motion along horizontal and vertical directions. Compare the amplitudes $A_{i,i+x(y)}$ for the hopping to the Cu site on the right and that on the top:

$$\begin{aligned} A_{i,i+x} &\propto \frac{\langle d_i | p_x \rangle \langle p_x | s_{i+x} \rangle}{[E_p - E_d][E_s - E_p]} \sim \frac{(-1) \exp(ik_x a)}{[E_p - E_d][E_s - E_p]} \\ A_{i,i+y} &\propto \frac{\langle d_i | p_y \rangle \langle p_y | s_{i+y} \rangle}{[E_p - E_d][E_s - E_p]} \sim \frac{(+1) \exp(ik_x a)}{[E_p - E_d][E_s - E_p]} . \end{aligned} \quad (9.1)$$

So far we consider plane waves that describe the states without impurity scattering. It was argued (Martin *et al.*, 2002) that the same holds for the states produced by impurity scattering. Quantum mechanical hopping from one site to its nearest neighbor s -orbital has contributions from four processes

$$\begin{aligned} A_{tot} &= A_{i,i+x} + A_{i,i-x} + A_{i,i+y} + A_{i,i-y} \\ &\sim \cos(k_x a) - \cos(k_y a) . \end{aligned} \quad (9.2)$$

Again, the second line refers to the pure plane wave to make contact with the bands structure calculations (Andersen *et al.*, 1995). Upon hopping on the s -orbitals electron moves to the next layer, and retraces its path. Therefore the net amplitude for the hopping will be pro-

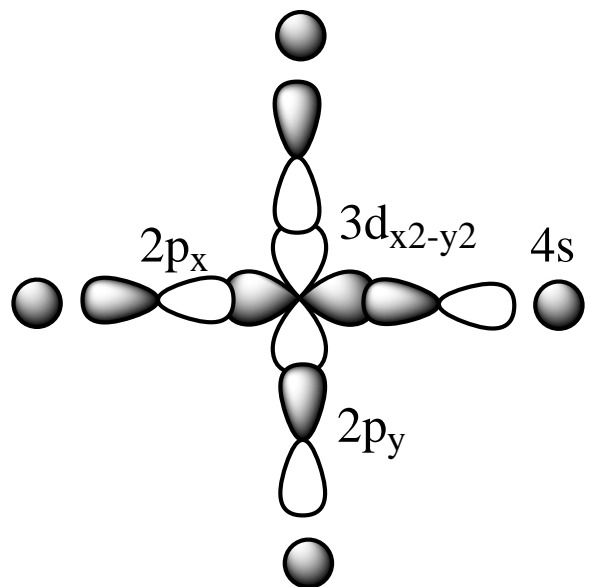


FIG. 19 The real space image of different orbitals on Cu, nearest O and nearest Cu sites are shown. Dark orbitals and lobes represent positive phase of the orbital wavefunction, white represent negative phase. Quantum mechanical interference produces the filter effect that changes the distribution of the impurity state intensity (Martin *et al.*, 2002).

portional to $|A_{tot}|^2$, and has $|d_{x^2-y^2}|$ modulations:

$$|A_{tot}|^2 \propto |\cos(k_x a) - \cos(k_y a)|^2 \quad (9.3)$$

This particular filter appears in the interplane hopping matrix element obtained within the band structure calculation (Andersen *et al.*, 1995; Xiang and Wheatley, 1995). However, the Cu s -orbitals are also relevant for probing an exposed Cu-O layer since the electrons tunnel from the STM tip predominantly into these states (Misra *et al.*, 2002). The $4s$ -orbital-assisted hopping was also argued to have profound consequences for the experimental measurement of vortex core states in cuprates (Wu *et al.*, 2000).

Filter of another type, due to blocking of certain hopping were considered by Zhu *et al.* (Zhu *et al.*, 2000c), who analyzed the local tunneling matrix elements that connect impurity orbitals to s -orbitals on neighboring Cu atoms. The net effect is to add probabilities $\sum_{nn\delta} |A_{i,i+\delta}|^2$ rather than the interfering amplitudes. This filter was argued to produce large spectral intensity on an impurity site and to suppress it on nearest neighbor sites. More recently, the STM data has been converted to a set of LDOS defined on a two-dimensional lattice (Wang and Hu, 2004), which allowed for a rigorous comparison between the tight-binding model studies and the STM experimental data.

An important observation arises from comparing STM and NMR results on Li doped YBCO superconductor (Bobroff *et al.*, 2001). Li appears to be a strong scatterer, and the maximum intensity of the NMR signal

comes from the four nearest neighbor Cu sites, hence is localized near the impurity. This is consistent with the notion that strongly scattering impurity produces large density of states on nearest sites. The crucial difference between NMR and STM is that no electron tunneling is associated with NMR observation, and therefore it measures real space distribution of spin. Consequently, NMR results provide another confirmation, albeit indirect, of the theory of the scattering resonance.

C. Spatial distribution of particle and hole components

It is clear from comparing the left and right panels of Fig. 16 that the tunneling intensity is not symmetric with the bias voltage. On the contrary, the maxima and minima in LDOS map are interchanged: bright spots in the STS map at a positive bias V correspond to dark spots at $-V$, and vice versa. This effect is a general property of superconductors, and is seen in both s and d -wave systems (Hudson *et al.*, 2001; Pan *et al.*, 2000a; Yazdani *et al.*, 1997), see also Sec. X. It results from the interplay between particle and hole components of the Bogoliubov quasiparticles, which are “native” elementary excitations of a superconductor. In the spatial LDOS pattern created by the quasiparticle resonance the sites with a large particle component have large intensity on positive bias site, while the sites with large hole component are bright at negative bias, Fig. 20.

Formally, define the amplitudes of particle and hole amplitudes of the Bogoliubov quasiparticle, $u_n(i)$ and $v_n(i)$ at site i and for a particular eigenstate n , see also Eq. (7.12). They obey the normalization condition $\sum_n |u_n(i)|^2 + |v_n(i)|^2 = 1$ at each site. Therefore at a site where $u_n(i)$ is large $v_n(i)$ is small, and vice versa. Large $u_n(i)$ component means that the quasiparticle state is predominantly electron-like at that site, and the probability for electron tunneling into superconductor is locally enhanced. Hence the tunneling intensity at the *positive sample bias* is large. At the same site the hole amplitude $|v_n(i)| \ll |u_n(i)|$ and the intensity at *negative sample bias* is small. Similarly, sites with large hole amplitudes $|v_n(i)|$ are bright at negative bias. It follows that if a particular intensity pattern is observed at positive bias (electron tunneling), quite generally, the complementary pattern is found at negative bias (hole tunneling). This is simply a consequence of particle-hole mixing in superconductors, and lies at the heart of the intensity pattern change upon switching bias, seen in experiments (Hudson *et al.*, 2001; Pan *et al.*, 2000a), see Fig. 16.

D. Fourier-transformed STM maps

The spatial dependence of the impurity-induced state has additional information about the underlying system. Consider the simple case of a metal surface with an impurity atom, see Sec. V. The modifications of the DOS

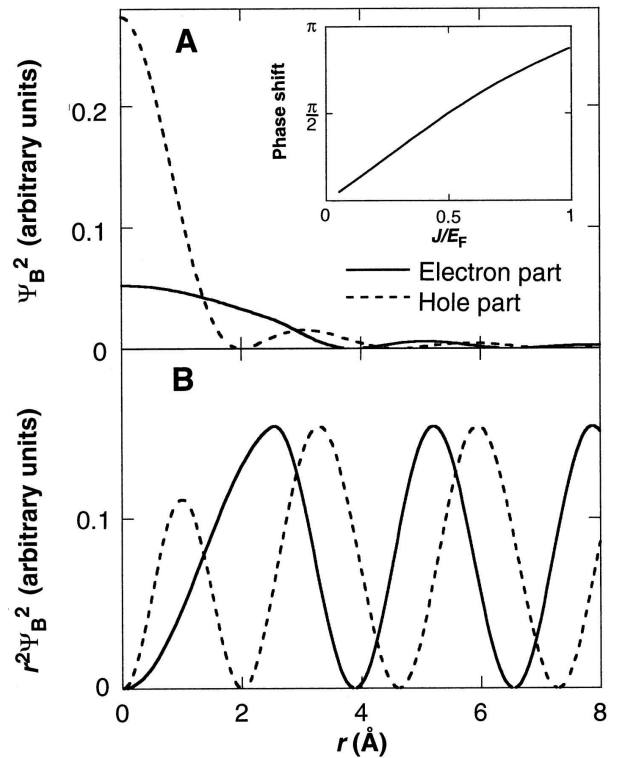


FIG. 20 Particle and hole components of the impurity wave function for a magnetic impurity in a s -wave superconductor. A) Impurity wave function $\Psi_B(r)$ and B) $r^2\Psi_B(r)$. The maxima of particle and hole components occur at different positions. This results in the different image of the impurity state, seen on positive and negative bias. This effect is a general property of a superconductor regardless of the symmetry of the pairing state. From (Yazdani *et al.*, 1997).

induced by the impurity, Friedel oscillations, vary at the wave vector k_F , and decay with the distance from the scattering center, see, for example, Eq. (5.12). Therefore if an area of the surface contains a number of dilute randomly distributed impurities, the LDOS exhibits a pattern of standing waves. Fourier transform (FT) of the intensity map at a given bias therefore shows pronounced maximum at the Fermi wave vector (or its 2D slice), and can be used to map out the Fermi surface of the underlying compound. This technique was pioneered by Sprunger *et al.* (Petersen *et al.*, 1998; Sprunger *et al.*, 1997) for Be, Cu, and other metallic surfaces, and became known as the Fourier-transform STM (FT-STM) method. In simple cases, the FT-STM directly reveals the Fermi surface of a metallic band, see Fig. 21.

The technique was recently successfully extended to the superconducting state of the cuprates (Hoffman *et al.*, 2002a,b; Howald *et al.*, 2003; McElroy *et al.*, 2003). In unconventional superconductors the information contained in the FT-STM maps is more extensive than in metals. In cuprates not all of the experimental features are understood, and theory generally followed experiment, so that here we review several aspects of the data.

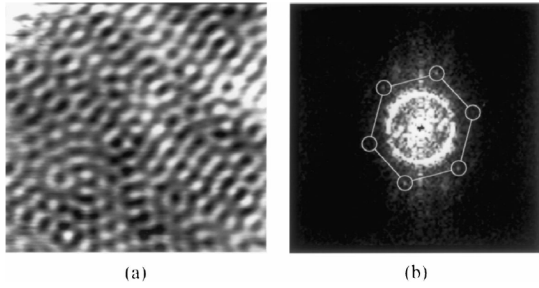


FIG. 21 Example of FT-STM. a) Be (001) surface, as seen by STM, with the standing waves (Friedel oscillations) produced by defects. b) Fourier transform of a) reveals a cut through the Fermi surface corresponding to the surface states. From (Petersen *et al.*, 1998; Sprunger *et al.*, 1997)

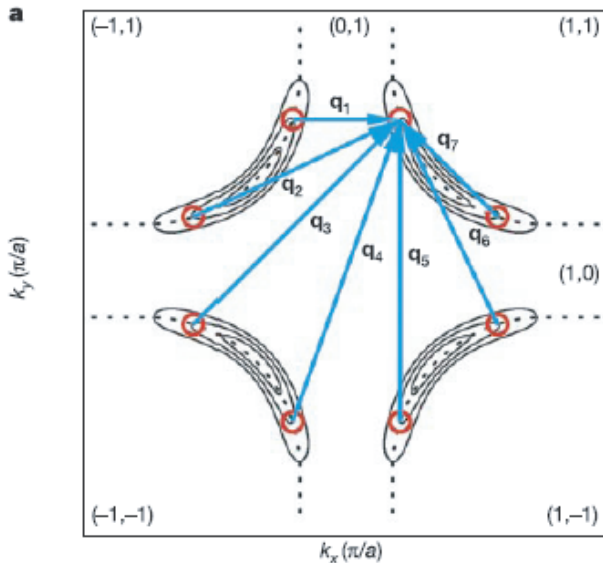


FIG. 22 A representative set of seven scattering vectors $\mathbf{q}_i(E)$ of the ‘octet’ model. Reproduced with permission from (McElroy *et al.*, 2003).

Enhanced signal in the FT-STM at a wave vector \mathbf{q} , and bias $eV = \omega$, corresponds to a large amplitude for scattering off of impurity. Qualitatively, this amplitude depends on the number of available initial at final states at a given energy in regions of the Brillouin Zone separated by \mathbf{q} , i.e. it is proportional to $\int N_{\mathbf{k}}(\omega)N_{\mathbf{k}+\mathbf{q}}(\omega)d\mathbf{k}$, where $N_{\mathbf{k}}(\omega)$ is the momentum dependent DOS. The greater the number of “matching” pairs of initial and final states, the more likely it is that a quasiparticle scatters from one of them into the other, producing a feature in the FT-STM image (we consider here low temperatures and therefore ignore Fermi factors). In most metals the density of states is essentially constant around the Fermi surface. In contrast, in nodal superconductors the loci of the low-energy excitations depend on the location of the nodes and the shape of

the Fermi surface. Experiment and analysis for BSCCO have been first carried out in (McElroy *et al.*, 2003). At energies below the gap maximum, $\omega \ll \Delta_0$, the energy contours $E(\mathbf{k} = \omega)$ are banana-shaped, as shown in Fig. 22. The dominant contribution to the density of states, $N(E = \omega) \propto \int \delta(E(\mathbf{k}) - \omega)|\nabla_{\mathbf{k}}E_{\mathbf{k}}|^{-1}d\mathbf{k}$ arises from regions of the greatest curvature of $E(\mathbf{k})$, i.e. from the tips of each banana. Therefore, the primary contributions to $N(\omega)$ is from the small regions around eight wave vectors (octet) $\mathbf{k}_j(E)$, $j = 1, 2, \dots, 8$, at the banana tips (red circles in Fig. 22.)

Consequently, maximal scattering intensity at a given ω is from one element of the octet to another, simply due to large DOS of initial and final states. For each \mathbf{k}_j , there are seven counterparts for enhanced scattering, producing a total of 56 scattering wave vectors. Of these, 32 are inequivalent, and therefore 16 distinct $\pm\mathbf{q}$ pairs can be detected by Fourier-transformed scanning tunneling spectroscopy. The experimental data (McElroy *et al.*, 2003) were found to be in good agreement with this model. The samples were not intentionally doped, so that the scattering was on intrinsic disorder. It is important to note that the model predicts the dispersion of each resonance wave vector with the energy (bias voltage) that is completely determined by the underlying Fermi surface and the shape of the gap, i.e. by the growth of bananas with energy. The peaks associated with these Friedel oscillations of quasiparticles scattering on impurities have been extensively investigated (Byers *et al.*, 1993; Wang and Lee, 2003; Zhang and Ting, 2003, 2004), and interference effects from many impurities was analyzed in Capriotti *et al.*, 2003; Zhu *et al.*, 2004b.

However, the results on the cuprates show features beyond the simple Fermi surface resonances. First, it has been argued that some of the FT features do not disperse (Howald *et al.*, 2003), and that these LDOS modulations should be interpreted by invoking a static (or fluctuating) competing charge- or spin-ordered state (Kivelson *et al.*, 2003; Podolsky *et al.*, 2003; Polkovnikov *et al.*, 2003). The experimentally observed nanoscale inhomogeneities (Howald *et al.*, 2001; Lang *et al.*, 2002; Pan *et al.*, 2001) may also indicate the proximity to such a state. Furthermore, the electronic states at low energies in the pseudogap state in BSCCO exhibit spatial modulations with an energy-independent incommensurate periodicity (Vershinin *et al.*, 2004).

Second, a static Cu-O bond-oriented “checkerboard” pattern with $4a_0$ periodicity was found near the vortex core in the mixed state (Hoffman *et al.*, 2002a). This charge modulation is consistent with the field-induced spin-modulation with the period $8a_0$ observed in neutron scattering (Khaykovich *et al.*, 2002; Lake *et al.*, 2001, 2002) in other cuprate materials. The “checkerboard” pattern was variously interpreted as the onset of the competing spin density wave order around the vortex core where the superconductivity is suppressed (Andersen and Hedegård, 2003; Takigawa *et al.*, 2003; Zhu *et al.*, 2002), the nucleation of the antiferromagnetic or-

der brought about by local quantum fluctuations of a vortex (Franz *et al.*, 2002), and the crystallization of the d -wave hole pairs by the magnetic field (Chen *et al.*, 2002). Similar pattern has also been predicted around a single strong impurity with induced local moment in the optimally doped cuprates (Chen and Ting, 2003, 2004; Liang and Lee, 2002; Zhu *et al.*, 2002). These predictions depend on the details of a complete microscopic model that has not been developed yet.

X. QUANTUM PHASE TRANSITION IN s -WAVE SUPERCONDUCTORS WITH MAGNETIC IMPURITY

A. Introduction

Here we revisit the well studied problem of a localized classical magnetic moment in a superconductor. We focus here on one remarkable aspect of this model: the *first-order zero temperature transition* that takes place in an s -wave superconductor as a function of the effective magnetic moment, $J_0 S$, where S is the local impurity spin and J_0 is the exchange coupling between that spin and the spins of the conduction electrons. In this transition, the spin quantum number s of the electronic ground state of the superconductor $|\Psi_0\rangle$ changes from zero for a subcritical moment $J_0 < J_{crit}$ to $1/2$ for $J_0 > J_{crit}$. The total spin becomes $S \pm 1/2$ depending on the sign of J_0 . Sakurai was the first to point out this transition (Sakurai, 1970), which corresponds to a level crossing between two ground states as a function of the exchange coupling. In a singlet superconductor the level crossing occurs between the state with the screened impurity spin and that with S unscreened or partially screened. The two states have different spin quantum numbers, and hence level crossing is generally allowed. This quantum phase transition is of the first order and hence is not associated with divergent time or length scales.

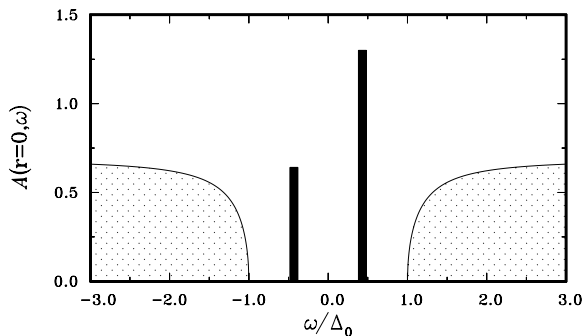


FIG. 23 The local effect of a magnetic moment on the low-energy spectral density in an s -wave superconductor.

We address the above problem at zero temperature by using the mean-field approximation within the T -matrix formulation and utilizing the self-consistent approach, which takes into account a local gap-function relaxation.

Local Coulomb interaction U breaks particle-hole symmetry and leads to an asymmetric spectral density for the impurity-induced quasiparticle states. Figure 23 illustrates the local effect of a magnetic moment on the low-energy spectral density in an s -wave superconductor. Since we limit our considerations to a classical spin, $S \gg 1$, the impurity moment cannot be screened completely by the quasiparticles. We show that the gross features of the impurity-induced quasiparticle states in s - and d -wave superconductors can be qualitatively understood within the non-self-consistent T -matrix formalism. The transition itself is not restricted to the classical spin: similar effect is found in a Kondo model, see Sec. XI.

B. Quantum phase transition as a level crossing

The physical picture of the quantum transition follows from the behavior of the impurity-induced bound state. The transition results from the instability of the spin unpolarized ground state. For a large enough value of J_0 , the energy of the impurity-induced quasiparticle state falls below the chemical potential.

In the Yu-Shiba-Rusinov solution for a classical spin, see Sec. VI, the impurity state always has the energy below the gap threshold:

$$\Omega_0/\Delta_0 = \frac{1 - (\pi J_0 S N_0)^2}{1 + (\pi J_0 S N_0)^2} \quad (10.1)$$

and the particle (u_{-1}) and hole (v_{-1}) amplitudes at positive and negative energies. The level crossing and change of the ground state follow already from this result. Ignoring the self-consistency, and using Eq. (10.1), we find that the transition occurs at

$$J_0 = J_{crit} = 1/\pi N_0 S \quad (10.2)$$

For a weak coupling $J_0 < J_{crit}$, the ground state of the superconductor is a paired state of time-reversed single-particle states in the presence of the impurity scattering, with the BCS-like ground state wave function:

$$|\Psi_0\rangle_{J_0 < J_{crit}} \sim \prod_n [u_n + v_n \psi_n^\dagger \psi_{-n}^\dagger] |0\rangle = |\Psi_0\rangle \quad (10.3)$$

Here, since the translational symmetry is broken by the impurity, we consider the eigenstates of the scattering problem in the presence of impurity. These states are labeled by a discrete index $n = 1, \dots, \infty$ and form the basis for the Bogoliubov Hamiltonian with an impurity. The $n = 1$ state corresponds to an impurity bound state, localized on impurity site. Index $-n$ correspond to a time reversal state, i.e. the localized state with opposite spin. The first excited state above the condensate corresponds, at $J_0 < J_{crit}$, to a single quasiparticle excitation, and its energy is that of the intragap Yu-Shiba-Rusinov state at energy Ω_0 , see Fig. 24.

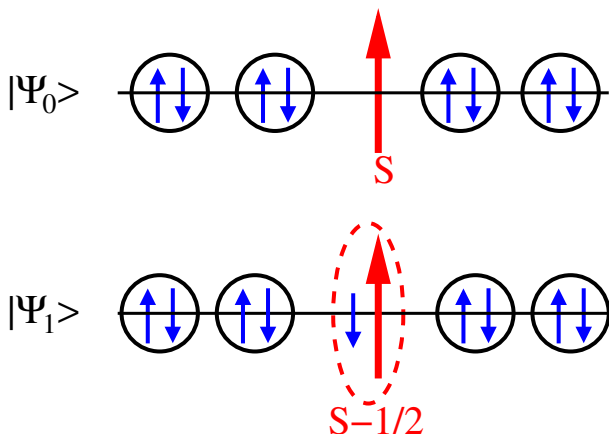


FIG. 24 Two variational states are shown schematically. $|\Psi_0\rangle$ is a standard BCS wave function that contains only paired particles and has unscreened impurity spin S . $|\Psi_1\rangle$ is a variational wave function that describes the formation of the bound state between particle with the spin opposite to the local spin (for antiferromagnetic coupling); this state is inherently a non BCS state and electronic spin quantum number differs by one unpaired spin compared to $|\Psi_0\rangle$.

The wave function of this excited state is

$$\begin{aligned} |\Psi_{-1}\rangle_{J_0 < J_{crit}} &\sim \gamma_{-1}^\dagger |\Psi_0\rangle = |\Phi_{-1}\rangle \\ |\Phi_{-1}\rangle &= \psi_{-1}^\dagger \prod_{n>1} [u_n + v_n \psi_n^\dagger \psi_{-n}^\dagger] |0\rangle \end{aligned} \quad (10.4)$$

with standard quasiparticle definitions of $\gamma_1 = u_1 \psi_1 - v_1 \psi_{-1}^\dagger$, $\gamma_1^\dagger = u_1 \psi_1^\dagger - v_1 \psi_{-1}$, $\gamma_{-1}^\dagger = u_{-1} \psi_{-1}^\dagger + v_{-1} \psi_1$, etc, with $u_n^2 + v_n^2 = 1$. We introduce a notation

$$|\widetilde{\Psi}_0\rangle = \prod_{n>1} [u_n + v_n \psi_n^\dagger \psi_{-n}^\dagger] |0\rangle, \quad (10.5)$$

so that $|\Phi_{-1}\rangle = \psi_{-1}^\dagger |\widetilde{\Psi}_0\rangle$. The state $\gamma_1^\dagger |\Psi_0\rangle$ is far above the superconducting gap and hence is not relevant for this discussion. Note that $|\Psi_0\rangle$ is a true vacuum for all quasiparticles: e.g. $\gamma_{\pm 1} \prod_{n>0} [u_n + v_n \psi_n^\dagger \psi_{-n}^\dagger] = 0$.⁷ This state is a true spin singlet $\langle \Psi_0 | \mathbf{S}_{electron} | \Psi_0 \rangle = 0$. To avoid confusion with impurity spin S we explicitly indicate that $\mathbf{S}_{electron}$ is the net spin of conduction electrons. Hence if $|\Psi_0\rangle_{J_0 < J_{crit}} = |\Psi_0\rangle$ is a ground state, the total spin of electrons is zero, and only the spin of impurity counts. The first excited state at energy Ω_0 has a spin $1/2$ quasiparticle in it: $\langle \Phi_{-1} | S_{electron}^z | \Phi_{-1} \rangle = -1/2$.

⁷ Here the spin of the state $n = 1$ is determined by the sign of exchange coupling J_0 . We will assume it to be antiferromagnetic. So the electronic spin of the state $n = -1$ in Eq. (10.4) is opposite to the local spin S assumed to be up without loss of generality. Case of ferromagnetic coupling is similar. Indeed classical spin solution Eq. (10.1) is symmetric between $J_0 \rightarrow -J_0$ as it contains only even powers of exchange.

Upon increasing the coupling constant J_0 one reaches the critical value where the energies of the two states cross, Fig. 25. Beyond that point the excited and the ground states changes the roles.

$$\begin{aligned} |\Psi_0\rangle_{J_0 > J_{crit}} &= |\Psi_{-1}\rangle = |\Phi_{-1}\rangle \\ |\Psi_{-1}\rangle_{J_0 > J_{crit}} &= |\Psi_0\rangle \end{aligned} \quad (10.6)$$

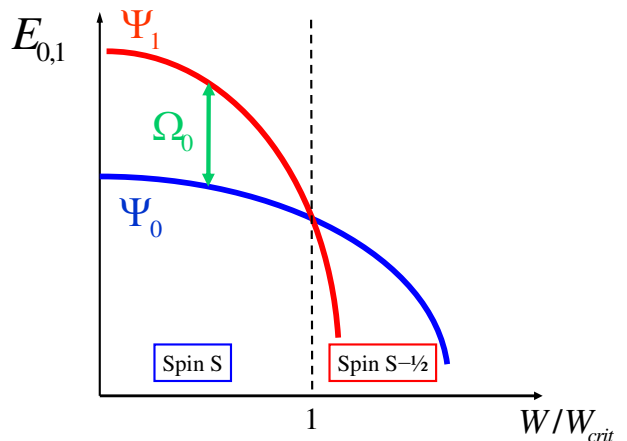


FIG. 25 Energies of two variational states are shown. $|\Psi_0\rangle$ is a standard BCS state with energy E_0 . $|\Psi_1\rangle$ is a variational state that describes the formation of the bound state between particle with the spin opposite to the local spin with energy E_1 . Level crossing between states with different symmetry occurs at some critical value of the coupling J_{crit} . This is an example of a first order quantum phase transition with no divergent length or time scale associated with it.

A clear way to see this quantum phase transition is via examining the energy levels as a function of J_0/J_{crit} . For variational wavefunctions $|\Psi_{0,-1}\rangle$ we define the respective energies as expectation values of the Hamiltonian:

$$E_{0,-1}(J_0/J_{crit}) = \langle \Psi_{0,-1} | H | \Psi_{0,-1} \rangle \quad (10.7)$$

Energy of the first excitation is then simply

$$\begin{aligned} \Omega_0(J_0/J_{crit}) &= E_{-1} - E_0, J_0 < J_{crit} \\ \Omega_0(J_0/J_{crit}) &= E_0 - E_{-1}, J_0 > J_{crit} \end{aligned} \quad (10.8)$$

There are several implications of this result. Firstly, the ground state of superconductor with a magnetic impurity in the strong coupling limit is a non-BCS state: there is one unpaired occupied single particle state in the ground state. In contrast, all states are paired in the BCS theory. A similar result was observed for a Kondo screening in superconductor (Sakai *et al.*, 1993). One can easily understand the result by considering a strong coupling limit $J_0 N_0 \gg 1$, when, long before any superconducting correlations are established, a single electron state is bound to the impurity site. This is equivalent to the strong coupling limit of Kondo screening. In our case the bound electron partially screens the large impurity spin. For spin $S = 1/2$ the screening is complete

and the state is a singlet (Sakai *et al.*, 1993). Thereafter a superconducting state emerges with one unpaired electron bound to the impurity; it is stabilized by the energy balance between superconducting and magnetic energies: Single electron state bound to a local spin yield energy gain $\sim J_0$ large compared to the pairing energy Δ_0 . The crossing point and related quantities are shown in the Fig. 26: This level crossing point corresponds to a quantum phase transition.

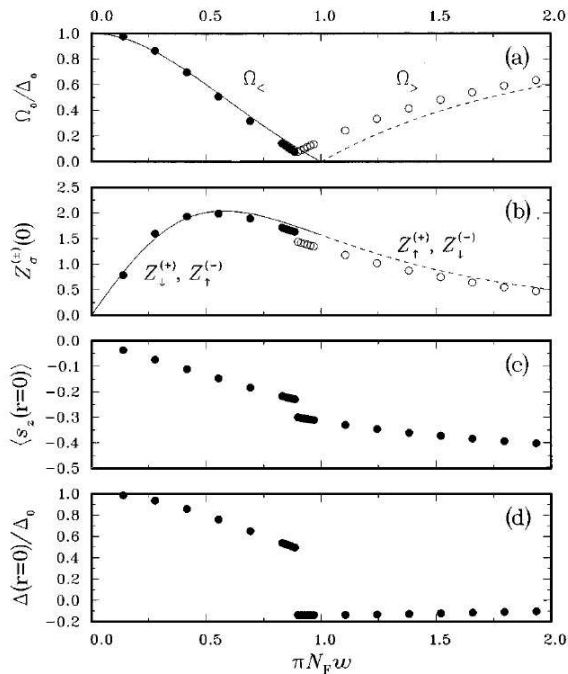


FIG. 26 a) The bound-state energy Ω_0 , b) the spectral weight of the pole Z^\pm for positive and negative energies in units of $N_0 J_0$, $N_0 = N_F$, c) the spin polarization $\langle s(\mathbf{r}=0) \rangle$, and d) the gap function $\Delta(\mathbf{r}=0)/\Delta_0$ at the impurity site $\mathbf{r}=0$ as a function of J_0 in the s-wave superconductor. Lines denote the T matrix results for the uniform order parameter and symbols the self-consistent mean-field results on a square lattice at half filling. The quantities of the impurity-induced intragap quasiparticle state belonging to the branch $J_0 < J_{crit}$ are denoted by solid lines and solid symbols, whereas those ones belonging to the branch $J_0 > J_{crit}$ are marked by dashed lines and open symbols. Taken from (Salkola *et al.*, 1997).

The crossing point occurs exactly at the critical point of Eq. (10.1) only in a non-self-consistent treatment where single particle levels provide the only contribution to total energy. The true phase transition occurs slightly earlier. The gap suppression and quasiparticle interaction also contribute to free energy and, in the self-consistent mean-field approximation, the order-parameter relaxation shifts J_{crit} downwards and the energy of the impurity-induced bound state does not reach zero when a first-order transition between the two ground states occurs. In practice the analytical results are within 10 percent of the numerical results obtained in a self-consistent treatment (Salkola *et al.*, 1997). In contrast,

a d-wave superconductor has no quantum transition for any value of the magnetic moment when its quasiparticle spectrum in the normal state has particle-hole symmetry. The absence of the transition follows from the behavior of the impurity-induced quasiparticle states which are pinned at the chemical potential for an arbitrarily large magnetic moment, see Sec. VII. However, if particle-hole symmetry is broken or if the pairing state acquires a small s-wave component, the transition is again possible for a large enough moment. The impurity moment induces two virtual-bound states which have four-fold symmetry and extend along the nodal directions of the energy gap.

C. Particle and hole component of impurity bound state

In this section we show that the excited states inside the gap in superconducting state appear in pairs at positive and negative energies. This is a direct consequence of the fact that natural excitations are Bogoliubov excitations. Particle and hole coefficients of the excited state $|\Psi_{-1}\rangle_{J_0 < J_{crit}}$ are given by the u and v components of the quasiparticle operators γ_n , see Sec. II. To be specific we confine subsequent discussion to s-wave case, however the results are applicable to a superconducting state of any symmetry.

Consider two independent processes: a) electron at energy Ω_0 and spin down, $n = -1$ and b) hole with spin up, $n = 1$ injected in superconductor with the same energy Ω_0 . Hole creation means that an electron with spin up is extracted from superconductor. In experiment, this is achieved by reversing the bias of the STM tip, and it corresponds to the negative energy axis. Variational wave functions that describes these processes are

$$\begin{aligned} \psi_{-1}^\dagger |\Psi_0\rangle_{J_0 < J_{crit}} &= -u_1 |\Phi_{-1}\rangle, \\ \psi_1 |\Psi_0\rangle &= v_1 |\Phi_{-1}\rangle. \end{aligned} \quad (10.9)$$

Here, to be specific, we consider the case of $J_0 < J_{crit}$. This illustrates the point that in BCS like ground state the particle excitation with energy Ω_0 and hole excitation with negative energy $-\Omega_0$, aside from irrelevant normalization factors, is the same excited state, namely $|\Phi_{-1}\rangle$. Therefore the poles in the density of states (and the contributions to the electronic LDOS) always come in pairs at positive and negative energies. The true quasiparticles in superconducting state are Bogoliubov excitations γ_n that have a finite component of particle and hole with amplitudes u_n and v_n . The strength of the electron absorption and emission process is controlled by the coherence factors. This is true for a BCS superconductor even without impurities. For the case at hand, the impurity states are distinct from the continuum. The two poles at $\pm\Omega_0$ are part of the same physical excitation. The local spectral function $A_1(\mathbf{r}, \omega) = -\text{Im}G_{11}(\mathbf{r}, \omega)/\pi$ at the impurity site is

$$A_1(\omega) = Z^+ \delta(\omega - \Omega_0) + Z^- \delta(\omega + \Omega_0) \quad (10.10)$$

and the relative strength of the particle and hole components is $Z^+ \sim u_{-1}^2$ and $Z^- \sim v_{-1}^2$, so that the net strength of the poles $Z^+ + Z^- \geq 1$ as it should for a physical excitation. For more details and references reader is referred to (Salkola *et al.*, 1997).

Analysis for $J_0 > J_{crit}$ is more involved. The ground state wave function is now $|\Phi_{-1}\rangle$. Injection of an electron with spin opposite to the spin of the bound state and extraction of an electron with the same spin produces

$$\psi_1^\dagger|\Phi_{-1}\rangle = \psi_1^\dagger\psi_{-1}^\dagger|\widetilde{\Psi}_0\rangle, \quad \psi_{-1}|\Phi_{-1}\rangle = |\widetilde{\Psi}_0\rangle \quad (10.11)$$

respectively, with the complementary annihilated states $\psi_1^\dagger|\Phi_{-1}\rangle = 0$ and $\psi_{-1}^\dagger|\Phi_{-1}\rangle = 0$. Although the two states written in Eq. (10.11) are different, the sole difference is that one of them has an extra Cooper pair. For a macroscopically large system with the number of Cooper pairs $N \gg 1$ this produces negligible difference in the energies and matrix elements. Therefore, again, the injection of electron with spin up (in our convention) and extraction of electron of spin down produce the same physical state. This state has a particle and a hole projection just as we discussed in case of $J_0 < J_{crit}$.

Similar quantum phase transition occurs in a d-wave superconductor even for a nonmagnetic impurity. In the case of particle-hole symmetric band the unitary scattering produces a zero energy state, see Sec. VII, Eq. (7.1). However for the particle hole asymmetric band the impurity state reaches zero energy and eventually changes the sign as a function of impurity strength. This transition occurs at $U_0 > U_{crit} \sim \mu$, where μ is the chemical potential that leads to a particle-hole asymmetric band. It is known that single quasiparticle bound state forms at $U_0 > U_{crit}$, and the ground state wavefunction has a single unpaired quasiparticle, in addition to the BCS pairs, see (Salkola *et al.*, 1996, 1997).

D. Intrinsic π phase shift for $J_0 > J_{crit}$ coupling

Here we would like to point a little noticed by important fact that near an impurity site the phase of the superconducting order parameter changes by π . As is shown Fig. 26d), the self-consistent solution indicates that at $J_0 > J_{crit}$ the phase of the order parameter on the impurity site is shifted by π with respect to the phase in the bulk. This is illustrated in Fig. 27.

In numerical calculation the spatial extent of the π shifted region was found to be few atomic sites. Such a sharp change in the phase of the order parameter costs significant superconducting condensate energy and is not preferred under normal circumstances. In the case at hand however, in the strong coupling limit near the impurity site, the condensate energy is secondary to the magnetic exchange energy, and physics is driven by magnetic interactions. Even though the phase shift is π , it does not lead to any time reversal violating observable effects, as there are no superconducting currents near

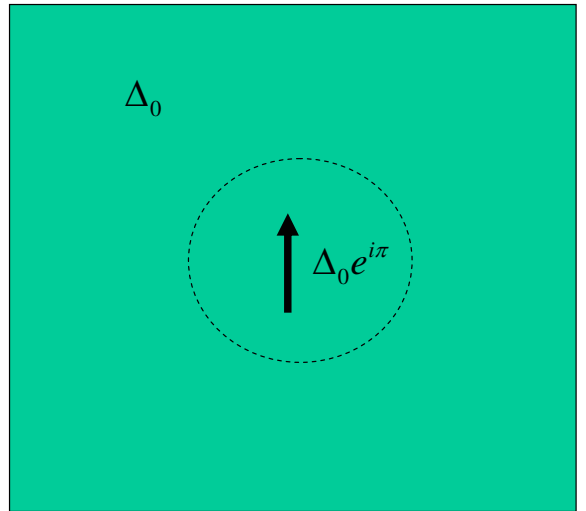


FIG. 27 Cartoon of the intrinsic π junction near magnetic impurity in s -wave superconductor.

the impurity: $I = I_c \sin \phi = 0$. These results were obtained in the self-consistent treatment within a negative U model that allows for the on-site pairing (Salkola *et al.*, 1997).

We are not aware of a simple explanation of this effect. It appears to be general and not restricted to a particular model. It is related to the π -shift superconducting junctions with tunneling barriers containing a magnetic impurity or a ferromagnetic layer. This subject is covered extensively, see e.g. recent review and other papers (Bulaevskii *et al.*, 1977; Buzdin *et al.*, 1982; Buzdin, 2005; Glazman and Matveev, 1989; Spivak and Kivelson, 1991).

XI. KONDO EFFECT AND QUANTUM IMPURITIES

Above we have concentrated on static impurities. In the next two Sections we consider examples when impurity atoms have their own internal degrees of freedom and impurities are dynamically coupled to conduction electrons. That dynamical behavior often leads to qualitatively new results is well known from the studies of the Kondo effect (Kondo, 1964): scattering of conduction electrons off of a single magnetic impurity.

At low T , dilute magnetic impurities doped into an otherwise nonmagnetic metallic host have dramatic effects on the resistivity and susceptibility. The anomalies are due to screening of the impurity spin by conduction electrons. For a local spin $S = \frac{1}{2}$ and antiferromagnetic exchange, a global singlet is formed by coupling an electron state to the impurity site; quantum dynamics of spin flips is crucial for its formation. The process is manifested in the crossover of the susceptibility from the Curie-like at high temperatures, $\chi = C/T$ with $C = 4\mu_B^2 S(S+1)/3k_B$, to Pauli-like below a characteristic Kondo temperature $T_K \simeq W \exp(-1/2JN_0)$. Here

W is the electron half band width and J is the exchange constant. Importantly: a) Kondo screening occurs *only* for antiferromagnetic exchange constant $J > 0$; and b) the process is non-perturbative, as is clear from the non-analytic dependence of T_K on the exchange constant. Full understanding of the single impurity Kondo problem in a metal required concerted use of the renormalization group (Anderson, 1970; Anderson *et al.*, 1970), numerical renormalization group (NRG) (Wilson, 1975), exact solutions via the Bethe ansatz (Andrei, 1980; Wiegmann, 1980), and large- N expansions (Coleman, 1984, 1985; Read, 1985; Read and Newns, 1983a,b). Many results are summarized in recent reviews (Cox and Zawadowski, 1998; Hewson, 1993).

Kondo screening involves mostly quasiparticles near the Fermi energy, E_F . In metals, the density of states near E_F varies weakly, and $N(\epsilon) \approx N_0$, which greatly simplifies the analysis. In contrast, if $N(\epsilon)$ varies strongly for $\epsilon \approx E_F$, Kondo effect is realized differently. In a band gap insulator this was investigated in (Ogura and Saso, 1993), who found that the ground state of the magnetic impurity changes from the singlet to multiplet when the band gap increases, as in the case of the magnetic impurity in a conventional BCS superconductor. In superconductors, however, the Cooper instability that gaps the Fermi surface and depletes the density of states is itself driven by the finite DOS in the normal state. Consequently, the two effects compete.

For simplicity and following the historical development, we so far considered properties of classical spin, for which no reduction in magnitude due to Kondo screening is possible, see Sec. VI. We now give the current understanding of the question of which conclusion of this analysis are robust for small spin values and in gapless superconductors.

A. Kondo effect in fully gapped superconductors

In normal metals antiferromagnetic exchange leads to Kondo screening below T_K , while ferromagnetic exchange does not. In superconductors, within the Shiba-Rusinov analysis the sign of the exchange interaction between the conduction electrons and impurity spins is irrelevant. Consequently, treatment of quantum impurity spins has to bring out the differences between two signs of J .

For $J > 0$ the opening of the superconducting gap competes with Kondo screening as both instabilities are driven by the finite DOS at zero energy. Clearly, if $T_K \gg T_c$, the impurity is completely screened by the time of the onset of superconductivity. In contrast, for $T_K \ll T_c$ Kondo screening is suppressed by the depletion of states upon opening of the superconducting gap.

In the RG picture Kondo screening is viewed as growth (and divergence) of the *effective* exchange coupling, J_{eff} , as we focus at the properties of the system at lower and lower energies. Therefore J_{eff} , and, with it, the phase shift of scattering on the impurity depends on the en-

ergy of the incoming electron. Consequently, the effect of scattering varies with temperature.

1. Ferromagnetic exchange

Early analytical attempts were carried out (Müller-Hartmann, 1973; Zittartz and Müller-Hartmann, 1970) in the framework of Nagaoka decoupling scheme (Hamann, 1967; Nagaoka, 1965, 1967). For $J < 0$ the bound state splits off the band edge and was found to move towards an asymptotic value

$$\epsilon \equiv \frac{E_0}{\Delta} = \left[1 + g^2 \pi^2 S(S+1) \right]^{-1/2}, \quad (11.1)$$

where $g = \lambda N_0$, and λ is the superconducting coupling constant. For weak coupling, $g \ll 1$, the bound state remains close to the gap edge for all values of $J < 0$. This qualitative result was later confirmed by NRG calculations (Sakai *et al.*, 1993; Satori *et al.*, 1992), which showed that the binding energy is well approximated by $\epsilon \approx 1 - \pi^2 J_{eff}^2 / 8$, where

$$J_{eff} = \frac{2|J|/W}{1 + (2|J|/W) \ln(W/\Delta)}. \quad (11.2)$$

Therefore the ferromagnetic case corresponds to weak coupling and small phase shift of scattering at low temperatures.

The ground state of this system was argued to be a doublet (Sakai *et al.*, 1993; Satori *et al.*, 1992; Soda *et al.*, 1967), since the ferromagnetic interaction renormalizes to weak coupling and the impurity spin remains essentially free. Recently it was suggested that superconducting interaction is relevant (in the RG sense) in this model, and therefore above a critical Δ -dependent coupling, J_C (J_C is larger for smaller Δ), the ground state of the coupled superconductor-impurity system is a triplet ($m_z = 0, \pm 1$) (Yoshioka and Ohashi, 1998). This suggestion needs exploring further.

2. Antiferromagnetic coupling

In a normal metal Kondo screening corresponds to $J_{eff} \rightarrow \infty$ and hence scattering in the unitarity limit, with the scattering phase shift, $\delta \rightarrow \pi/2$. The Hartree-Fock analysis (Shiba, 1973) is insufficient to fully describe this effect.

Several authors considered the limit $T_K \ll \Delta$ (Müller-Hartmann, 1973; Soda *et al.*, 1967; Zittartz and Müller-Hartmann, 1970), and found the position of the localized excited state with various degrees of accuracy. In this regime the localized state lies close to the gap edge, as it does for the ferromagnetic coupling. In the opposite limit, $T_K \gg \Delta$ approximate solution for the position and the residue of the bound state was obtained

in Refs. (Müller-Hartmann, 1973; Zittartz and Müller-Hartmann, 1970), however, the results were inexact due to the nature of their approximation. Later, within the local Fermi liquid approach, the energy of the bound state in this limit was found to be (Matsuura, 1977)

$$\epsilon = \frac{1 - \alpha^2}{1 + \alpha^2}, \quad (11.3)$$

where

$$\alpha \approx \frac{\pi\Delta}{4T_K} \ln \frac{4eT_K}{\pi\Delta}. \quad (11.4)$$

This result clearly shows that the phase shift of scattering depends on the ratio T_c/T_K .

The properties of the bound state, including its position and spectral weight, for arbitrary values of T_K/T_c were obtained with the help of NRG (Sakai *et al.*, 1993; Satori *et al.*, 1992). They found level crossing similar to the quantum phase transition (discussed above) at $T_K/\Delta \sim 0.3$. For $T_K/\Delta > 0.3$ the impurity moment is largely quenched by the time the depletion of states caused by superconductivity affects screening. In that case the ground state is a Kondo-screened singlet, while the excited intra-gap state is a doublet with the spectral weight $\nu \approx 2$ for $T_K\Delta \gg 1$, corresponding to a single-particle state. Here ν is defined from

$$-\frac{1}{\pi} \text{Im}G(\omega + i\delta)/\pi = \frac{\nu}{2} \left[\delta(\omega - E_0) + \delta(\omega + E_0) \right]. \quad (11.5)$$

On the other hand, for $T_K\Delta < 0.3$ the Kondo effect is suppressed by the opening of the superconducting gap, the ground state is a doublet corresponding to a free spin state, while the bound excited state is a Kondo singlet. The spectral weight, $\nu \approx 0.5$ for $T_K \ll \Delta$, and changes discontinuously at the phase transition point.

Level crossing means that the bound state is at zero energy for $T_K/\Delta \approx 0.3$, while it is close to the gap edge for both $T_K \gg \Delta$ and $T_K \ll \Delta$. Numerical results show that the energy of the bound state is not symmetric with respect to the crossing point: $E_0/\Delta < 0.5$ for $0.03 \lesssim T_K/\Delta \lesssim 1$ (Satori *et al.*, 1992).

3. Anisotropic exchange and orbital effects

Several more complicated aspects of Kondo screening in superconductors attracted attention in recent years, and we review them briefly, referring the reader to the original papers for further information. Anisotropic exchange interaction, $J_z \neq J_{\pm}$, allows the investigation of the crossover between the Ising regime, $J_{\pm} = 0$, when the spin-flip is disallowed and there is no Kondo screening, and the isotropic exchange considered so far. The main features of the phase diagram are discussed by (Yoshioka and Ohashi, 1998), and new phases occur on the ferromagnetic side. In particular, these authors find an extended regime of Ising-dominated ground state even

for $J_{\pm} \neq 0$. In addition, they find small regions of the phase diagram around isotropic ferromagnetic and Ising antiferromagnetic lines, where there exist two localized intra-gap states. They also obtain a perturbative analytic expression for the shift of the bound state energy due to anisotropy of the interaction.

Using the numerical RG approach to analyse Anderson's model allows to interpolate between asymmetric magnetic scattering, Kondo problem, and non-magnetic scattering, including resonance $U = 0$ limit (Yoshioka and Ohashi, 2000). In particular, the crossover from magnetically induced bound state to the resonance non-magnetic scattering regime (Machida and Shibata, 1972) was studied.

Finally, so far we only discussed purely s -wave superconductors. Fully gapped systems include also materials with a complex order parameter combining two (or more) out of phase unconventional gaps, such as $d_{x^2-y^2} + id_{xy}$, or $p_x + ip_y$. In both of these cases Cooper pairs have orbital degrees of freedom that also couple to the impurity spins, leading to multichannel Kondo effect. In addition, for p -wave pairing, the total spin of Cooper pairs is $s = 1$, so that non-trivial changes in screening occur depending on whether the impurity spin $S = 1/2$ or $S = 1$. The NRG analysis of the Kondo problem in this system was carried out very recently (Koga and Matsumoto, 2002a,b; Matsumoto and Koga, 2002). They found that the two order parameters are indistinguishable when only $l = 0$ impurity scattering partial wave is taken into account, i.e. only the depletion of the density of states due to the gap, rather the spin structure of the Cooper pair dictated the Kondo screening. In that case the moment of the ground state is determined by the orbital structure of the Cooper pair. However, inclusion of higher harmonics with $l \neq 0$ for scattering (extended impurity potential), leads to some novel dependencies of the screening and ground states on the exchange couplings.

B. Kondo effect in gapless superconductors

The systems analysed above are either metals with a constant DOS at the Fermi surface, or superconductors with a hard gap. Gapless superconductors, such as d -wave, with the power law DOS, $N(E) \propto |E|^r$ with $r > 0$, present a new situation that attracted much attention in recent years. The Kondo effect in systems where the host single particle density of states follows a power law, has been studied intensively (Borkowski and Hirschfeld, 1992, 1994; Bulla *et al.*, 2000, 1997; Cassanello and Fradkin, 1996, 1997; Chen and Jayaprakash, 1995; Gonzalez-Buxton and Ingersent, 1998; Han *et al.*, 2002, 2004; Ingersent, 1996; Ingersent and Si, 1998; Itoh, 1993; Logan and Glossop, 2000; Polkovnikov, 2002; Polkovnikov *et al.*, 2001; Vojta, 2001; Vojta and Bulla, 2001; Withoff and Fradkin, 1990; Zhang *et al.*, 2001, 2002; Zhu and Ting, 2001a,c). Notice that considering the Kondo effect in a system with the power law dependence of the DOS is not

the same as analysing the competition between superconducting and Kondo correlations for a d -wave systems.

Fradkin and co-workers (Cassanello and Fradkin, 1996, 1997; Withoff and Fradkin, 1990) first employed a combination of the poor man's scaling argument and the large- N approach to spin- $\frac{1}{2}$ impurity for $0 < r \leq 1$, and showed that for all $r > 0$, there is a critical coupling value, J_c , such that (i) at $J < J_c$ the system is in the weak-coupling regime when the Kondo interaction is irrelevant ($J = 0$ is a stable fixed point), and the impurity decouples from the band; (ii) For $J > J_c$ Kondo screening takes place. Further studies based on the NRG approach (Chen and Jayaprakash, 1995; Ingersent, 1996) identified particle-hole asymmetry as a key factor in determining the low-temperature physics. Their analysis indicated that even at $J = \infty$ the impurity spin is only partially screened. In the particle-hole symmetric case, for $0 < r \leq \frac{1}{2}$, there exists a critical coupling J_c , above which the $J = \infty$ fixed point becomes stable. In contrast, for $r > \frac{1}{2}$, the moment remains unscreened as the exchange $0 < J < \infty$ renormalizes to zero. When the particle-hole symmetry is broken by introducing a static potential scattering at the impurity, a critical J_c exists for an arbitrary r . For a fixed value of r ($\geq \frac{1}{2}$), the critical coupling depends strongly on the potential scattering. Detailed dependence of J_c on the potential scattering is complicated and readers are referred to (Ingersent, 1996).

In real systems, the power-law variation of $N(\epsilon)$ is restricted to an energy range $|\epsilon| \leq \Delta_0$, with $N(\epsilon) \approx N(\Delta)$ for $\Delta_0 < |\epsilon| \leq W$. The NRG approach gave results entirely consistent with those known for gapped systems (The full gap $2\Delta_0$ in the spectrum corresponds to $r = \infty$ limit). For the particle-hole symmetric case, an impurity in an insulator retains its moment, no matter how large J is. Away from particle-hole symmetry, the spin is screened provided that $J > J_c \approx 2W/\ln(W/\Delta_0)$ (Takegahara *et al.*, 1992). Formation and screening of the local moments in d -wave superconductors has been investigated using the variational wave function approach (Simon and Varma, 1999).

The Hamiltonian of a magnetic impurity in a metal with a non-trivial DOS is

$$H = \sum_{\sigma} \int_{-\infty}^{\infty} d\epsilon N(\epsilon) \epsilon c_{\epsilon\sigma}^{\dagger} c_{\epsilon\sigma} + \frac{1}{N_L} \sum_{k,k'} [(U_0 + \frac{J}{2}) c_{k\uparrow}^{\dagger} c_{k'\uparrow} + (U_0 - \frac{J}{2}) c_{k\downarrow}^{\dagger} c_{k'\downarrow}] + \frac{J}{2} \sum_{k,k'} [c_{k\uparrow}^{\dagger} c_{k'\downarrow} S_- + c_{k\downarrow}^{\dagger} c_{k'\uparrow} S_+], \quad (11.6)$$

where $N(\epsilon)$ is the electron density of states, N_L is the lattice size, and we included both potential scattering and exchange.

Interest in the Kondo impurities in d -wave systems is motivated by the recent STM and NMR experiments around single impurities in the high- T_c cuprates. Zn and Ni are believed to replace Cu in the cooper-oxide plane and change the local electronic structure without changing net carrier concentration. Simple valence counting

suggests that, if Zn and Ni impurities maintain a nominal Cu^{2+} charge, the Zn^{2+} has $(3d)^{10}$, $S = 0$ configuration and acts as a nonmagnetic impurity. In contrast Ni^{2+} is in $(3d)^8$, $S = 1$ state and is magnetic. Direct comparison between the two cases is difficult.

Nuclear magnetic resonance (NMR) experiments performed with nonmagnetic spin-0 (Zn,Li,Al) in doped cuprates (Alloul *et al.*, 1991; Ishida *et al.*, 1993, 1996; Mahajan *et al.*, 1994, 2000; Mendels *et al.*, 1999) showed clearly that these impurities induce a local $S = \frac{1}{2}$ moment on the nearest-neighbor Cu. It was also demonstrated that the magnetic properties associated with the substitution of these impurities strongly depend on the hole doping: In the underdoped regime, the susceptibility obeys Curie's law below the superconducting transition temperature T_c . Near optimal doping, the Kondo screening (albeit strongly reduced) may persist to the lowest T .

NMR shows that the induced moment is spatially distributed around the impurity. It is important to emphasize that this moment is merely a particular bound state of conduction electrons near the impurity and the precise form of the interaction of the induced moment with other conduction electrons is *a priori* unknown. Kondo effect in the cuprates does not simply stem from the screening of the pre-formed local moment: Moment formation and screening (as well as pairing) result from the same bare interactions.

Nonetheless, in the absence of the microscopic theory of high- T_c superconductivity, many authors use the ideas of the Kondo screening as a starting point for the analysis of experiments. Moreover, in most unconventional superconductors other than cuprates, the properties of a magnetic impurity embedded in a superconductor is a well defined theoretical problem. The Hamiltonian consists of an unconventional (d -wave in our case) BCS state \mathcal{H}_{BCS} , a potential scattering term \mathcal{H}_{pot} , and a magnetic term \mathcal{H}_{mag} . The magnetic term can be described by either Anderson impurity model or Kondo exchange model, and the impurity spin can be either localized at a single site or spatially distributed in its vicinity. For the Anderson model with the single-site coupling, the magnetic term is given by:

$$\mathcal{H}_{mag} = \sum_{k\sigma} [V_{kd} c_{k\sigma}^{\dagger} d_{\sigma} + H.c.] + \epsilon_d \sum_{\sigma} d_{\sigma}^{\dagger} d_{\sigma} + U_d n_{d\uparrow} n_{d\downarrow}. \quad (11.7)$$

In the strong U_d limit, the Anderson model can be mapped onto a Kondo s-d exchange model through the Schrieffer-Wolff transformation (Hewson, 1993), leading to

$$\mathcal{H}_{mag} = J \mathbf{s}_0 \cdot \mathbf{S}, \quad (11.8)$$

where $\mathbf{s}_0 = \frac{1}{2} \sum_{\sigma\sigma'} c_{0\sigma}^{\dagger} \boldsymbol{\sigma}_{\sigma\sigma'} c_{0\sigma'}$ is the spin operator for the conduction electron at the impurity site. For multi-site coupling

$$\mathcal{H}_{mag} = \sum_{I\sigma} [V_{Id} c_{I\sigma}^{\dagger} d_{\sigma} + H.c.] + \epsilon_d \sum_{\sigma} d_{\sigma}^{\dagger} d_{\sigma} + U_d n_{d\uparrow} n_{d\downarrow}, \quad (11.9)$$

where I is the set of nearest neighbors sites

$$\mathcal{H}_{mag} = \sum_I J_I \mathbf{s}_I \cdot \mathbf{S}. \quad (11.10)$$

The Anderson impurity model for a single-site coupling in d -wave superconductors, Eq. (11.7), was studied by Zhang, Hu, and Yu (Zhang *et al.*, 2001). A sharp localized resonance above the Fermi energy was predicted for the impurity state. The marginal Fermi liquid behavior, i.e. logarithmic, in frequency, self-energy, and a linear relaxation rate were also obtained, indicating a new universality class for the strong coupling fixed point. Almost at the same time, the multi-site coupling Anderson impurity model, Eq. (11.9) was considered by Zhu and Ting (Zhu and Ting, 2001a,b) while the multi-site coupling Kondo impurity was studied by Polkovnikov, Sachdev, and Vojta (Polkovnikov, 2002; Polkovnikov *et al.*, 2001). All these works show the existence of Kondo resonance. The low energy structure of spectral weight of the conduction electrons was found to be sensitive to the local environment surrounding the dynamic impurity. The on-site potential scattering was taken to be either zero (Zhang *et al.*, 2001) or very weak (Polkovnikov, 2002; Polkovnikov *et al.*, 2001) and the resonance peak was close to the Fermi energy. Zhu and Ting (Zhu and Ting, 2001a) took into account the quasiparticle scattering from a geometrical hole, where electrons are allowed to hop onto the four neighbors of the impurity site, and obtained a double-peak structure around the Fermi energy. Further (Zhu and Ting, 2001b) considered the potential scattering term to be in the unitary limit ($U \rightarrow \infty$), and found that the Kondo screening and the strong potential scattering together determine the low energy quasiparticle states. The delicate influence of the potential scattering on the Kondo physics as well as the local electronic structure in d -wave superconductors has been re-emphasized by Vojta and Bulla (Vojta and Bulla, 2001).

Here we present a discussion based on the multi-site coupling Kondo impurity model, as given by Eq. (11.10). As demonstrated in previous sections, the problem of a single-site potential scattering can be exactly solved. In the Nambu space, the full matrix Green's function is

$$G(i, j; i\omega_n) = G^0(i, j; i\omega_n) + G^0(i, 0; i\omega_n) T(i\omega_n) G^0(0, j; i\omega_n) \quad (11.11)$$

where the T -matrix due to the potential scatterer is

$$T^{-1}(i\omega_n) = \tau_3/U - G^0(0, 0; i\omega_n), \quad (11.12)$$

and G^0 is the Green's function for the clean system. In the presence of both potential and magnetic scattering the Green's function is:

$$\begin{aligned} \tilde{G}(i, j; i\omega_n) &= G(i, j; i\omega_n) + \sum_{l, l'} \varphi_l \varphi_{l'} G(i, l; i\omega_n) \mathcal{T}_K(i\omega_n) \\ &\quad \times G(l', j; i\omega_n). \end{aligned} \quad (11.13)$$

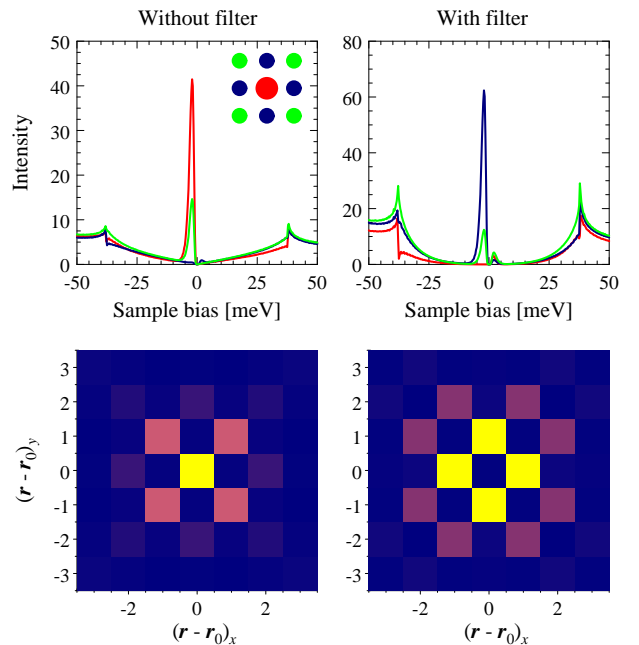


FIG. 28 Calculated tunneling density of states for the four-site Kondo impurity model at 15% hole doping with a realistic band structure ($t = 0.15$ eV, $t' = -t/4$, $t'' = t/12$), $\Delta_0 = 0.04$ eV, and $\mu = -0.14$ eV. The Kondo coupling is $J = 0.09$ eV, the potential scattering $U = 0$. Top: Local DOS vs. energy for the impurity site (red) and the nearest (blue) and second (green) neighbor sites. Bottom: Spatial dependence of the local DOS at $\omega = -2$ meV. Left: Local DOS in the CuO_2 plane. Right: Local DOS after applying the filter effect proposed by Martin, Balatsky, and Zaanen (Martin *et al.*, 2002). From Vojta and Bulla (Vojta and Bulla, 2001)

Here l and l' label the nearest neighbors to the impurity site at $(0,0)$, and \mathcal{T}_K is the T -matrix for the Kondo impurity. The variables φ_l have different meaning depending on the approach to \mathcal{T}_K . In the large- N approximation (equivalent to the slave-boson mean-field theory)

$$\mathcal{T}_K^{-1} = i\omega_n - \lambda\tau_3 - \sum_{l, l'} \varphi_l \varphi_{l'} \tau_3 G(l, l'; i\omega_n) \tau_3, \quad (11.14)$$

and φ_l are the complex Hubbard-Stratonovich fields, which are determined, together with the Lagrange multiplier λ , by the saddle point solution. Within the NRG approach only the strongest d -wave scattering channel is considered, and the variables are taken to be $\varphi_l = +(-)1$ depending on the bond orientation. Note that this d -wave pattern is simply a band structure effect and is not related to the d -wave symmetry of the superconducting order parameter of the host. The LDOS is:

$$\rho_i(\omega) = -\frac{1}{\pi} \text{Im} \left\{ \text{Tr} \left[\tilde{G}(i, i; \omega + i0^+) \frac{1 + \tau_3}{2} \right] \right\}. \quad (11.15)$$

Figures 28–30 show the LDOS for a four-site Kondo impurity and different strength of the potential scattering, calculated using the NRG technique (Vojta and

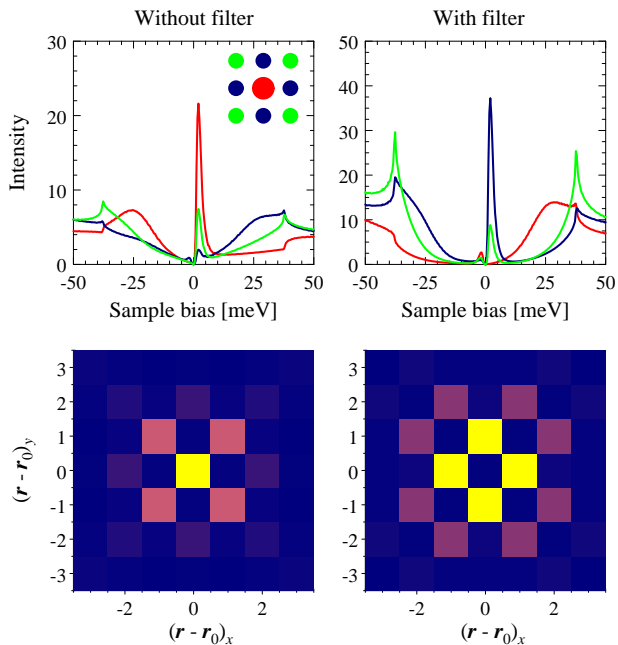


FIG. 29 Same as Fig. 28, but with potential scattering $U = t = 0.15$ eV. Here, $J = 0.065$ eV. The lower panel shows the local DOS at $\omega = +2$ meV. From Vojta and Bulla (Vojta and Bulla, 2001).

Bulla, 2001). It is clear that the spatial structure of the resonance state is sensitive to the strength of the potential scattering: if it is absent, sharp resonance peak appears directly on the impurity site, as well as on its next-nearest neighbors, with reduced intensity. This is consistent with the experimental observations (Pan *et al.*, 2000b). For a moderate value of the potential scattering, as shown in Fig. 29, the global particle-hole asymmetry changes its sign and the Kondo peak appears at the opposite side of the Fermi level compared to Fig. 28. For strong (but finite) potential scattering, the resonance peak due to impurity scattering becomes dominant, and the Kondo effect is weaved into the overall structure of the LDOS. In this case, the intensity of the on-site peak is strongly suppressed, and a double-peak structure with enhanced intensity is seen in the LDOS at the nearest-neighbor sites. The same results were also obtained by Zhu and Ting (Zhu and Ting, 2001a) based on the Anderson impurity model. In this simple model the large LDOS from the resonance state induced by the strong potential scatterer reduces dramatically the critical Kondo coupling, indicating that the fate of the Kondo effect is determined by local rather than global environment in which the magnetic impurity is embedded. In the unitary limit (infinite impurity potential) LDOS has a zero intensity at the impurity site and a sharp single peak at its nearest neighbors. Consequently, to achieve agreement with the pattern observed in experiment, one needs to invoke the filter effect (Martin *et al.*, 2002; Zhu *et al.*, 2000c), which is detailed in Sec. IX.

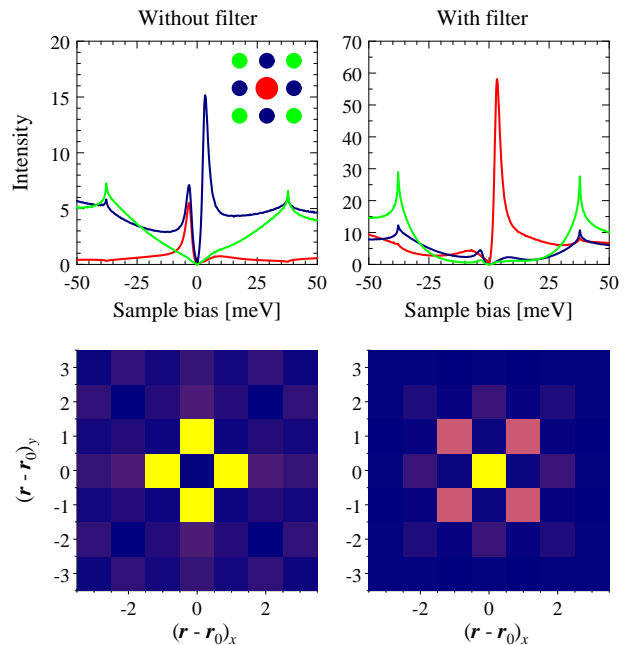


FIG. 30 Same as Fig. 28, but with potential scattering $U = 4t = 0.6$ eV. Here, $J = 0.04$ eV. The lower panel shows the local DOS at $\omega = +3$ meV. From Vojta and Bulla (Vojta and Bulla, 2001).

XII. INELASTIC SCATTERING IN d -WAVE SUPERCONDUCTOR

A. Inelastic scattering: general remarks

Previous section provided the simplest example of an impurity with an internal degree of freedom – spin for the Kondo effect. As a result, we had to extend the previous treatment of static impurities to account for the scattering processes that involve spin flips, which resulted in a qualitatively new behavior. We now take this idea further and explore inelastic scattering processes.

By definition, impurity scattering changes the direction of the quasiparticle momentum. However, purely potential scattering is elastic, i.e. the quasiparticle energy does not change. Kondo impurity affects electron spin, however, the scattering remains elastic: the energies of the spin-up and spin-down impurity states are identical; this degeneracy is at the origin of the Kondo singlet formation. In this section we consider inelastic scattering processes that involve not only momentum but also energy transfer. There are two distinct scenarios for inelastic scattering. One possibility is that impurities themselves are dynamic, and energy is transferred to/from electrons during scattering, only when they are in the immediate vicinity of the impurity. This is an extension of the previous treatment. Another possibility is that electrons scatter off of a delocalized (extended) collective mode, such as a spin wave or a phonon, while the scattering on impurities remains elastic.

We consider the two situations separately. In the former case the impurity induced electron self energy contains the information both about the spatial and the temporal, or dynamical, structure of the impurity. The latter case is even more interesting, as the information about the extended collective mode is encoded in real space Friedel oscillations around the impurity site, and its determination is only possible due to the presence of impurities. Below we discuss a proposal to combine Fourier transform and inelastic tunneling spectroscopy (IETS). Fourier Transformed IETS, which is an extension of the FT-STM discussed above, allows, in principle, the investigation of *both characteristic momentum and energy* of the inelastic scattering. The central object we deal with in this technique is $d^2I(\mathbf{q}, eV)/dV^2$, similar to real space IETS STM (Hahn and Ho, 2001; Stipe *et al.*, 1998). Extension of the IETS analysis to reciprocal space reveals nontrivial features in the spectra with simultaneous momentum and energy resolution.

The rest of the section is devoted to IETS in d-wave superconductors. Similar analysis can be done for the s-wave case, (Brandt, 1970). We expect the IETS features at energies above the gap to be similar for s- and d-wave superconductors, while below the gap a detailed analysis is required.

B. Localized modes in d-wave superconductors

Two examples that we review explicitly are the local vibrational mode (arising, for example, from a substitution atom in the lattice), and the scattering on an impurity spin in an applied magnetic field. Essentially the same techniques are used to analyze both situations, and here we follow (Balatsky *et al.*, 2003; Morr and Nyberg, 2003).

The Hamiltonian for a local distortion coupled to electrons is known from the standard electron-phonon coupling theory. Here, however, the interaction occurs only at the impurity site, so that

$$H = \sum_{k\sigma} \xi_k c_{k\sigma}^\dagger c_{k\sigma} + \sum_k [\Delta_k c_{k\uparrow}^\dagger c_{-k\downarrow}^\dagger + h.c.] + g \sum_\sigma (b^\dagger + b) c_{0\sigma}^\dagger c_{0\sigma}, \quad (12.1)$$

The Hamiltonian for a spin S interacting with the electrons via a contact exchange $J\mathbf{S} \cdot \boldsymbol{\sigma}$ is quite different

$$H = \sum_{\mathbf{k}} \xi(\mathbf{k}) c_{\mathbf{k}\sigma}^\dagger c_{\mathbf{k}\sigma} + \sum_{\mathbf{k}} [\Delta(\mathbf{k}) c_{\mathbf{k}\uparrow}^\dagger c_{-\mathbf{k}\downarrow}^\dagger + h.c.] + \sum_{\mathbf{k}, \mathbf{k}', \sigma, \sigma'} J\mathbf{S} \cdot c_{\mathbf{k}\sigma}^\dagger \boldsymbol{\sigma}_{\sigma\sigma'} c_{\mathbf{k}'\sigma'} + g\mu_B \mathbf{S} \cdot \mathbf{B}. \quad (12.2)$$

The external magnetic field $\mathbf{B} \parallel \hat{\mathbf{z}}$ leads to Zeeman splitting of the spin states by the Larmor frequency, $\omega_0 = g\mu_B B$. If the spin is in an equilibrium with a thermal bath, Zeeman splitting of spin levels is exactly analogous to the frequency of a local mode, and electron can scatter off the spin inelastically. We focus on the latter case.

In Eq.(12.2) we used a mean field description of superconducting state, and ignored both orbital and Zeeman effect of the field on the conduction electrons. This is justified for $B \ll H_{c2}$ ⁸. In the following we choose $|S| = 1/2$, and consider a d-wave superconductor, $\Delta(\mathbf{k}) = \frac{\Delta}{2}(\cos k_x - \cos k_y)$ at low temperatures $T \ll T_c$. Clearly, this treatment is only justified when the spin is not screened via Kondo interaction at low T .

Since spin splitting (and hence the inelastic scattering) involves only the components transverse to the field, the information about the scattering, to second order, is contained in the self-energy with normal Green's function:

$$\Sigma(\omega_l) = J^2 T \sum_{\mathbf{k}, \Omega_n} G(\mathbf{k}, \omega_l - \Omega_n) \chi^{+-}(\Omega_n), \quad (12.3)$$

Here the spin propagator $\chi(\tau) = \langle T_\tau S^+(\tau) S^-(0) \rangle$ in the frequency space is given by $\chi_0(\omega) = \langle S^z \rangle / (\omega_0^2 - (\omega + i\delta)^2)$. For local mode that present on a single site there is no contribution to Σ from the anomalous Green's function as $\sum_{\mathbf{k}} F(\mathbf{k}, \omega) = 0$. For a free spin in a field $\langle S_z \rangle = \tanh(\omega_0/2T)/2$, but we keep the notation $\langle S_z \rangle$ to account for magnetic anisotropy. The functional form of the propagator is identical to that of a phonon mode, and therefore subsequent analysis is applicable to both situations.

In Eq.(12.3) the Green's function is determined self-consistently, $G^{-1} = G^{(0)-1} - \Sigma$, where $G^{(0)}$ is the Green's function of the pure d-wave superconductor, and $\Omega_l(\omega_l)$ are the bosonic (fermionic) Matsubara frequencies. After analytic continuation to real axis, $i\omega_n \rightarrow \omega + i\delta$, we find for the imaginary part of the self energy

$$\text{Im}\Sigma(\omega) = -J^2 \langle S_z \rangle \text{Im}G(\omega - \omega_0) [n_F(\omega - \omega_0) - n_B(\omega_0) - 1], \quad (12.4)$$

where $n_{F(B)}(\omega) = 1/[1 + (-)\exp(\beta\omega)]$ are Fermi (Bose) distribution functions. All the information about the tunneling DOS is contained in the self-energy. The modifications of the superconducting order parameter and bosonic propagator are ignored here.

Fig. 31 shows the results for local density of states at the impurity site, solved numerically by finding Σ and G . To proceed with analytical treatment we limit ourselves below to second order scattering in Σ . We find that the differences between the self-consistent solution and the second order calculation are only quantitative. To that accuracy, the corrections to the Green's function are $G(\mathbf{r}, \mathbf{r}', \omega) = G^0(\mathbf{r}, \mathbf{r}', \omega) + G^0(\mathbf{r}, 0, \omega) \Sigma(\omega) G^0(0, \mathbf{r}', \omega) + F^0(\mathbf{r}, 0, \omega) \Sigma(\omega) F^{*0}(0, \mathbf{r}, \omega)$. We define $K(T, \omega, \omega_0) = -[n_F(\omega - \omega_0) - n_B(\omega_0) - 1]$, and focus on the $T \ll \omega_0$, when $K(T, \omega, \omega_0) \simeq \Theta(\omega - \omega_0)$. From this expression, the correction to the LDOS at point

⁸ To minimize the orbital effect of magnetic field one can apply it parallel to the surface of a superconductor. The magnetic field is screened on the scale of penetration depth so that its effect on the superconducting electrons is small.

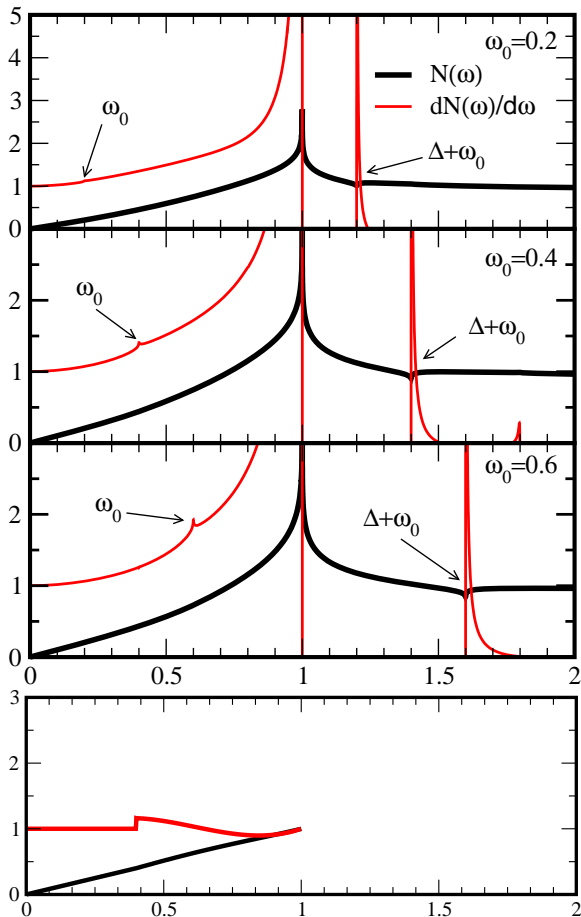


FIG. 31 The DOS (black line) and its derivative (red line) for a local boson mode scattering in a d -wave superconductor. The normal self-energy was treated self-consistently in Eq. (12.4). We ignored vertex corrections and gap modification. In addition to the feature at $\omega = \omega_0$ we find strong satellite peaks at $\Delta + \omega_0$ resulting from the coherence peak in the DOS of a d -wave superconductor. Satellites are not present in the pseudogap state with no ODLRO. These features are best seen in $\frac{dN}{d\omega}$. Energy is in units of Δ , the dimensionless coupling constant is 1. The top three panels are for local mode frequencies $\omega_0/\Delta = 0.2, 0.4, 0.6$. The lower panel shows the asymptotic analytic solution, that assumes $\omega_0 \ll \Delta$ and uses Eq. (12.2), for $\omega_0 = 0.4$. The overall features are similar for both cases, however the analytic solution shows a somewhat larger feature. From (Balatsky *et al.*, 2003)

\mathbf{r} is: $\delta N(\mathbf{r}, \omega) = (1/\pi)\text{Im}[G^0(\mathbf{r}, 0, \omega)\Sigma(\omega)G^0(0, \mathbf{r}, \omega) \pm F^0(\mathbf{r}, 0, \omega)\Sigma(\omega)F^{*0}(0, \mathbf{r}, \omega)]$. Here plus (minus) sign corresponds to the coupling to the local vibrational (spin) mode, i.e to the cases of preserved (broken) time-reversal symmetry. The modification of the LDOS is most pronounced at the impurity site, where we find

$$\frac{\delta N(\mathbf{r} = 0, \omega)}{N_0} = \frac{\pi^2}{2}(JSN_0)^2 \frac{\omega - \omega_0}{\Delta} K(T, \omega, \omega_0) \times \left(\frac{2\omega}{\Delta} \ln \left(\frac{\Delta}{\omega} \right) \right)^2, \quad \omega \ll \Delta, \quad (12.5)$$

$$\frac{\delta N(\mathbf{r} = 0, \omega)}{N_0} = 2\pi^2(JSN_0)^2 K(T, \omega, \omega_0) \ln^2 \left(\frac{|\omega - \Delta|}{4\Delta} \right) \times \ln \left(\frac{4\Delta}{|\omega + \omega_0 - \Delta|} \right) + (\omega_0 \rightarrow -\omega_0), \quad \omega \simeq |\Delta|. \quad (12.6)$$

To obtain this result we retained only the dominant real part of $G^0(0, 0, \omega) = N_0 \frac{2\omega}{\Delta} \ln(\frac{4\Delta}{\omega})$ for $\omega \ll \Delta$, and the dominant imaginary part of $G^0(0, 0, \omega) = i\pi N(\omega) = -2iN_0 \ln(\frac{|\omega - \Delta|}{4\Delta})$, in the opposite limit $\omega \simeq \Delta$. The results for the LDOS $N(\omega)$ and its derivative $\frac{dN(\omega)}{d\omega}$ are shown in the lower panel of Fig. 31.

Away from the impurity site $N(\mathbf{r}, \omega)$ exhibits Friedel oscillations. Standing wave produced by inelastic scattering has fingerprints of the energy transfer: there is a peak (or a cusp) in the derivative of the DOS with respect to energy. These oscillations can be called *inelastic* Friedel oscillation, stressing oscillation nature of inelastic signal d^2I/dV^2 in real space. These oscillations can also be analyzed in reciprocal space, similar to the elastic case IX.D. The real space pattern at $\omega \ll \Delta$ is given by $\Lambda(\mathbf{r}) = [|G^0(\mathbf{r}, \omega)|^2 \pm |F^0(\mathbf{r}, \omega)|^2] \sim \frac{\sin(k_F r)}{(k_F r_{\parallel})^2 + (r_{\perp}/\xi)^2}$. Here we separated $\mathbf{r} = (\mathbf{r}_{\perp}, \mathbf{r}_{\parallel})$ into the components along (\mathbf{r}_{\perp}) and normal to (\mathbf{r}_{\parallel}) the Fermi surface near the nodal point. Existence of the nodes in the superconducting gap leads to the power law decay of $\Lambda(\mathbf{r})$ in all directions, and to its four fold modulation due to gap anisotropy; See (Salkola *et al.*, 1997), and Sec. VII.

It is important to emphasize the differences between the resulting LDOS behavior for a nodal superconductor and a normal metal. For a d -wave superconductor, using the connection between the differential conductance in STM experiments and DOS, we find

$$\delta \frac{dI}{dV} / \frac{dI}{dV} \sim \delta N(\mathbf{r} = 0, V)/N_0 \sim (JSN_0)^2 \frac{V - \omega_0}{\Delta} \Theta(V - \omega_0), \quad \delta \frac{d^2I}{dV^2} \sim (JSN_0)^2 \Theta(V - \omega_0). \quad (12.7)$$

In contrast, for a metal with the energy independent normal state DOS, from Eq. (12.5) for $T \ll \omega_0$

$$\frac{dI}{dV} \sim \delta N(\mathbf{r} = 0, V) \sim J^2 N_0^3 \Theta(V - \omega_0), \quad (12.8)$$

and the second derivative reveal a delta function $d^2I/dV^2 \sim J^2 N_0^3 \delta(\omega - \omega_0)$. We emphasize that the dominant effect is purely due to the energy dependence of the DOS, and therefore both in a d -wave superconductor and in a metal with vanishing DOS $N(\omega) = N_0 \frac{\omega}{\Delta}$ (such as in some of the models of the pseudogap) there is a *step discontinuity* in d^2I/dV^2 at the energy of a local mode with the strength $J^2 N_0^2$ (see Fig. 31).

The result can be generalized to a metal with a power law DOS, $N(\omega) = 1/\pi \text{Im} G^0(0, 0, \omega) = (\omega/\Delta)^\gamma N_0$, with $\gamma > 0$. From Eqs. (12.4-12.5) we have for $\omega \ll \Delta$:

$$\delta \frac{dI}{dV} / \frac{dI}{dV} \sim \delta N(\mathbf{r} = 0, V)/N_0 \sim (V - \omega_0)^\gamma \Theta(V - \omega_0), \quad \delta \frac{d^2I}{dV^2} \sim (V - \omega_0)^{\gamma-1} \Theta(V - \omega_0). \quad (12.9)$$

Thus we find a singularity at ω_0 for $\gamma < 1$, and a power law for $\gamma \geq 1$. For $\gamma = 1$ we recover the result for d -wave superconductor.

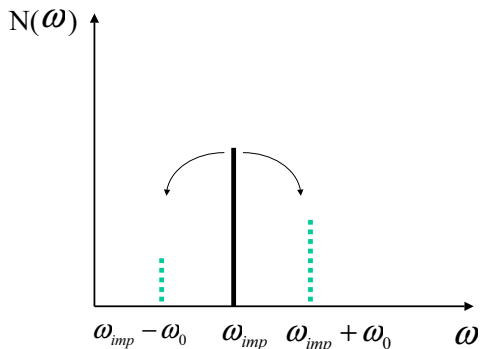


FIG. 32 Satellite peaks for an impurity resonance ω_{imp} at $\omega_{imp} \pm \omega_0$ are shown schematically. The satellites have different spectral weight. If an electron with energy $\omega_{imp} + \omega_0$ is injected into the system, it can excite a local mode and form the bound state at ω_{imp} . Similarly, an injected electron at energy $\omega_{imp} - \omega_0$ can absorb local mode energy to reach ω_{imp} . For the latter process to occur the mode has to be excited, and hence this peak has very low weight at low T. The two processes have different matrix elements. Relative weight of the side peaks is proportional to $J^2 N_0^2$ which we assumed to be small. For magnetic scattering ($\omega_0 = g\mu_B B$) the splitting is tunable by the field. From (Balatsky *et al.*, 2003)

These results can be expressed more generally via the energy spectrum of the superconductor. Using spectral representation for $G(\mathbf{r}, \omega)$ with Bogoliubov's functions $u_\alpha(\mathbf{r}), v_\alpha(\mathbf{r})$ for the eigenstate α ,

$$G(\mathbf{r}, \omega) = \sum_{\alpha} \left[\frac{|u_{\alpha}(\mathbf{r})|^2}{\omega - E_{\alpha} + i\delta} + \frac{|v_{\alpha}(\mathbf{r})|^2}{\omega + E_{\alpha} + i\delta} \right]. \quad (12.10)$$

For $T \ll \omega_0$ we find

$$\text{Im}\Sigma(\omega) = \frac{\pi J^2}{2\omega_0} \langle S_z \rangle [|u_{\alpha}(\mathbf{r} = 0)|^2 \delta(\omega - \omega_0 - E_{\alpha}) + |v_{\alpha}(\mathbf{r} = 0)|^2 \delta(\omega - \omega_0 + E_{\alpha})], \quad \omega > 0. \quad (12.11)$$

In the last equation for $\omega < 0$ we need to symmetrize, $\omega_0 \rightarrow -\omega_0$. Consider a magnetic impurity resonance in a d-wave superconductor at energy ω_{imp} , (such as a Ni resonance in cuprates (Hudson *et al.*, 2001; Salkola *et al.*, 1997)). Then the sum is dominated by the term with resonance level $E_{\alpha} = \omega_{imp}$ in the vicinity of the impurity site. Inelastic scattering produces satellites of the main level *split from it by the energy* ω_0 , see Fig. 32. Similar splitting of occurs for a phonon mode with energy ω_0 .

For cuprates, taking the experimentally measured DOS $N_0 \simeq 1/eV$ with $JN_0 \simeq 0.14$, $\Delta = 30meV$ (Hudson *et al.*, 2001) and assuming the field of $\sim 10T$ we find $\omega_0 = 1meV$. Then from Eqs. (12.5-12.7)

$$\delta N(\mathbf{r} = 0, \omega)/N_0 \simeq 10^{-2} \frac{\omega - \omega_0}{\Delta} \Theta(\omega - \omega_0). \quad (12.12)$$

For observation of this effect one has to sample DOS in the vicinity of $eV = \omega_0 \propto B$. Assuming $\omega - \omega_0 = \omega_0$ we have from Eq. (12.12) $\delta \frac{dI}{dV} / \frac{dI}{dV} \sim 10^{-2}$. Expressed as a relative change of DOS of a superconductor $N(\omega) = N_0 \omega / \Delta$ effect is:

$$\delta \frac{dI}{dV} / \frac{dI}{dV} \sim \delta N(\mathbf{r} = 0, \omega) / N(\omega_0) \sim 10^{-2} \frac{\omega - \omega_0}{\omega_0} \Theta(\omega - \omega_0). \quad (12.13)$$

It is of the same order as the observed vibrational modes of localized molecules in inelastic electron tunneling spectroscopy STM, IETS-STM (Hahn and Ho, 2001; Stipe *et al.*, 1998). The satellites at $\Delta + \omega_0$ produce the effect of the order unity, and are clearly seen even for small coupling. The important difference with phonons is that for a localized spin scattering the kink in DOS is *tunable* with magnetic field which makes its detection easier.

The proposed extension of the inelastic tunneling spectroscopy on the strongly correlated electrons states, such as a d-wave superconductor and pseudogap normal state opens possibilities to study the dynamics of local spin and vibrational excitations. The DOS in these systems often has power law energy dependence, $N(\omega) \sim \omega^{\gamma}$, $\gamma > 0$, resulting in weaker features than in normal metals. This technique allows for Zeeman level spectroscopy of a single magnetic center, thus allowing, in principle, single spin detection. The feature in $dI/dV \sim (\omega - \omega_0)^{\gamma-1} \Theta(\omega - \omega_0)$ near the threshold energy ω_0 is due to inelastic scattering. One also finds strong satellite features near the gap edge due to coherence peak for a superconducting case. The singularity in the derivative of the conductance is of a power law type, and qualitatively different from the results for metallic DOS (Hahn and Ho, 2001; Stipe *et al.*, 1998). For the relevant values of parameters for high- T_c the feature is expected to be on the order of several percents and should be observable. Similar predictions are also applicable to the local vibrational modes, where ω_0 is the mode frequency.

C. Interplay between collective modes and impurities in d-wave superconductors

We have focused so far on the IETS for local modes, where inelastic scattering occurs only on one site. Here we extend the discussion to the case of a collective mode. In real systems this may be a spin (Abanov *et al.*, 2002; Campuzano *et al.*, 1999; Eschrig and Norman, 2000; Kee *et al.*, 2002; Norman and Ding, 1998) or lattice (Damascelli *et al.*, 2003; Gweon *et al.*, 2004; Lanzara *et al.*, 2004) mode.

We are motivated by the possible connection between the kink in the quasiparticle dispersion found in ARPES data on cuprates, and phonon modes (and, possibly, interactions that lead to superconductivity) (Damascelli *et al.*, 2003; Gweon *et al.*, 2004; Lanzara *et al.*, 2004). Efforts to relate the data from ARPES, STM, and transport measurements in cuprates have recently intensified (Scalapino *et al.*, 2004; Zhu *et al.*, 2004c). It was

also suggested that the full Eliashberg function in frequency *and momentum* space may be extracted from ARPES (Vekhter and Varma, 2003), and the challenge is to design a similar procedure to use with IETS STM.

At first glance it seems that local probes have poor momentum resolution since they couple to LDOS, which is summed over all momenta, and cannot identify the momentum dependence of the collective modes. We argue that this is a misconception, and the FT IETS can provide the momentum spectroscopy of the modes that produce inelastic scattering.

The elastic FT STM can identify the Fermi wave vectors because of Friedel oscillations in the electron density due to impurities, see Sec. IX.D. For the FT IETS, we need impurity scattering to produce interference waves in real space. Hence we look at the features arising from the interplay between dynamic scattering off the collective mode and static disorder. We use the Fourier transform of the LDOS as a tool to investigate the characteristic momentum and energy features containing the fingerprints of the bosonic excitations (Zhu *et al.*, 2004a).

We call this approach the Fourier transformed inelastic electron tunneling spectroscopy STM (FT-IETS STM). The central object in this technique is the Fourier transform of the second derivative of the tunneling current, $d^2I/dV^2(\mathbf{q}, eV)$. The energy signatures of the quasiparticle interaction with the collective mode, and the real space pattern of the scattering of the same quasiparticles from a local impurity combine to produce features containing the information about the energy and momentum of the mode in $d^2I/dV^2(\mathbf{r}, eV)$. Fourier transform map of this quantity could help to uncover the characteristic momenta of the mode, just as conventional Friedel oscillations encode the Fermi wavevector in $d^2I/dV^2(\mathbf{r}, E)$, see Sec. XII.B.

To illustrate this idea consider a spin resonance mode, such as that revealed by neutron scattering in cuprates (Abanov *et al.*, 2002; Campuzano *et al.*, 1999; Eschrig and Norman, 2000; Kee *et al.*, 2002; Norman and Ding, 1998). STM was proposed to be used for its detection (Zhu *et al.*, 2004a). We limit consideration to the example of a sharp mode at the wave vector $\mathbf{Q} = (\pi, \pi)$ with energy $\omega_0 = 42$ meV. This assumption allows to highlight the effect, but the formalism presented here is equally applicable to the case where mode spectral density is distributed in energy and momentum.

We have to keep track of the self-energy effects as a function of energy as well as momentum. Inelastic scattering of quasiparticles requires considering the off shell excitations, up to energies $\Delta + \Omega_0 \sim 70$ meV. At these energies the Fermi surface effects, typical wave vectors of the collective mode and typical wave vectors of the impurity potential all determine the momentum dependence of the inelastic tunneling features seen in FT IETS

STM.⁹

We start with a model Hamiltonian describing two-dimensional electrons coupled to a collective spin mode and in the presence of disorder:

$$\mathcal{H} = \mathcal{H}_{BCS} + \mathcal{H}_{sp} + \mathcal{H}_{imp}. \quad (12.14)$$

Here the BCS-type Hamiltonian is given by $\mathcal{H}_{BCS} = \sum_{\mathbf{k}, \sigma} (\varepsilon_{\mathbf{k}} - \mu) c_{\mathbf{k}\sigma}^\dagger c_{\mathbf{k}\sigma} + \sum_{\mathbf{k}} (\Delta_{\mathbf{k}} c_{\mathbf{k}\uparrow}^\dagger c_{-\mathbf{k}\downarrow}^\dagger + \Delta_{\mathbf{k}}^* c_{-\mathbf{k}\downarrow} c_{\mathbf{k}\uparrow})$, where $\varepsilon_{\mathbf{k}}$ is the normal state dispersion, μ the chemical potential, and $\Delta_{\mathbf{k}} = \frac{\Delta_0}{2} (\cos k_x - \cos k_y)$ the d -wave superconducting energy gap. The coupling between the electrons and the resonance mode is modeled by $\mathcal{H}_{sp} = g \sum_i \mathbf{S}_i \cdot \mathbf{s}_i$, where g , \mathbf{s}_i , and \mathbf{S}_i are the coupling strength, the electron spin operator at site i , and the operator for the collective spin degrees of freedom, respectively. Dynamics of the collective mode is specified by spin \mathbf{S} susceptibility $\chi_{ij}(\tau)$, defined below. The quasiparticle scattering from impurities in the Hamiltonian is given by $H_{imp} = \sum_{i\sigma} U_i c_{i\sigma}^\dagger c_{i\sigma}$, where U_i is the strength of the impurity potential, and we consider weak (Born) scattering. One of the interesting findings is that characteristic wave vectors of the impurity potential $U_{\mathbf{q}} = \sum_i U_i \exp(i\mathbf{q} \cdot \mathbf{r}_i)$ play a crucial role in defining characteristic wave vectors of the DOS modulation. For simplicity, we consider only nonmagnetic scattering.

By introducing a two-component Nambu spinor operator, $\Psi_i = (c_{i\uparrow}, c_{i\downarrow}^\dagger)^T$, one can define the matrix Green's function for the full Hamiltonian system, $\hat{G}(i, j; \tau, \tau') = -\langle T_\tau [\Psi_i(\tau) \otimes \Psi_j^\dagger(\tau')] \rangle$. Simple algebra leads to the full electron Green's function with impurity scattering:

$$\begin{aligned} G(i, j; i\omega_n) &= \tilde{G}^{(0)}(i, j; i\omega_n) \\ &+ \sum_{j'} U_{j'} [\tilde{G}^{(0)}(i, j'; i\omega_n) \tilde{G}(j', j; i\omega_n) \\ &- \tilde{F}^{(0)}(i, j'; i\omega_n) \tilde{F}^{(0)}(j', i; i\omega_n)] \end{aligned} \quad (12.15)$$

Here $\tilde{G}^{(0)}$, $\tilde{F}^{(0)}$, $\tilde{F}^{*(0)}$ are the dressed by collective mode scattering normal and anomalous Green's function, with its Fourier component given by 11, 12 and 21 components of the full matrix Green's function:

$$[\hat{G}^{(0)}]^{-1}(\mathbf{k}; i\omega_n) = \begin{pmatrix} i\omega_n - \xi_{\mathbf{k}} - \Sigma_{11} & -\Delta_{\mathbf{k}} - \Sigma_{12} \\ -\Delta_{\mathbf{k}} - \Sigma_{21} & i\omega_n + \xi_{\mathbf{k}} - \Sigma_{22} \end{pmatrix}, \quad (12.16)$$

where $\xi_{\mathbf{k}} = \varepsilon_{\mathbf{k}} - \mu$, $\omega_n = (2n + 1)\pi T$ is the fermionic Matsubara frequency. When quasiparticles scatter inelastically off of the collective mode, the self-energy, to the second order in the coupling constant, is

$$\hat{\Sigma}(\mathbf{k}; i\omega_n) = \frac{3g^2T}{4} \sum_{\mathbf{q}} \sum_{\Omega_l} \chi(\mathbf{q}; i\Omega_l) \hat{G}^{(0)}(\mathbf{k} - \mathbf{q}; i\omega_n - i\Omega_l), \quad (12.17)$$

⁹ We limit ourselves to the second order scattering between carriers and bosonic excitations and at this level there is no conceptual difference in the method for spin or phonon bosonic mode.

where $\chi(\mathbf{q}; i\Omega_l)$ is the dynamical spin susceptibility $\chi_{ij}(\tau) = \langle T_\tau(S_i^x(\tau)S_j^x(0)) \rangle$ and $\Omega_l = 2l\pi T$ the bosonic Matsubara frequency, $\hat{G}^{(0)}$ is the bare superconducting Green's function and $\hat{G}^{(0)}$ is the superconducting Green's function dressed by scattering of the collective mode, but without disorder. We assume that the d -wave pair potential is real. For a single-site impurity, the equation of motion for the full Green's function can be exactly solved, see above. For multiple impurities, and especially for the inhomogeneous situation, an approximation scheme for $\hat{\Sigma}$ is in order. In the Born limit, the normal Green's G function is found to be:

$$G(i, j; i\omega_n) = \tilde{G}^{(0)}(i, j; i\omega_n) + \delta G(i, j; i\omega_n) \quad (12.18)$$

with

$$\delta G(i, j; i\omega_n) = \sum_{j'} U_{j'} [\tilde{G}^{(0)}(i, j'; i\omega_n) \tilde{G}^{(0)}(j', j; i\omega_n) - \tilde{F}^{(0)}(i, j'; i\omega) \tilde{F}^{*(0)}(j', j; i\omega_n)] . \quad (12.19)$$

The LDOS at site i , summed over spin components, is

$$\rho(\mathbf{r}_i, E) = -\frac{2}{\pi} \text{Im} G(i, i; E + i\gamma) , \quad (12.20)$$

where $\gamma = 0^+$. We are especially interested in the correction to the LDOS from the impurity scattering,

$$\delta\rho(\mathbf{r}_i, E) = -\frac{2}{\pi} \text{Im} \delta G(i, i; E + i\gamma) , \quad (12.21)$$

and its Fourier transform,

$$\begin{aligned} \delta\rho(\mathbf{q}, E) &= \sum_i \delta\rho(i, E) e^{-i\mathbf{q}\cdot\mathbf{r}_i} \\ &= -\frac{U_{\mathbf{q}}}{N\pi i} \sum_{\mathbf{k}} [\tilde{G}^{(0)}(\mathbf{k} + \mathbf{q}; E + i\gamma) \tilde{G}^{(0)}(\mathbf{k}; E + i\gamma) \\ &\quad - \tilde{G}^{(0)*}(\mathbf{k} - \mathbf{q}; E + i\gamma) \tilde{G}^{(0)*}(\mathbf{k}; E + i\gamma) \\ &\quad - \tilde{F}^{(0)}(\mathbf{k} + \mathbf{q}; E + i\gamma) \tilde{F}^{*(0)}(\mathbf{k}; E + i\gamma) \\ &\quad + \tilde{F}^{(0)*}(\mathbf{k} - \mathbf{q}; E + i\gamma) \tilde{F}^{(0)}(\mathbf{k}; E + i\gamma)] \quad (12.22) \end{aligned}$$

Here $U_{\mathbf{q}} = \sum_i U_i e^{-i\mathbf{q}\cdot\mathbf{r}_i}$ is the Fourier transform of the scattering potential. It multiplies the entire result, and directly affects the FT IETS image. For example, if $U_{\mathbf{q}}$ has a strong peak at $\mathbf{q} = \mathbf{q}_0$, it will result in a spurious peak in the FT IETS image, not related to the characteristic momenta for the inelastic scattering. Detailed knowledge of the impurity scattering is necessary for extracting the intrinsic scattering momenta from FT IETS STM.

The local density of states is proportional to the local differential tunneling conductance (i.e., dI/dV). To look into the renormalization effect of collective bosonic excitations in the STM, the energy derivative of the LDOS, corresponding to the derivative of the local differential tunneling conductance (i.e., d^2I/dV^2), is more favorable to enhance the signal. For a fixed value of energy, one first gets a set of $\delta\rho'(i, E)$ (the prime \prime means the energy

derivative) in real space, and then performs the Fourier transform:

$$\delta\rho'(\mathbf{q}, E) = \sum_i \delta\rho'(\mathbf{r}_i, E) e^{-i\mathbf{q}\cdot\mathbf{r}_i} , \quad (12.23)$$

to obtain a map of the Fourier spectrum in \mathbf{q} space,

$$P(\mathbf{q}, E) = |\delta\rho'(\mathbf{q}, E)| . \quad (12.24)$$

Up to now discussion and formulation are quite general and can be used to study the effects of any dynamic mode once the susceptibility χ is known. For the specific case of magnetic mode, we take a phenomenological form (based on the inelastic neutron scattering observations), see also (Eschrig and Norman, 2000):

$$\chi(\mathbf{q}; i\Omega_l) = -\frac{f(\mathbf{q})}{2} \left[\frac{1}{i\Omega_l - \Omega_0} - \frac{1}{i\Omega_l + \Omega_0} \right] . \quad (12.25)$$

Here the spin resonance mode energy is also denoted by Ω_0 . The quantity $f(\mathbf{q})$ describes the momentum dependence of the mode and is assumed to be enhanced at the $\mathbf{Q} = (\pi, \pi)$ point. Using the correlation length ξ_{sf} (chosen to be 2 here), it can be written as

$$f(\mathbf{q}) = \frac{1}{1 + 4\xi_{sf}^2 [\cos^2 \frac{q_x}{2} + \cos^2 \frac{q_y}{2}]} . \quad (12.26)$$

This form captures the essential feature of resonant peak observed by neutron scattering experiments in the superconducting state of cuprates (Zhu *et al.*, 2004a). Note that strong impurity scattering will shift the position and broaden the width of (π, π) spin resonance peak (Li *et al.*, 1998). However, in the Born limit, the above form of the susceptibility should still be valid for the purpose of this discussion. For the normal-state energy dispersion, we adopt a six-parameter fit to the band structure used previously for optimally doped Bi-2212 systems (Norman *et al.*, 1995), having the form

$$\begin{aligned} \xi_{\mathbf{k}} &= -2t_1(\cos k_x + \cos k_y) - 4t_2 \cos k_x \cos k_y \\ &\quad - 2t_3(\cos 2k_x + \cos 2k_y) \\ &\quad - 4t_4(\cos 2k_x \cos k_y + \cos k_x \cos 2k_y) \\ &\quad - 4t_5 \cos 2k_x \cos 2k_y - \mu , \quad (12.27) \end{aligned}$$

where $t_1 = 1$, $t_2 = -0.2749$, $t_3 = 0.0872$, $t_4 = 0.0938$, $t_5 = -0.0857$, and $\mu = -0.8772$. Unless specified explicitly, the energy is measured in units of t_1 hereafter. Since the maximum energy gap for most of the cuprates at the optimal doping is about 30 meV, while the resonance mode energy is in the range between 35 and 47 meV, we take $\Delta_0 = 0.1$ and $\Omega_0 = 0.15$ (i.e., $1.5\Delta_0$). To mimic the intrinsic life time broadening, in our numerical calculation we use $\gamma = 0.005$ in Eq. (12.20). System size is $N_x \times N_y = 1024 \times 1024$.

We present in Fig. 33 the results of the DOS and its energy derivative as a function of energy for a clean (i.e., $U_0 = 0$) d -wave superconductor with the electronic coupling to the (π, π) spin resonance modes. For comparison, the DOS for the case of no mode coupling is also

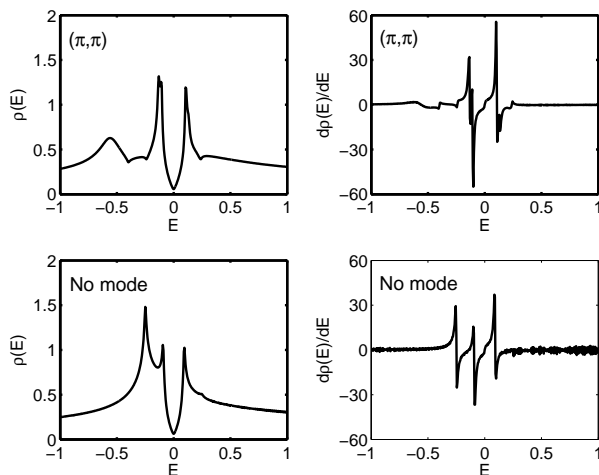


FIG. 33 Density of states (left column) and its energy derivative (right column) as a function of energy for a clean d -wave superconductor with the electronic coupling to the (π, π) spin resonance mode ($g = 2.30$). The case of no mode coupling ($g = 0$) is also shown for comparison.

shown. When there is no electron-mode coupling, there is a van Hove singularity peak appearing outside the superconducting gap edge. When the electrons are coupled to the (π, π) -spin resonance modes, the van Hove singularity peak is strongly suppressed. Instead, one sees a dip structure following the coherent peak at the gap edge. The distance between this dip and the coherent peak defines the resonance energy Ω_0 . These results, for the clean case, are consistent with earlier studies of the ARPES (Abanov *et al.*, 2002; Campuzano *et al.*, 1999; Dessau *et al.*, 1991; Eschrig and Norman, 2000; Kee *et al.*, 2002; Norman and Ding, 1998; Shen and Schrieffer, 1997) and DOS (Abanov and Chubukov, 2000). The shift of states due to inelastic scattering is also expected for scattering off local mode XII.B. Taking the second derivative, d^2I/dV^2 , emphasizes these features. As shown in the right column of Fig. 33, when the electrons are coupled to the spin resonance modes, there is a strong peak structure at $E = -(\Delta_0 + \Omega_0)$ in the $\rho'(E)$ spectrum.

In Fig. 34, we show the Fourier spectrum of the derivative of the LDOS at the energy $-(\Delta_0 + \Omega_0)$ (i.e., the peak position in d^2I/dV^2 in the presence of the mode coupling) with a structureless scattering potential $U_{\mathbf{q}} = U_0$, arising from a single-site impurity. In the absence of the electron-mode coupling, the Fourier spectrum intensity is strongest at $\mathbf{q} = (0, 0)$ and its equivalent points, and has moderate weight along the edges of the square around $\mathbf{q} = (\pi, \pi)$. When the electron-spin mode coupling is present, as shown in Fig. 34, the spectrum has the strongest intensity at the diamonds around (π, π) . Independently of the coupling to the collective mode, the spectrum has an intensity minimum $\mathbf{q} = (\pi, \pi)$. FT image of d^2I/dV^2 is greatly affected in this case by the underlying band structure.

In this simple model the inelastic feature is expected

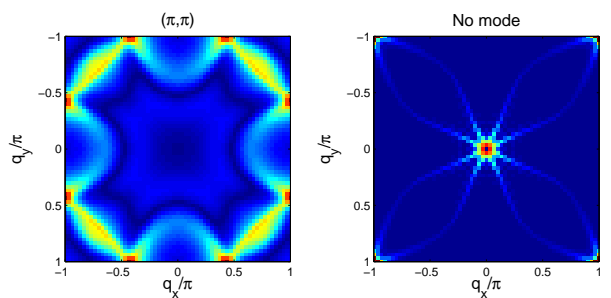


FIG. 34 The Fourier spectral weight of the energy derivative of the LDOS at $E = -(\Delta_0 + \Omega_0)$ for a d -wave superconductor with the electronic coupling to the spin resonance modes ($g = 2.30$). For comparison, the quantity is also shown for the case of no mode coupling ($g = 0$).

at $E_r = \Delta_0 + \Omega_0 \sim 70$ meV for optimal doping. Since the observed gap is position dependent, so is E_r . The wave vectors where the inelastic features are most prominent depend on the momentum dependence of the disorder potential, $U(\mathbf{q})$, doping and the band structure. All these combine to produce the “diamonds” seen in Figs. 34. In addition to structure at large momenta, there are features at small \mathbf{q} in $d^2I(\mathbf{q}, V)/dV^2$ (Zhu *et al.*, 2005a,b). Although we focused on spin mode, FT IETS STM is applicable to lattice (Zhu *et al.*, 2005a,b) and local inelastic modes (Balatsky *et al.*, 2003; Morr and Nyberg, 2003).

The FT-IETS STM technique can be applied to a variety of systems, such as conventional and organic superconductors, and systems exhibiting charge and spin density waves. Disorder and “inelastic Friedel” oscillations produced by disorder are necessary ingredients of this new technique. Real potential of this technique can only be assessed when a comparison is made between experimental data and theoretical predictions on model systems. We are optimistic that this technique will be useful in the near future, and refer the reader to recent literature on this new and rapidly developing field (Balatsky *et al.*, 2003; Morr and Nyberg, 2003; Zhu *et al.*, 2005a,b, 2004a).

XIII. AVERAGE DENSITY OF STATES IN SUPERCONDUCTORS WITH IMPURITIES

The Green’s function formalism is well suited to the analysis of the combined effect of many uncorrelated impurities in the bulk of a superconductor. The first such treatment was given in a pioneering paper by Abrikosov and Gor’kov (Abrikosov and Gorkov, 1960). The basic assumptions underlying the calculations were given in Sec. III.C. After averaging over different impurity distributions following Eq. (3.14), the translational symmetry is restored, and the Green’s function takes the form

$$\hat{G}^{-1}(\mathbf{k}, \omega) = i\omega_n - \xi(\mathbf{k})\tau_3 - \Delta_0\sigma_2\tau_2 - \hat{\Sigma} \quad (13.1)$$

$$\equiv i\tilde{\omega} - \tilde{\varepsilon}(\mathbf{k})\tau_3 - \tilde{\Delta}\sigma_2\tau_2. \quad (13.2)$$

Here we took into account the matrix structure of the self-energy, $\widehat{\Sigma} = \sum_i \Sigma_i \widehat{\tau}_i$. The superconducting gap in the presence of impurities is determined by the self-consistency condition, Eq. (2.22), which reads here

$$\Delta(\widehat{\Omega}) = \pi T N_0 \sum_{\omega_n} \int d\widehat{\Omega}' V(\widehat{\Omega}, \widehat{\Omega}') \frac{\widetilde{\Delta}(\widehat{\Omega}')}{\sqrt{\widetilde{\omega}_n^2 + \Delta^2(\widehat{\Omega}')}}. \quad (13.3)$$

T_c is the temperature at which a non-trivial solution of the self-consistency equation first appears. Eq.(13.3) with the recipe for computing the self-energy form the basis for treating superconductors with impurities. We always ignore the contribution of Σ_3 , as it simply renormalizes the chemical potential. This is justified in computing the density of states, although the corrections may be relevant for some response functions (Hirschfeld *et al.*, 1988). In computing the self-energy we neglect the interaction between spins on different impurity sites (Galitskii and Larkin, 2002; Larkin *et al.*, 1971) and the interference effects of scattering on different impurities (of the order $(pFl)^{-1}$, where l is the mean free path).

A. s-wave

1. Born approximation and the Abrikosov-Gor'kov theory

We begin by reviewing the seminal results of Abrikosov and Gor'kov (AG) for impurity scattering in the Born limit (phase shift $\delta_0 \ll 1$). This sets the standard for comparison with theories going beyond the Born approximation. We follow the notations of (Maki, 1969).

Consider an impurity potential combining the potential and the magnetic scattering,

$$\widehat{U}_{imp}(\mathbf{k} - \mathbf{k}') = U_{pot}(\mathbf{k} - \mathbf{k}')\tau_3 + J(\mathbf{k} - \mathbf{k}')\mathbf{S} \cdot \boldsymbol{\alpha}, \quad (13.4)$$

where $\boldsymbol{\alpha}$ is defined in Eq. (3.5). AG considered the self energy in the second order (Born approximation),

$$\widehat{\Sigma}(\omega, \mathbf{k}) = n_{imp} \int \frac{d\mathbf{k}'}{(2\pi)^3} \widehat{U}_{imp}(\mathbf{k} - \mathbf{k}') \widehat{G}(\mathbf{k}', \omega) \widehat{U}_{imp}(\mathbf{k}' - \mathbf{k}). \quad (13.5)$$

Integrating over \mathbf{k}' we find

$$\widetilde{\omega} = \omega_n + \frac{1}{2} \left(\frac{1}{\tau_p} + \frac{1}{\tau_s} \right) \frac{\widetilde{\omega}}{\sqrt{\widetilde{\omega}_n^2 + \Delta^2}}, \quad (13.6)$$

$$\widetilde{\Delta} = \Delta + \left(\frac{1}{\tau_p} - \frac{1}{\tau_s} \right) \frac{\widetilde{\Delta}}{\sqrt{\widetilde{\omega}_n^2 + \Delta^2}}. \quad (13.7)$$

The potential (τ_p) and spin-flip (τ_s) scattering times are

$$\frac{1}{\tau_p} = n_{imp} N_0 \int d\widehat{\Omega} |U_{pot}(\mathbf{k} - \mathbf{k}')|^2, \quad (13.8)$$

$$\frac{1}{\tau_s} = n_{imp} N_0 S(S+1) \int d\widehat{\Omega} |J(\mathbf{k} - \mathbf{k}')|^2, \quad (13.9)$$

and we averaged over the directions of the impurity spin.

In the absence of spin-flip scattering both Δ and ω are renormalized identically, and it follows from Eq. (13.3) that the gap remains unchanged compared to the pure case. This is in accordance with Anderson's theorem. The spin flip scattering violates the time-reversal symmetry, and τ_s enters the equations for $\widetilde{\omega}$ and $\widetilde{\Delta}$ with the opposite sign. Introducing $u = \widetilde{\omega}/\widetilde{\Delta}$, we find

$$\frac{\omega}{\Delta} = u \left(1 - \frac{(\Delta\tau_s)^{-1}}{\sqrt{1+u^2}} \right). \quad (13.10)$$

It follows that the gap in the single particle spectrum is $E_{gap} = \Delta(1 - (\Delta\tau_s)^{-2/3})^{3/2}$ for $\Delta\tau_s > 1$, and vanishes for $\Delta\tau_s < 1$. This gapless region starts at the value of pairbreaking parameter α

$$\alpha' = \tau_s^{-1} = \Delta_{00} \exp(-\pi/4), \quad (13.11)$$

where Δ_{00} is the gap in the pure material at $T = 0$.

The transition temperature is determined from

$$\psi\left(\frac{1}{2} + \frac{1}{2\pi\tau_s T_c}\right) - \psi\left(\frac{1}{2}\right) = \ln \frac{T_{c0}}{T_c}, \quad (13.12)$$

where $\psi(x)$ is the digamma function and T_{c0} is the transition temperature of the pure material. Consequently, superconductivity is destroyed ($T_c = 0$) when

$$\alpha_c = \tau_s^{-1} = \pi T_{c0}/2\gamma = \Delta_{00}/2 > \alpha', \quad (13.13)$$

where $\gamma \approx 1.78$. As $\alpha' \approx 0.912\alpha_c$ AG predicted that gapless superconductivity exists for a range of impurity scattering (Abrikosov and Gorkov, 1960). This was later confirmed in experiment (Woolf and Reif, 1965).

The evolution of the density of states with increasing disorder was investigated in detail (Ambegaokar and Griffin, 1965; Gong and Cai, 1966; Skalski *et al.*, 1964), and is shown in Fig. 35. For $\alpha < \alpha'$ a hard gap in the single particle spectrum persists up to the critical impurity concentration, as shown in Fig. 36. This result is clearly at odds with our discussion in Sec. VI, which shows that even a single magnetic impurity creates a localized state in the superconducting gap.

2. Shiba impurity bands

In the AG theory the impurity concentration and the strength of the exchange coupling contribute to the suppression of superconductivity as a single pairbreaking parameter, $\alpha = \tau_s^{-1} = (2n_{imp}/\pi N_0) \sin^2 \delta_0 \propto n_{imp} J^2 S(S+1)$ for isotropic exchange, see Eq. (13.9). This is a result of the Born approximation; in general, the phase shift δ_0 and the concentration of impurities n_{imp} are separate variables that control different aspects of impurity scattering. For example, in the limit of dilute concentration of strong magnetic impurities, the AG approach yields a small scattering rate, and a single-particle spectral gap virtually identical to that in a pure limit. On the other

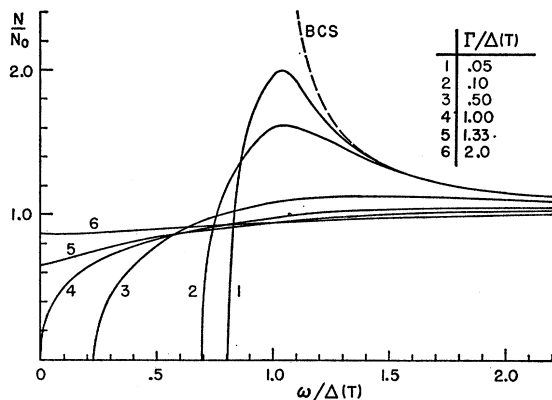


FIG. 35 Density of states in the Abrikosov-Gorkov theory of magnetic impurities in superconductors. Here $\Gamma = \tau_s^{-1}$. Reproduced with permission from (Skalski *et al.*, 1964).

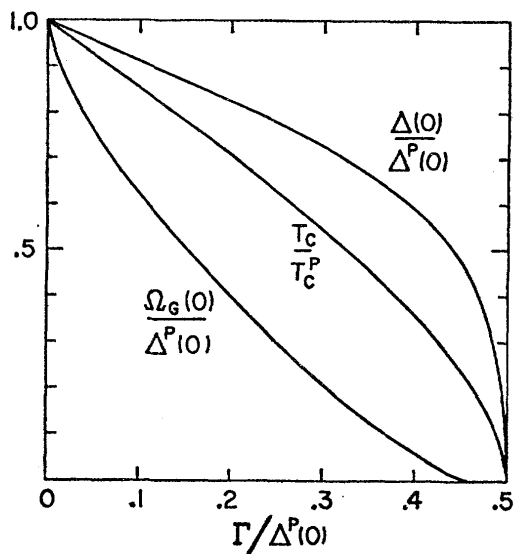


FIG. 36 Plot of the dependence of the order parameter, Δ , transition temperature, T_c , and the single particle spectral gap, Ω_G here, on the scattering rate $\Gamma = \tau_s^{-1}$. Reproduced with permission from (Skalski *et al.*, 1964).

hand, we have learned that in this regime each impurity is accompanied by a bound state with the energy below the gap, and therefore we expect a finite number of these sub-gap states to exist in a superconductor. This section addresses this dichotomy.

Analysis of the strong scattering regime requires use of the self-consistent T -matrix approach (Hirschfeld *et al.*, 1986; Schmitt-Rink *et al.*, 1986), where the self-energy $\hat{\Sigma}(\mathbf{p}, \omega) = n_{imp} \hat{T}_{\mathbf{p}, \mathbf{p}}$, and

$$\hat{T}_{\mathbf{p}, \mathbf{p}'} = \hat{U}_{\mathbf{p}, \mathbf{p}'} + \int d\mathbf{p}_1 \hat{U}_{\mathbf{p}, \mathbf{p}_1} \hat{G}(\mathbf{p}_1, \omega) \hat{T}_{\mathbf{p}_1, \mathbf{p}'}. \quad (13.14)$$

Following the treatment described in Sec. VI, we analyse the pairbreaking in different angular momentum channels. The effective pairbreaking parameter in the l -th channel is $\alpha_l = n_{imp}(1 - \epsilon_l^2)/(2\pi N_0)$, where ϵ_l is the

position of the corresponding bound state, see Eq. (6.10). In analogy with the AG treatment, we find that the ratio $u_n = \tilde{\omega}_n/\tilde{\Delta}(\omega_n)$ satisfies the equation (Chaba and Nagi, 1972; Rusinov, 1969)

$$\frac{\omega_n}{\Delta} = u_n \left[1 - \sum_{l=0}^{\infty} (2l+1) \frac{\alpha_l}{\Delta} \frac{\sqrt{1+u_n^2}}{\epsilon_l^2 + u_n^2} \right], \quad (13.15)$$

where the gap is determined self-consistently from

$$\Delta = 2\pi T N_0 g \sum_n (1 + u_n^2)^{-1/2}. \quad (13.16)$$

This equation should be contrasted with Eq. (13.10). The pairbreaking parameter, α_l now depends *separately* on the position of the single-impurity resonance state, ϵ_l and the impurity concentration, in contrast to the AG theory.

The growth of the impurity band has been investigated for the spherically symmetric case of purely magnetic scattering (Chaba and Nagi, 1972; Rusinov, 1969; Shiba, 1968). The critical concentration of impurities at which the transition temperature vanishes is obtained by setting $T_c = 0$ in the gap equation,

$$\ln \frac{T_{c0}}{T_c} = \psi(1/2 + \alpha/2\pi T_c) - \psi(1/2), \quad (13.17)$$

where now (Ginzberg, 1979)

$$\alpha = \sum_l (2l+1) \alpha_l. \quad (13.18)$$

Since the gap equation is identical to that considered by AG, the critical pairbreaking, $\alpha_{cr} = \Delta_0/2$. However, now the critical concentration of impurities depends on the phase shift of scattering by individual impurities, and on the position of the single impurity resonance, see Fig. 37,

$$n_{cr} = \pi N_0 \Delta_0 \left[\sum_l (2l+1) (1 - \epsilon_l^2) \right]^{-1}. \quad (13.19)$$

The width of the gapless regime depends on the details of scattering. For $l = 0$ the gap vanishes when the pairbreaking exceeds the value (Rusinov, 1969; Shiba, 1968)

$$\frac{\alpha'}{\alpha_{cr}} = 2\epsilon_0^2 \exp[-\pi\epsilon_0^2/2(1 + \epsilon_0)]. \quad (13.20)$$

In the Born approximation the bound state moves to the gap edge, $\epsilon_0 = 1$, and we regain the result of Abrikosov and Gorkov. For stronger scattering, $\epsilon_0 < 1$, the realm of gapless superconductivity is enhanced compared to the AG theory. As higher order harmonics are included, the threshold at which the density of states at the Fermi energy becomes non-zero shifts even lower (Ginzberg, 1979). This behavior is modified by the inclusion of Kondo screening (see next section), but the overall shape of the DOS observed in planar tunneling measurements (Bauriedl *et al.*, 1981; Dumoulin *et al.*, 1975, 1977) is in agreement with these expectations.

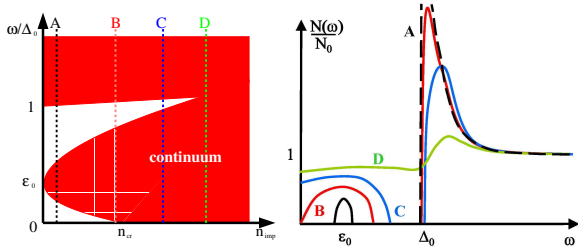


FIG. 37 Evolution of the spectral gaps and density of states for strong magnetic impurities ($\epsilon_0 \ll \Delta_0$). Left panel: available states (shaded) as a function of the impurity concentration. Right panel: qualitative features of the DOS for different impurity concentrations; following cuts A, B, C, D on the left. Critical concentration corresponds to line B, when the impurity band touches $\omega = 0$. The spectral gap between the top of the impurity band and the bottom of the continuum persists to higher impurity concentration (line D).

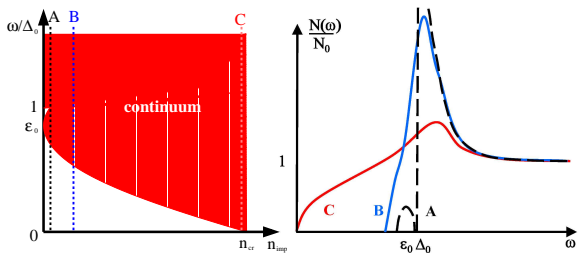


FIG. 38 Evolution of the spectral gaps and density of states for weak magnetic impurities ($\epsilon_0 \lesssim \Delta_0$). Left panel: available states (shaded) as a function of the impurity concentration. Right panel: qualitative features of the DOS for different impurity concentrations, following cuts A, B, C on the left. The impurity band and the continuum merge at a low impurity concentration (line B), and further evolution of the DOSs is very close to the predictions of the AG theory. At the critical concentration (line C) gapless superconductivity sets in.

For $l = 0$ in the limit $\alpha_0 \ll \Delta$ the width of the impurity band around E_0 is estimated to be $W = (8\alpha_0\Delta)^{1/2}(1 - \epsilon_0)^{1/4}$, and therefore varies as $n_{imp}^{1/2}$ (Shiba, 1968). Therefore if the resonance state at E_0 is sufficiently close to the gap edge, the concentration, c_0 , at which the top of the impurity band merges with the continuum above Δ is smaller than the critical concentration, c' , at which the bottom of the impurity band reaches the Fermi surface and the superconductor becomes gapless (Shiba, 1968), see Fig. 38. The AG result is an extreme example of this behavior when the states due to individual impurities are infinitely close to the gap edge, and therefore upon increasing impurity concentration the gap decreases until the onset of the gapless behavior.

3. Quantum spins and density of states

In the quantum treatment of the impurity spin, Sec. XI, we discussed the competition between gapping the density of states due to superconductivity, and the

onset of the Kondo screening of the impurity moment. We concluded that, in contrast to classical spin, the position of the bound state is not simply given by the value of the bare exchange coupling but depends on the ratio T_K/T_c . Once the position of the bound state is established, for independent impurities the growth of the impurity band is analogous to that in the previous section. As discussed above, for ferromagnetic coupling of the impurity to the conduction electrons the bound state is always close to the gap edge, the scattering is weak, and the Abrikosov-Gor'kov theory gives correct results.

When Kondo screening is effective, for antiferromagnetic coupling, the behavior of the density of states and the transition temperature was studied in the 70s (Müller-Hartmann, 1973; Müller-Hartmann and Zittartz, 1971; Schuh and Müller-Hartmann, 1978; Zittartz *et al.*, 1972). Appearance of the predicted subgap band of localized states (qualitatively similar to Shiba-Rusinov band, above) was confirmed experimentally (Bauriedl *et al.*, 1981; Dumoulin *et al.*, 1975, 1977). The main new result was the prediction of the re-entrant behavior for small $T_K/T_c \lesssim 1$. In that case the phase shift of the scattering increases upon lowering temperature, but remains moderate at T_c enabling the transition to the superconducting state. Upon further decrease in temperature, scattering becomes stronger and suppresses superconductivity in a range of phase diagram of Fig. 39. Finally, at lowest temperatures below T_K , the system re-enters local Fermi liquid regime and superconductivity may re-appear. While further work (Jarrell, 1990; Matsuura *et al.*, 1977) cast doubt on the existence of the third transition, region of two solutions for $T_c(n_{imp})$ was confirmed by theoretical studies. In particular, a combination of quantum Monte Carlo technique with Eliashberg equations gave the dependence of the re-entrance transition on the electron-phonon coupling constant, while accounting non-perturbatively for the Kondo effect (Jarrell, 1990), see Fig. 39. Moreover, the initial decrease of T_c with increasing impurity concentration is fast (Jarrell, 1990; Müller-Hartmann and Zittartz, 1971), and depends on the coupling strength (Jarrell, 1990). The behavior of the density of states in this limit was investigated in detail (Bickers and Zwicky, 1987; Jarrell *et al.*, 1990). The overall shape of the transition temperature as a function of impurity concentration with re-entrant transition was observed in (LaCe)Al₂ alloy series (Maple, 1973).

B. *d*-wave

As mentioned above, scalar (non-magnetic) impurities are pair-breakers for any nonconventional superconductor, and substantially change the low-energy quasiparticle spectrum. This problem has been addressed via the self-consistent T -matrix approximation (Balatsky *et al.*, 1994; Gorkov and Kalugin, 1985; Hirschfeld and Goldenfeld, 1993; Hirschfeld *et al.*, 1986, 1988; Lee, 1993; Schmitt-Rink *et al.*, 1986), which gives a finite density

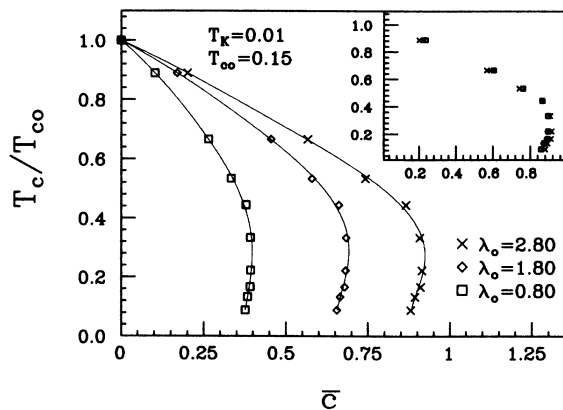


FIG. 39 Reduced transition temperature normalized to pure system as a function of the impurity concentration for different electron-phonon coupling, λ_0 . The impurity concentration $\bar{c} = n_{imp}/(2\pi)^2 N_0 T_{c0}$. From (Jarrell, 1990).

of states at the Fermi level. Here we briefly review only the main results, see Sec.I.D for details.

The self-consistent Green's function, averaged over impurity positions, is

$$\hat{G}^{-1}(\mathbf{k}, \omega) = \hat{G}_0^{-1}(\mathbf{k}, \omega) - \hat{\Sigma}(\omega). \quad (13.21)$$

with $\hat{\Sigma}(\omega) = n_{imp} \hat{T}(\omega)$. For particle-hole symmetry (Hirschfeld *et al.*, 1988), and unconventional gap (defined as having a zero average over the Fermi surface, see Sec. I) the only non-vanishing component of the T -matrix is proportional to τ_0 ,

$$T_0(\omega) = \frac{g_0(\omega)}{c^2 - g_0(\omega)}. \quad (13.22)$$

The T -matrix has to be determined self-consistently with $g_0(\omega) = (2\pi N_0)^{-1} \sum_{\mathbf{k}} \text{Tr} \hat{G}(\mathbf{k}, \omega) \hat{\tau}_0$.

Solution of this equation leads to a finite density of states at the Fermi level. This result was first obtained for Born scattering (Gorkov and Kalugin, 1985; Ueda and Rice, 1985), leading to an exponentially small $N(0)/N_0 \approx 4\tau^2 \Delta_0^2 \exp(-2\Delta_0\tau)$, where τ is the normal state scattering rate. The results are much more dramatic for unitarity scattering ($c = 0$) (Hirschfeld *et al.*, 1986; Schmitt-Rink *et al.*, 1986), when

$$\gamma \simeq \sqrt{n_{imp}(\Delta_0/\pi N_0)}, \quad (13.23)$$

where $\gamma = -\text{Im} \Sigma(\omega \rightarrow 0)$ is the scattering rate for low-energy quasiparticles. For $\omega \lesssim \gamma$, the density of states is determined by impurities and is finite: $N_{imp}(0)/N_0 = 2\gamma/\pi\Delta_0$. The characteristic width of the impurity-dominated region is $\omega^* \simeq \gamma \propto \sqrt{n_{imp}}$.

The origin of the finite DOS is the impurity band, growing from the impurity-induced states. Scaling of the impurity bandwidth $\gamma \propto \sqrt{n_{imp}}$ was found for paramagnetic impurities in an s -wave superconductor (Shiba, 1968). The fact that $\gamma \propto \sqrt{n_{imp}}$ is valid for a d -wave

superconductor is consistent with the picture of the low-energy states formed from the bound states at finite impurity concentration. Many questions about localization of low-energy quasiparticles in unconventional superconductors remain unanswered, see Sec. I).

The results above are for isotropic impurity scattering. Anisotropic impurities may preferentially scatter electrons between regions with the same, or close values of the gap, so that the scattering is inefficient in suppressing T_c . For general impurity phase shifts this has been considered by (Choi, 1999; Golubov and Mazin, 1999; Haran and Nagi, 1996, 1998; Kulic and Dolgov, 1999), while for a model with dominant small angle scattering in cuprates (Abrahams and Varma, 2000) the effect was analyzed by Kee (Kee, 2001).

XIV. OPTIMAL FLUCTUATION

A. Introduction

So far we discussed the effect of a single impurity on its immediate surrounding and the combined effect of an ensemble of scattering centers on the spatially averaged properties of a superconductor. In the case of a single pairbreaking impurity the characteristic length is simply the superconducting coherence length, ξ_0 . In the Abrikosov-Gorkov approach the gap is assumed to be uniformly suppressed, after averaging over all the possible configurations of impurity atoms at the mean field level (Abrikosov *et al.*, 1963).

It is clear, however, that some physics is missing in such an approach. Among all the realizations of the impurity distribution in a sample of size L_0 there exist regions where the *local* impurity concentration, on some characteristic scale $L \ll L_0$, differs significantly from the average concentration, n_i . If the local impurity concentration is sufficiently high, for $L > \xi_0$ superconductivity may be locally destroyed or sufficiently suppressed to generate a bound quasiparticle state at an energy $E \ll \Delta_0$.

Of course, such regions are rare. There is a high entropy cost to create an impurity droplet with the concentration significantly different from the average, hence the probability of finding these regions is small. However, the states localized in such droplets make a non-perturbative contribution to the density of states averaged over the entire sample, $N(E)$, and qualitatively modify its behavior compared to the mean field (Abrikosov-Gorkov and Shiba) treatment. Quite dramatically, they make any s -wave superconductor with a small concentration of magnetic impurities ($\Delta\tau_s \gg 1$) *gapless* (Balatsky and Trugman, 1997). It is due to such a dramatic modification that the interest in these "tail" states stretching below the mean field gap edge has peaked in recent years.

The problem of tail states did not originate in the study of superconductivity. The contribution of regions of anomalous impurity concentration to the net density of states below the gap edge was first considered in doped

semiconductors by Lifshitz (Lifshitz, 1964a,b, 1967). He showed that such rare impurity configurations create a local profile in the Coulomb potential that can have bound states, and therefore gives rise to the non-vanishing density of states below the bottom of the band, E_g . Henceforth the states localized in the droplets of impurities have become known as ‘Lifshitz tails’, and have been extensively studied (Halperin and Lax, 1966; Van Mieghem, 1992; Zittartz and Langer, 1966).

While, in retrospect, it is natural that inhomogeneities lead to a low-energy tail in the density of states in superconductors in much the same way, little attention has been paid to this problem until the paper by Balatsky and Trugman (Balatsky and Trugman, 1997). Their study was stimulated by the experimental observations that the tunneling density of states in s -wave superconductors with magnetic impurities is far greater at low energies than the Abrikosov-Gorkov theory suggests (Bader *et al.*, 1975; Edelstein, 1967; Woolf and Reif, 1965). A number of theoretical studies of the tail states followed, and this topic is now a subject of active interest.

Below we first briefly review the physical picture of the tail states in semiconductors, and then apply it to the subgap states in superconductors.

B. Tail states in semiconductors and optimal fluctuation

We distinguish between heavily doped and lightly doped semiconductors. In the former case a localized tail state with energy $E < E_g$ forms in the impurity-rich region, and the extent of its wave function greatly exceeds the average distance between individual shallow sites. Therefore the exact impurity potential can be replaced by a smooth function, averaged over regions containing many impurities. The probability of realization of the potential with the ‘‘right’’ energy of the bound state among all the possible impurity distributions determines its contribution to the DOS. In the latter case the number of impurity sites needed to form a bound state depends on how deep below the band edge the energy of such a state is. For example, if each impurity binds an electron at energy E_1 , while E_2 is the energy of the state bound by two impurities on neighboring lattice sites, to obtain a localized state below E_1 but above E_2 , one simply needs to find a region where the two impurities are at a particular finite distance from each other. The probability of finding such an impurity pair determines the density of states (Lifshitz, 1964b, 1967). As we go to energies below E_2 we need to position three impurities etc.

For energy, E , the most probable (albeit still rare) configuration of impurities that creates a potential U , such that $[H_{band} + U]\psi = \mathcal{E}[U]\psi$, with $\mathcal{E}[U] = E$, and therefore contributes the most to $N(E)$ is called the optimal fluctuation (OF). Given the probability density for the potential, $P[U]$, and the density of states in it,

$$N(E) = \int \mathcal{D}U P[U] \delta(E - \mathcal{E}[U]), \quad (14.1)$$

the optimal fluctuation is obtained by using the saddle point approximation and minimizing the resulting functional with respect to U . This approach finds the entropically cheapest impurity potential that creates a bound state at E . Therefore it optimizes the non-uniform impurity distribution (fluctuation from the uniform average) to the given energy, hence the name. The technical difficulty of minimization lies in its essential nonlinearity: the optimal potential depends on the wave function of the particle in this potential.

Consider many uncorrelated shallow impurity centers forming an extended potential. It is described by the Gaussian probability density,

$$P[U] \propto \exp\left[-\frac{1}{2U_0} \int d^d \mathbf{r} U^2(\mathbf{r})\right]. \quad (14.2)$$

Saddle point approximation for Eq.(14.1) gives

$$\ln \frac{N(E)}{N_0} \approx -\mathcal{S}[U_{opt}], \quad (14.3)$$

where the OF is obtained by minimizing the functional

$$\mathcal{S}[U] = \frac{1}{2U_0^2} \int d^d \mathbf{r} U^2(\mathbf{r}) + \lambda \left(\mathcal{E}[U] - E \right) \quad (14.4)$$

with respect to the potential U and the Lagrange multiplier λ . At the simplest level it is sufficient to consider only the potentials where $\mathcal{E}[U] = E$ is the lowest energy state in the potential U ; fluctuations where E coincides with the higher eigenstates are exponentially less probable. In a semiconductor the kinetic energy of the quasiparticle is $p^2/2m^*$, where m^* is the effective mass. Consequently, in a potential well of depth U (all energies are measured from the band edge) and size L the energy of the localized state is of the order of $U + 1/(mL^2) = E$ ($\hbar = 1$). In the optimal fluctuation $E \sim U \sim L^{-2}$, so that the action is $\mathcal{S}[U] \approx L^d U^2/U_0^2$, or $\ln [N(E)/N_0] \approx -|E|^{2-d/2}/U_0^2$ (Halperin and Lax, 1966; Lifshitz, 1964b). Importantly, the size of the optimal fluctuation, $L \propto |E|^{-1/2}$, increases as the energy approaches the band edge, while its depth, $|U| \sim |E|$ decreases.

More formally, since the energy of the bound state is the expectation value of the hamiltonian over the wave function of the bound state, $\psi(\mathbf{r})$, we have

$$\mathcal{E}[U] = \langle \hat{H} \rangle = \langle \psi | \frac{\mathbf{p}^2}{2m^*} + U | \psi \rangle = E \quad (14.5)$$

Minimization in Eq.(14.4) with respect to U dictates that

$$U(x) = -\lambda U_0^2 \langle \psi | \frac{\delta \hat{H}}{\delta U} | \psi \rangle = -\lambda U_0^2 \psi^2(x), \quad (14.6)$$

while minimization with respect to λ requires that the bound state is at energy E , i.e. (setting $m^* = 1$)

$$\left[-\frac{1}{2} \nabla^2 - \lambda U_0^2 \psi^2(\mathbf{r}) \right] \psi(\mathbf{r}) = E \psi(\mathbf{r}). \quad (14.7)$$

In one dimension this equation is exactly solved to give (Halperin and Lax, 1966)

$$\psi(x) = \sqrt{\frac{\kappa}{2}} \operatorname{sech} \kappa x, \quad (14.8)$$

$$\lambda U_0^2 = 8\kappa, \quad (14.9)$$

with $E = -\kappa^2/2$. Therefore the ‘‘optimal action’’ $\mathcal{S}(U_{opt}) \simeq \kappa^2/U_0^2 \sim |E|^{3/2}$ as expected.

In higher dimensions the corresponding equation is not solvable. However, one can extract the energy dependence of the action by assuming a spherically symmetric optimal fluctuation and an exponentially decaying, at large distances, bound state to find the Lifshitz tail $N(E) \propto \exp(-|E|^{2-d/2})$ (Lifshitz, 1964b; Lifshitz *et al.*, 1988). To obtain the pre-exponential factor one needs to consider all the wave functions in the potential, and this analysis has only been carried out in low dimensions (Halperin and Lax, 1966).

C. *s*-wave superconductors

1. Magnetic and non-magnetic disorder

The effect of the tails is most dramatic for fully gapped superconductors with magnetic impurities. The general route is similar to the approach above: given the probability density of different impurity configurations, we find the most probable configuration of impurities that gives rise to a state at a given energy within the gap. Technical implementations of this algorithm vary depending on the specifics of the problem at hand, see below.

There are important differences between the physics of the optimal fluctuation in a superconductor and a semiconductor. First, since the superconducting quasiparticles consist of electron pairs close to the Fermi surface, their kinetic energy is not simply that of a band particle, but is given instead by the Hamiltonian

$$\hat{H} = \hat{\xi} \tau_3 + \Delta(\mathbf{r}) \tau_1 \sigma_2. \quad (14.10)$$

Here we use Nambu’s notations with τ_i and σ_i the Pauli matrices in the particle-hole and the spin space respectively. Therefore, while the envelope of the tail state wave function still varies smoothly over the length scale of inhomogeneities in the impurity distribution, there are also rapid oscillations on the atomic scale due to the Fermi surface. As is shown below, these considerations substantially modify the behavior of the tail states.

Second, the scattering potential is a matrix in particle-hole and spin space,

$$\hat{U}(\mathbf{r}) = \sum_i \left[U_0 \tau_3 \delta(\mathbf{r} - \mathbf{r}_i) + J(\mathbf{r} - \mathbf{r}_i) \mathbf{S}_i \cdot \boldsymbol{\alpha} \right]. \quad (14.11)$$

The potential part of the scattering, U_0 , is not pairbreaking in accordance with Anderson’s theorem. However, since the size of the optimal fluctuation is large compared

to the correlation length, it is necessary to distinguish between the cases where the motion of quasiparticles within the OF is diffusive (strong potential scattering, $\Delta\tau \ll 1$, $\tau \ll \tau_s$, where τ is the transport lifetime) and ballistic (weak potential scattering, $\tau \gg \tau_s$). Moreover, we also distinguish between strong and weak *magnetic* scattering: if the magnetic scattering is strong there are resonance (Shiba-Rusinov) states in the gap, and the tails stretch not from the mean-field gap edge, but from the localized impurity band. If the magnetic scattering can be treated in the self-consistent Born approximation, the tail states emerge below the Abrikosov-Gorkov renormalized single particle spectral gap, $\Delta_0 = \Delta(1 - (\Delta\tau_s)^{-2/3})^{3/2}$, where Δ is the superconducting order parameter. In the AG limit the probability density for the magnetic impurity potential is Gaussian, as it is averaged over a large number of impurity sites. In contrast, in the unitarity limit there are subgap states localized on one or a few impurities; consequently, Poisson density distribution is appropriate. These possibilities provide for a rich variety of behavior that is still a subject of active interest.

All models ignore interactions between the impurity spins: this is justified as discussed in Sec.III.C. The models also treat impurity spins as classical, and therefore do not account for the Kondo effect. This is justified either when the Kondo temperature $T_K \ll T_c$ (and depletion of states at the Fermi level prevents screening of the local moment), or in the opposite limit, $T_K \gg T_c$, when the moments are quenched already in the normal state (Müller-Hartmann and Zittartz, 1971).

To our knowledge, the first discussion of the influence of non-uniform impurity distribution on the transition temperature appeared in 1968 (Kulik and Itskovich, 1968). These authors found that, in the limit of average impurity concentration $n \ll n_{cr}$ of the Abrikosov-Gorkov theory, there are localized regions that become superconducting at a temperature $T'_c > T_c(n)$, where $T_c(n)$ is the corresponding AG transition temperature. The difference between the two was evaluated for parabolic one-dimensional variation of the effective impurity potential. (Kulik and Itskovich, 1968) noted that their results are modified if there is non-magnetic as well as magnetic scattering, but did not address this further.

2. Diffusive limit, weak magnetic scattering

If the scattering on individual magnetic impurities is weak, the optimal fluctuation is created by large droplets of these scattering centers. Since the impurities are uncorrelated, the probability density for the impurity potential is Gaussian, which greatly simplifies the analysis.

Historically, most of the studies have been carried out in the diffusive limit. Larkin and Ovchinnikov investigated the smearing of the gap edge due to local fluctuations in the effective interaction between electrons (Larkin and Ovchinnikov, 1972). If the correlation length of the inhomogeneities, $r_c \gg \xi$, where ξ is the coherence

length of the dirty superconductor, $\xi \sim (D/\Delta)^{1/2}$, and D is the diffusion constant, the order parameter simply locally adjusts to the value of the interaction and the density of state is determined by the local gap amplitude,

$$N(E) = \int_0^\infty N(E, \Delta)W(\Delta)d\Delta, \quad (14.12)$$

where $W(\Delta)$ is the probability density of the gap.

In the opposite limit of short-range correlations in the pairing interaction, the finite density of states below the mean field gap edge is due to the states spatially localized in correlated droplets of size $r_0 \sim \xi[(\Delta_0 - E)/\Delta]^{-1/4}$ (increasing rapidly as $E \rightarrow \Delta_0$ as in a semiconductor), which leads to $N(E) \propto \exp[-[(\Delta_0 - E)/\Delta]^{5/4}]$ in $d = 3$. As in semiconductors, the high entropy cost of a large droplet is offset by the lowering of the kinetic energy of the bound state. Indeed, in a clean system with $\Delta\tau_s \gg 1$, and therefore $\Delta_0 \approx \Delta$, we find the characteristic kinetic energy, $D/r_0^2 \simeq \sqrt{\Delta_0^2 - E^2}$.

Recently it was argued that the above result is flawed since it does not account properly for the rapid oscillations of the wave function of the bound state on the scale of the Fermi wavelength (Meyer and Simons, 2001). These authors used a field-theoretical approach that maps the disordered superconducting system onto a non-linear σ -model (for a review, see (Altland *et al.*, 2000)) to show that, while the droplet size for the optimal fluctuation is identical to that obtained by Larkin and Ovchinnikov, the subgap density of states is $N(E) \propto \exp\{-[(\Delta_0 - E)/\Delta]^{(6-d)/4}\}$, which gives the exponent $3/4$, rather than $5/4$, for $d = 3$.

The paper that brought the investigation of the subgap states in superconductors into the limelight after a quarter-century-long hiatus was the study of the density of states due to regions where the impurity concentration is sufficient to locally destroy superconductivity (Balatsky and Trugman, 1997). The spectrum of the fluctuation region is similar to that of a disordered metallic grain of the same size, L , and depends on the mean level spacing, δ_L . The average density of states was obtained in two steps. First, an average over all realizations of disorder for grains of size L yielded $N_L(E) \sim \delta_L^{-1}$. Second, the probability of finding a fluctuation region of size L with the critical concentration of impurities, n_c , for a given average impurity concentration, n , $P_L(n_c; n)$ was used to define the average DOS, $N(E) \sim \int dV P_L(n_c; n)N_L(E)$. This integral was estimated to give

$$N(E) \sim \delta_{L_0}^{-1} \exp[-L_0^d(n_c \ln(n_c/n) - n_c + n)], \quad (14.13)$$

as $E \rightarrow 0$. Here $L_0 = (\xi_0 l)^{1/2}$ is of the order of the coherence length in a dirty superconductor with $l \ll \xi_0$.

At energies closer to the gap edge it is not necessary to destroy superconductivity completely to generate the tail states. Using the instanton approach for the nonlinear σ -model, Lamacraft and Simons demonstrated how these states arise out of inhomogeneous instanton configurations for the action (Lamacraft and Simons, 2000,

2001). The resulting optimal action reads

$$S_0 = a_d(\Delta_0\tau_s)^{2/3}(1-\Delta_0\tau_s)^{-2/3}-(2+d)/8 \left(\frac{\Delta_0 - E}{\Delta}\right)^{(6-d)/4} \quad (14.14)$$

and the DOS varies as $N(E) \sim \exp[-4\pi g(\xi/L)^{d-2}S_0] \sim \exp\{-[(\Delta_0 - E)/\Delta]^{(6-d)/4}\}$. Here g is the bare conductance and $a_d \sim 1$.

The same approach was used to derive (Lamacraft and Simons, 2001) the universal gap fluctuations in small metallic grains, first obtained using random-matrix theory (Vavilov *et al.*, 2001), namely $N(E) \sim \exp[-(\Delta_0 - E)^{3/2}]$, valid for $\Delta_0 - E \ll \Delta_0$. In this regime the spatial extent of the optimal fluctuation is greater than the size of the grain, so that effectively we are in dimension $d = 0$, and the exponent $3/2$ agrees with the general result of Lamacraft and Simons, $(6 - d)/4$. In the same $d = 0$ limit, but at $E \ll \Delta_0$, the random matrix theory gives $N(E) \sim (|E|/\delta^{3/2}\Delta^{1/2}) \exp[-\pi\tau_s(\Delta_0 - E)^2/\delta]$, where δ is the mean level spacing in the grain (Beloborodov *et al.*, 2000).

3. Diffusive limit, strong scattering

Recently the field theoretical treatment has been extended to the case of strong scatterers (Marchetti and Simons, 2002). When the probability distribution of scattering strength is Poissonian rather than Gaussian, the action cannot be expanded to second order in the magnetic potential, as it was for the weak potential. Marchetti and Simons circumvented this difficulty by considering the dominant contribution of droplets densely populated by magnetic impurities, so that $\xi \ll l_s \ll l$. As we saw above, an impurity band emerges within superconducting gap in the limit of near-unitary scattering already at the level of the mean field theory. Consequently, the tail states extend from the edge of the continuum above Δ_0 as well as from the top and bottom of the impurity band, see Fig. 41. According to Marchetti and Simons in all these cases the density of states varies as $N(E) \propto \exp[-(|E - E_i|/\Delta)^{(6-d)/4}]$, where E_i is the appropriate band edge. The exponent of the action is identical to that found above in the diffusive limit.

4. Ballistic limit, weak scattering

It was noticed early on that in some systems the magnetic scattering is dominant: upon increasing the concentration of impurities the increase in residual resistivity ratio correlates with the suppression of the superconducting transition temperature (Edelstein, 1967). Since both magnetic and nonmagnetic scattering contribute to the resistivity, but only the magnetic part suppresses T_c , this is an indication of almost purely spin-dependent scattering. Shytov and co-workers (Shytov *et al.*, 2003) considered the subgap states in this limit in clean ($l \gg \xi_0$ or

$\Delta\tau_s \gg 1$) limit, when the spectral gap obtained in the self-consistent Born approximation nearly coincides with the order parameter, $\Delta_0 \approx \Delta$.

Once again, since the impurities are weak, the optimal fluctuation is large and shallow, and the spin-dependent potential has the Gaussian probability density. When the size of the optimal fluctuation is much greater than the coherence length, $l \gg L \gg \xi_0$, the motion of the quasiparticles in this potential is ballistic. As a result, mapping on the non-linear σ -model is not feasible, and the problem requires quantum mechanical treatment akin to that in a semiconductor.

As in that case, we first consider the one-dimensional problem. An important assumption (discussed below) is that a ferromagnetic fluctuation maximizes the effect of the impurity potential. Choosing the direction of the impurity spins along the y axis, performing rotation $\sigma_2 \rightarrow \sigma_3$, we remove the vector character of the slowly varying potential \mathbf{U} , and consider the hamiltonian

$$\hat{H}_\pm = \hat{\xi}\tau_3 \pm \Delta_0\tau_1 \pm U(\mathbf{r}). \quad (14.15)$$

The hamiltonian, however, still remains a matrix in the particle-hole space, and the wave functions of the optimal fluctuation are the Nambu spinors Ψ .

Let us discuss the physical behavior qualitatively. We linearize the kinetic energy near the Fermi surface, so that typical kinetic energy in an OF of size L is $\xi \simeq v_F/L$. Then the energy of a quasiparticle in the optimal fluctuation (measured from the Fermi energy) is $E \simeq U + \sqrt{\Delta_0^2 + v_F^2/L^2}$. For the energies close to the superconducting gap, $(\Delta_0 - E)/\Delta_0 \ll 1$, the OF is large ($L \gg \xi_0 = v_F/\Delta_0$) and shallow ($|U|/\Delta_0 \ll 1$), so that $E - \Delta_0 \approx U + v_F^2/(\Delta_0 L^2)$. Introducing the dimensionless energy $\epsilon = E/\Delta_0$, we obtain, in analogy with the arguments above, $|U|/\Delta_0 \simeq \xi_0^2/L^2 \simeq 1 - \epsilon$. Notice that the size of the fluctuation is $L \simeq \xi_0/\sqrt{1 - \epsilon} \gg \xi_0$. As a result, we find (see Eq.(14.4)) $\mathcal{S}[U] \approx LU^2/U_0^2 = \Delta_0^2 \xi_0 (1 - \epsilon)^{3/2}/U_0^2$. From the definition of U_0 ,

$$-\ln \frac{N(E)}{N_0} \approx \mathcal{S}[U_{opt}] \simeq (\Delta_0\tau_s)(1 - \epsilon)^{3/2}. \quad (14.16)$$

The energy dependence in Eq. (14.16) is identical to the result of Lifshits in $d = 1$, despite the linear, rather than quadratic, dependence of the kinetic energy on the size of the droplet. This follows from the smallness of this energy compared to the gap: even though $\xi \propto 1/L$, the expansion is in ξ^2 .

The minimization of the saddle-point action proceeds exactly as in Sec. XIV.B. For spin ‘‘up’’ particles $\mathcal{E}_+[U] = \langle \Psi | \hat{H}_+ | \Psi \rangle$. Minimization with respect to U gives

$$U(x) = -\lambda U_0^2 \langle \Psi | \frac{\delta \hat{H}_+}{\delta U} | \Psi \rangle. \quad (14.17)$$

In principle this variational derivative includes the effect of the self-consistent suppression of the gap. However, this effect is small (Shytov *et al.*, 2003). Then,

in exact analogy to the semiconductor problem, $U(x) = -\lambda U_0^2 \langle \Psi^*(x) \Psi(x) \rangle$, where $(\Psi^* \Psi)$ denotes the scalar product in particle-hole space. In turn, Schrödinger equation takes the form

$$\left[-iv_F \frac{\partial}{\partial x} \tau_3 + \Delta_0 \tau_1 - \lambda U_0^2 (\Psi^* \Psi) \right] \Psi = E \Psi. \quad (14.18)$$

This equation is solved by introducing the bilinear forms $R_i = \Psi^*(x) \hat{\tau}_i \Psi(x)$, which play the role of the Halperin-Lax wave function in the Nambu space. We find

$$R_0 = \frac{1 - \epsilon^2}{\xi_0 \arccos \epsilon} \frac{1}{\epsilon + \cosh(2x\sqrt{1 - \epsilon^2}/\xi_0)}, \quad (14.19)$$

$$R_1 = R_0(\epsilon + \xi_0 R_0 \arccos \epsilon), \quad (14.20)$$

$$R_2 = \sqrt{R_0^2 - R_1^2}, \quad (14.21)$$

and $R_3 = 0$ (Shytov *et al.*, 2004). The physical potential of the optimal fluctuation is (Shytov *et al.*, 2003)

$$\frac{U(x)}{2\Delta_0} = -\frac{1 - \epsilon^2}{\epsilon + \cosh(2x\sqrt{1 - \epsilon^2}/\xi_0)}. \quad (14.22)$$

which corresponds to the value of the action

$$\mathcal{S}[U] = 8\pi(\Delta_0\tau_s) \left[\sqrt{1 - \epsilon^2} - \epsilon \arccos \epsilon \right]. \quad (14.23)$$

For $\epsilon \approx 1$ the length scale of the optimal fluctuation is $\xi_0/\sqrt{1 - \epsilon^2}$, its depth is $U \sim \Delta_0(1 - \epsilon^2)$, and the density of states $N(E) \sim \exp[-(1 - \epsilon^2)^{3/2}]$, in complete agreement with qualitative estimates.

The most important observation of (Shytov *et al.*, 2003) is that in higher dimensions the optimal fluctuation is strongly anisotropic, in contrast to both the conventional semiconductors and superconductors in the diffusive limit. This is a direct consequence of the composite nature of superconducting quasiparticles: they are made out of objects that move with the Fermi velocity. The wave function of the subgap state is concentrated along the quasiclassical trajectory, which is a chord in a potential of any shape. Consequently, there is little energy cost in reducing the size of the OF in the ‘‘transverse’’ direction, while the smaller volume makes such fluctuations more probable, see Fig. 40. As a result, the optimal fluctuation is strongly elongated in one (x) direction. The wave function of the bound state can be written as $\Psi(x, \mathbf{y}) = \exp(ik_F x) \Phi(x, \mathbf{y})$, where \mathbf{y} denotes the transverse $d-1$ coordinates, and Φ is a slowly varying function. The kinetic energy of the quasiparticle is

$$\hat{\xi} \Psi \approx -e^{ik_F x} \left(iv_F \frac{\partial}{\partial x} + \frac{\nabla_y^2}{2m} \right) \Phi \sim \left(\frac{v_F}{L_x} + \frac{1}{mL_y^2} \right) \Psi. \quad (14.24)$$

The transverse size of the fluctuation can therefore be reduced until the second term becomes comparable to the first, i.e. $L_y \simeq (\lambda_F L_x)^{1/2}$, where $\lambda_F \simeq k_F^{-1}$ is the

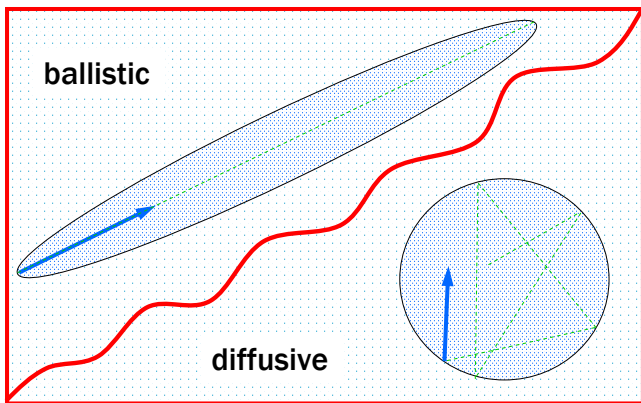


FIG. 40 The spatial structure of the optimal fluctuation in the ballistic and the diffusive limits.

Fermi wavelength. Consequently, $|U|/\Delta_0 \sim 1 - \epsilon$ and $L_x \sim \xi_0/\sqrt{1 - \epsilon}$, and

$$\mathcal{S}[U_{opt}] \simeq L_x L_y^{d-1} \frac{U^2}{U_0^2} \simeq (\Delta_0 \tau_s) \left(\frac{E_F}{\Delta_0} \right)^{\frac{d-1}{2}} (1 - \epsilon)^{\frac{7-d}{4}}, \quad (14.25)$$

where E_F is the Fermi energy. Consequently, the density of states, $N(E) \sim \exp[-(1 - \epsilon)^{(7-d)/4}]$.

The action for this anisotropic fluctuation is smaller than that for an isotropic droplet with the same energy of the bound state, by a factor of $(E_F/\Delta_0)^{(d-1)/2} (1 - \epsilon)^{-(d-1)/4}$, so that the corresponding DOS is exponentially higher.

Since the optimal fluctuation is a result of a saddle point approximation for the functional integral, Eq. (14.1), it is only valid when $\mathcal{S}[U_{opt}] \gg 1$, or

$$1 - \epsilon \gg (\Delta_0 \tau_s)^{\frac{4}{d-7}} \left(\frac{\Delta_0}{E_F} \right)^{\frac{2(d-1)}{7-d}}. \quad (14.26)$$

For $d = 1$ this condition is $1 - \epsilon \gg (\Delta_0 \tau_s)^{-2/3}$, while for $d = 3$ it does not depend on the gap, $1 - \epsilon \gg (k_F l)^{-1}$.

It is possible to compare the DOS given by different approaches at the crossover scale between the diffusive and the ballistic regimes (Vekhter *et al.*, 2003). A transition to the diffusive regime occurs when the size of OF $L \geq v_F \tau_s$, or $1 - \epsilon \leq (\Delta_0 \tau_s)^{-2}$. The result of Ref. (Lamacraft and Simons, 2000) for $\Delta_0 \tau_s \gg 1$ is $S_D = (\Delta_0 \tau_s)^{5/3} (E_F/\Delta_0)^{d-1} (1 - \epsilon)^{(6-d)/4}$. Consequently, at the crossover point the action from Eq. (14.25) is smaller, $S_D/S_0 \simeq (E_F/\Delta_0)^{(d-1)/2} (\Delta_0 \tau_s)^{7/6} \gg 1$, and the OF found by Shytov *et al.* corresponds to a greater DOS. Therefore the structure of the OF near the crossover between the ballistic and diffusive regimes still resembles closely that given above. As the size of the OF increases even further, the anisotropic fluctuation becomes insupportable due to diffusive motion.

Balatsky and Trugman (Balatsky and Trugman, 1997) considered only the DOS at $E = 0$ due to the suppres-

sion of superconductivity by paramagnetic impurity potential. They needed a large volume fluctuation, $V \geq \xi^d$, which is less probable and yields lower DOS than that of Eq. (14.25). (Vekhter *et al.*, 2003) checked whether local suppression of the gap from Δ_0 to E due to a large number of impurities with *uncorrelated* spins (as opposed to a ferromagnetic OF above) is advantageous. For $1 - \epsilon \ll 1$ the local pairbreaking rate, γ , needed to reduce the gap to E is $\gamma \tau_s \approx 1 + (1 - \epsilon)(\Delta_0 \tau_s)^{2/3}$, and the volume of the region has to be at least equal to that of the anisotropic OF to avoid high kinetic energy cost (this is an underestimate since it ignores proximity coupling to bulk). In that case the optimal action $S_{BT}/S_0 \approx (\Delta_0 \tau_s)^{1/3} (E_F/\Delta_0) \bar{c}$, where $\bar{c} = n_{imp} \lambda_F^d$ is the atomic concentration of impurity atoms. As a result, for realistic values of \bar{c} and clean samples $S_{BT} \gg S_0$, and the DOS given by the action in Eq. (14.25) is higher. Therefore the ballistic limit of the action obtained by (Shytov *et al.*, 2003) is expected to be valid up to the crossover to the diffusive regime.

5. Ballistic regime, strong scattering

As of today, we are not aware of any investigations of the structure of the optimal fluctuation in the ballistic regime, when there exist bound states on individual magnetic impurities. It is reasonable to assume that the result differs from the standard Lifshitz formula for the same reason as in the section above: the wave functions of the states localized on magnetic impurities in superconductors oscillate with the Fermi wavelength, see Sec. VI. As a result, in the dilute impurity limit, the shift of the energy level localized on, for example, two impurities located at distance $R \gg p_F^{-1}$, will be suppressed by the typical factor $\exp(-R/\xi_0)$ (Rusinov, 1968). Consequently, the states significantly below the impurity band must be created by a large number of impurities or impurities located on neighboring lattice sites. This problem still awaits further investigation.

6. Summary

In *s*-wave superconductors with magnetic impurities the density of states does not vanish *irrespective of the concentration and nature of the impurity scattering*. The tails of the density of states extend into the mean field gap. Therefore *all superconductors with magnetic impurities are gapless*. This behavior is illustrated in Fig. 41.

XV. SUMMARY AND OUTLOOK

While considering the role of impurities in conventional and unconventional superconductors, this review focused on theoretical and experimental results that highlight the new physics beyond standard Abrikosov-Gor'kov theory, Anderson theorem and average lifetime effects. The studies of disorder in *s*-wave superconductors were carried out

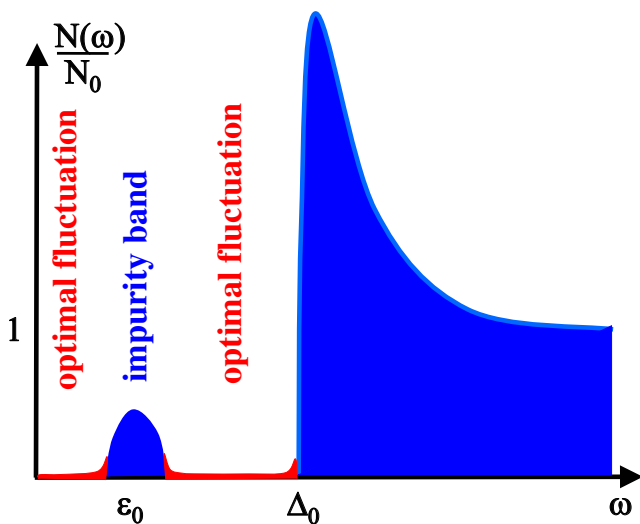


FIG. 41 Sketch of the density of states in an s -wave superconductor with magnetic impurities. Blue shade denotes regions where the mean field density of states is finite. Red shading signifies the finite, but exponentially small DOS induced by the fluctuations in the local impurity distribution. If the impurities are weak, the impurity band is absent and the tail extend from the mean field gap edge.

in detail in the 1960's. We discussed more recent results in this field. Our main emphasis has been on how individual impurities influence local electronic states in their immediate vicinity, and on deviations from the standard Abrikosov-Gorkov theory on mesoscopic scales. This focus is dictated both by the advances in experimental techniques, which can now use NMR methods and STS measurements to probe electronic states with atomic spatial resolution, at the scales where impurities perturb their surrounding, (Fischer *et al.*, 2005), and the concomitant development of new theoretical approaches.

The stimulus for such extensive studies is that impurities are markers that allow to reveal the nature of correlations and pairing of the state where impurities are placed. Indeed particular pattern of impurity-induced electronic states is closely connected to the symmetry of the superconducting gap and to the underlying electronic band structure and helps us to understand the nature of superconducting pairing. If strong electronic correlations in the ground state are present, they also are reflected in details of impurity induced states. Therefore watching the waves created by throwing a pebble in the pond of correlated electrons helps us understand the properties of the underlying electronic liquid.

We kept the discussion general to allow applications to other systems and materials. For instance, this was our rationale for employing the BCS state to describe superconductivity. We believe that it is a good approximation in heavy fermion, organic superconductors and SrRuO_4 , at very low energy. At the same time, deviations from this mean field picture may provide additional details on the underlying physics of the particular material. Ma-

majority of the data at a moment are obtained in high- T_c materials. It is clear that similar local effects are present around impurities in other unconventional superconductors, e.g. in $\text{Na}_x\text{CoO}_2 \cdot y\text{H}_2\text{O}$ superconductors (Wang and Wang, 2004), although we are not aware of any data on single impurity states in these materials. Given the importance of the impurity states, this field will undoubtedly be extended to other systems by future experiments.

Outlook for the future. New ideas and directions continue to emerge in the studies of electronic properties induced by impurities. The suite of new experimental tools that address local electronic effects, such as STM, will help to clarify the role of interference between several impurities, and pave the way towards connecting the microscopic local states with average properties. Recent theoretical work addressed some aspects of this subject (Andersen, 2003; Atkinson *et al.*, 2003; Morr and Balatsky, 2003; Morr and Stavropoulos, 2003b; Zhu *et al.*, 2003, 2004b), and is awaiting direct comparison with experiment.

Another promising avenue is combining the spatial resolution of STM-STs with the time resolution. The subject is still in its infancy, both theoretically and experimentally, but hold immense promise for the future. Sec. XI reviewed some of very recent work in this direction. Temporal and spatial characterization of the states generated by dynamical impurities allow exploration of the correlations inside the electronic state in which impurity is placed. One obvious example where such characterization is crucial is the Kondo effect in a superconducting state. It is desirable to have a time resolved measurements that allow to visualize the Kondo effect in a superconductor. Another interesting problem that needs further elaboration is a role of collective modes in impurity-induced states. We are only starting to investigate these questions, as discussed in Sec. XII.C.

Real progress on these problems will be made when we have real data. As usual, one should expect that the data will have surprises that were not anticipated in simple theoretical models. This will motivate further theoretical studies, stimulate more measurements, and therefore will lead to a rapid further development of the field. They can provide space (and time) resolved window into the intimate workings of the correlated electron matter. We have every reason to be enthusiastic and optimistic about the future the field of impurity states in superconductors, and in other correlated electron systems.

Acknowledgments

We would like to thank many of our colleagues for useful discussions. We are especially grateful to our collaborators over many years who were instrumental in our work on the subjects that are reviewed here. Without their insights and knowledge this work would be impossible. We thank Ar. Abanov, E. Abrahams, H. Al-loul, B. Altshuler, K. Bedell, A. R. Bishop, D. Bonn, P.

Bourges, J. Carbotte, C. Capan, A. H. Castro Neto, S. Chakravarty, N. Curro, J. C. Davis, D. Eigler, M. Franz, C. D. Gong, L. P. Gor'kov, M. J. Graf, I. A. Gruzberg, W. Hardy, P. J. Hirschfeld, W. Ho, C. R. Hu, A. Kapitulnik, S. Kivelson, T. K. Lee, I. Martin, D. K. Morr, S.H. Pan, D. Pines, A. Rosengren, M. I. Salkola, J. Sar-

rao, J. A. Sauls, D. J. Scalapino, K. Scharnberg, J. R. Schrieffer, A. V. Shytov, Q. Si, C. S. Ting, J.D. Thompson, M. Vojta, Z. D. Wang, A. Yazdani and J. Zaanen for fruitful discussions. This work was supported by the U.S. Department of Energy (A.V.B. and J.X.Z.) and by the Board of Regents of Louisiana (I. V.).

List of Symbols

Quantity	Explanation
a	Lattice parameter
$b(b^\dagger)$	Bosonic annihilation (creation) operators
$c(c^\dagger)$	Fermionic annihilation (creation) operators
d	Spatial dimension
D	Half energy bandwidth
Δ_0	Superconducting energy gap
Δ_k	Momentum-dependent superconducting energy gap
$\phi_n(\mathbf{r})$	Electron eigenfunction
E_F	Electron Fermi energy
$G(\tau, \tau'), G(\tau, \mathbf{r})$	Electron Green's function in coordinate space
$G(\omega_n, \mathbf{k}), G(\mathbf{k}, \omega_n)$	Electron Green's function in Matsubara frequency and momentum space
H, \mathcal{H}, H_{int}	Hamiltonian
J, J_0, J_c	Exchange coupling
L	Linear dimension of a system
μ	Chemical potential
$N(\epsilon)$	Electron density of states
$N(\epsilon, \mathbf{r}), N(E, i)$	Electron local density of states
$\psi(\mathbf{r})(\psi^\dagger(\mathbf{r}))$	Fermionic field operators in continuum space
$ \Psi\rangle, \Psi_0\rangle$	BCS variational wavefunction
$ \Psi_{-1}\rangle, \Phi_{-1}\rangle$	Excited variational wavefunction with single particle excitation present
\mathbf{r}	Spatial coordinates
$\boldsymbol{\sigma}$	Pauli matrices in spin space
$\boldsymbol{\tau}$	Pauli matrices in Nambu space
$V_{\alpha\beta\gamma\delta}, \tilde{V}_{\alpha\beta}$	Superconducting pairing interaction
\mathbf{S}	Local spin operator
t, t'	Electron hopping integral
u	Electron-like Bogoliubov quasiparticle wavefunction amplitude
$T(\omega)$	T -matrix
T	Temperature
v	Hole-like Bogoliubov quasiparticle wavefunction amplitude
U	Hubbard on-site electron-electron interaction
U_0	Impurity scattering potential
W	Half energy bandwidth
$W_{\mathbf{k}}$	D -density-wave order parameter
ξ_0	BCS superconducting coherence length at low temperatures
$\xi(T)$	BCS temperature dependent coherence length

References

Abanov, A., and A. V. Chubukov, 2000, Phys. Rev. B **61**, R9241.

Abanov, A., A. V. Chubukov, M. Eschrig, M. R. Norman, and J. Schmalian, 2002, Phys. Rev. Lett. **89**, 177002.
 Abrahams, E., and C. M. Varma, 2000, Proc. Natl. Acad. Sci.

- 97**, 5714.
- Abrikosov, A. A., and L. P. Gorkov, 1960, *Zh. Eksp. Teor. Fiz.* **39**, 1781, [Sov. Phys. JETP **12**, 1243 (1961)].
- Abrikosov, A. A., L. P. Gorkov, and I. E. Dzyaloshinski, 1963, *Methods of Quantum Field Theory in Statistical Physics* (Dover Publications, Inc., New York).
- Adagideli, I., P. M. Goldbart, A. Shnirman, and A. Yazdani, 1999, *Phys. Rev. Lett.* **83**, 5571.
- Affleck, I., and J. B. Marston, 1988, *Phys. Rev. B* **37**, 3774.
- Alloul, H., P. Mendels, H. Casalta, J.-F. Marucco, and J. Arabski, 1991, *Phys. Rev. Lett.* **67**, 3140.
- Altland, A., B. D. Simons, and D. Taras-Semchuk, 2000, *Adv. Phys.* **49**, 321.
- Altland, A., B. D. Simons, and M. R. Zirnbauer, 2002, *Physics Reports* **359**, 283.
- Altland, A., and M. Zirnbauer, 1997, *Phys. Rev. B* **55**, 1142.
- Altshuler, B. L., 1985, *Pis'ma ZhETF* **51**, 530, [JETP Lett. **41**, 648 (1985)].
- Ambegaokar, V., and A. Griffin, 1965, *Phys. Rev.* **137**, A1151.
- Andersen, B. M., 2003, *Phys. Rev. B* **68**, 094518.
- Andersen, B. M., and P. Hedegård, 2003, *Phys. Rev. B* **67**, 172505.
- Andersen, O. K., A. I. Lichtenstein, O. Jepsen, and F. Paulsen, 1995, *J. Phys. Chem. Solids* **56**, 1573.
- Anderson, P. W., 1959, *Phys. Rev. Lett.* **3**, 325.
- Anderson, P. W., 1970, *J. Phys. C* **3**, 2436.
- Anderson, P. W., G. Yuval, and D. R. Hamann, 1970, *Phys. Rev. B* **1**, 4464.
- Andrei, N., 1980, *Phys. Rev. Lett.* **45**, 379.
- Annett, J., 1990, *Adv. Phys.* **39**, 83.
- Aprili, M., M. Covington, E. Paraoanu, B. Niedermeier, and L. H. Greene, 1998, *Phys. Rev. B* **57**, R8139.
- Arfi, B., H. Bahlouli, C. Pethick, and D. Pines, 1988, *Phys. Rev. Lett.* **60**, 2206.
- Aristov, D. N., and A. G. Yashenkin, 1998, *Phys. Rev. Lett.* **80**, 1116.
- Atkinson, W. A., and P. J. Hirschfeld, 2002, *Phys. Rev. Lett.* **88**, 187003.
- Atkinson, W. A., P. J. Hirschfeld, A. H. MacDonald, and K. Ziegler, 2000, *Phys. Rev. Lett.* **85**, 3926.
- Atkinson, W. A., P. J. Hirschfeld, and L. Zhu, 2003, *Phys. Rev. B* **68**, 054501.
- Bader, S. D., N. E. Phillips, M. B. Maple, and C. A. Luengo, 1975, *Solid State Commun.* **16**, 1263.
- Balatsky, A., 1998, *Phys. Rev. Lett.* **80**, 1972.
- Balatsky, A., 2000, *Phys. Rev. B* **61**, 6940.
- Balatsky, A., and E. Abrahams, 1992, *Phys. Rev. B* **45**, 13125.
- Balatsky, A. V., A. Abanov, and J.-X. Zhu, 2003, *Phys. Rev. B* **68**, 214506.
- Balatsky, A. V., A. Rosengren, and B. L. Altshuler, 1994, *Phys. Rev. Lett.* **73**, 720.
- Balatsky, A. V., and M. I. Salkola, 1998, *Phys. Rev. Lett.* **80**, 1117.
- Balatsky, A. V., M. I. Salkola, and A. Rosengren, 1995, *Phys. Rev. B* **51**, 15547.
- Balatsky, A. V., and S. A. Trugman, 1997, *Phys. Rev. Lett.* **79**, 3767.
- Barash, Y. S., A. Grishin, and M. Sigrist, 1997, *Zh. Eksp. Teor. Fiz.* **112**, 304, [JETP **85**, 168 (1997)].
- Barash, Y. S., M. S. Kalenkov, and J. Kurkijrvi, 2000, *Phys. Rev. B* **62**, 6665.
- Bauriedl, W., P. Ziemann, and W. Buckel, 1981, *Phys. Rev. Lett.* **47**, 1163.
- Beloborodov, I. S., B. N. Narozhny, and I. L. Aleiner, 2000, *Phys. Rev. Lett.* **85**, 816.
- Berezinskii, V., 1974, *Pisma Zhurn. Eksp. Teor. Fiz.* **20**, 628, [JETP Lett. **20**, 287 (1974)].
- Berlinsky, A. J., D. A. Bonn, R. Harris, and C. Kallin, 2000, *Phys. Rev. B* **61**, 9088.
- Bhaseen, M. J., J. S. Caux, I. I. Kogan, and A. M. Tsvelik, 2001, *Nucl. Phys. B* **618**, 465.
- Bickers, N. E., and G. E. Zwicknagl, 1987, *Phys. Rev. B* **36**, 6746.
- Blonder, G. E., M. Tinkham, and T. M. Klapwijk, 1982, *Phys. Rev. B* **25**, 4515.
- Blount, E. I., 1985, *Phys. Rev. B* **32**, 2935.
- Bobroff, J., H. Alloul, W. MacFarlane, P. Mendels, N. Blanchard, G. Collin, and J. Marucco, 2001, *Phys. Rev. Lett.* **86**, 4116.
- Borkowski, L. S., and P. J. Hirschfeld, 1992, *Phys. Rev. B* **46**, 9274.
- Borkowski, L. S., and P. J. Hirschfeld, 1994, *J. Low Temp. Phys.* **96**, 185.
- Brandt, U., 1970, *J. Low Temp. Phys.* **2**, 573.
- Buchholtz, L. J., and G. Zwicknagl, 1981, *Phys. Rev. B* **23**, 5788.
- Bulaevskii, L., V. Kuzii, and A. Sobyenin, 1977, *Pisma Zh. Eksp. Teor. Phys.* **25**, 314, [JETP Lett. **25**, 290 (1977)].
- Bulla, R., M. T. Glossop, D. E. Logan, and T. Pruschke, 2000, *J. Phys.: Condens. Matter* **12**, 4899.
- Bulla, R., T. Pruschke, and A. C. Hewson, 1997, *J. Phys.: Condens. Matter* **9**, 10463.
- Buzdin, A., L. Bulaevskii, and S. Panyukov, 1982, *Pisma Zh. Eksp. Teor. Phys.* **35**, 147, [JETP Lett. **35**, 178 (1982)].
- Buzdin, A. I., 2005, *Rev. Mod. Phys.* **XX**, ****.
- Byers, J. M., M. E. Flatté, and D. J. Scalapino, 1993, *Phys. Rev. Lett.* **71**, 3363.
- Campuzano, J. C., H. Ding, M. R. Norman, H. M. Fretwell, M. Randeria, A. Kaminski, J. Mesot, T. Takeuchi, T. Sato, T. Yokoya, T. Takahashi, T. Mochiku, *et al.*, 1999, *Phys. Rev. Lett.* **83**, 3709.
- Campuzano, J. C., M. R. Norman, and M. Randeria, 2004, in *Physics of Superconductors* (Springer, Berlin), volume II, p. 167.
- Capriotti, L., D. J. Scalapino, and R. D. Sedgewick, 2003, *Phys. Rev. B* **68**, 014508.
- Carbotte, J. P., 1990, *Rev. Mod. Phys.* **62**, 1027.
- Carr, G. L., R. P. S. M. Lobo, J. LaVeigne, D. H. Reitze, and D. B. Tanner, 2000, *Phys. Rev. Lett.* **88**, 3001.
- Cassanello, C. R., and E. Fradkin, 1996, *Phys. Rev. B* **53**, 15079.
- Cassanello, C. R., and E. Fradkin, 1997, *Phys. Rev. B* **56**, 11246.
- Chaba, A. N., and A. D. S. Nagi, 1972, *Can. J. Phys.* **50**, 1736.
- Chakravarty, S., R. B. Laughlin, D. K. Morr, and C. Nayak, 2001, *Phys. Rev. B* **63**, 094503.
- Chamon, C., and C. Mudry, 2001, *Phys. Rev. B* **63**, 100503.
- Chen, D. C., D. Rainer, and J. Sauls, 1999, in *Proceedings of the International Conference on Quasiclassical Methods in Superconductivity and Superfluidity, VERDITZ 96*, edited by D. Rainer and J. A. Sauls.
- Chen, H.-D., J.-P. Hu, S. Capponi, E. Arrighoni, and S.-C. Zhang, 2002, *Phys. Rev. Lett.* **89**, 137004.
- Chen, H. Y., and C. S. Ting, 2003, *Phys. Rev. B* **68**, 212502.
- Chen, K., and C. Jayaprakash, 1995, *J. Phys.:Condens. Matter* **7**, L491.

- Chen, Q., I. Kosztin, B. Janko, and K. Levin, 1998, Phys. Rev. Lett. **81**, 4708.
- Chen, Y., and C. S. Ting, 2004, Phys. Rev. Lett. **92**, 077203.
- Chiao, M., R. W. Hill, C. Lupien, L. Taillefer, P. Lambert, R. Gagnon, and P. Fournier, 2000, Phys. Rev. B **62**, 3554.
- Choi, C., and P. Muzikar, 1990, Phys. Rev. B **41**, 1812.
- Choi, C. H., 1999, Phys. Rev. B **60**, 6884.
- Chubukov, A. V., A. Abanov, and D. N. Basov, 2003, Phys. Rev. B **68**, 024504.
- Coleman, P., 1984, Phys. Rev. B **29**, 3035.
- Coleman, P., 1985, J. Magn. Mater. **47**, 323.
- Corson, J., J. Orenstein, S. Oh, J. O'Donnell, and J. N. Eckstein, 2000, Phys. Rev. Lett. **85**, 2569.
- Covington, M., M. Aprili, E. Paraoanu, L. H. Greene, F. Xu, J. Zhu, and C. A. Mirkin, 1997, Phys. Rev. Lett. **79**, 277, [Erratum: Phys. Rev. Lett. **79**, 2598 (1997)].
- Cox, D. L., and A. Zawadowski, 1998, Adv. Phys. **47**, 599.
- Damascelli, A., Z. Hussain, and Z.-X. Shen, 2003, Rev. Mod. Phys. **75**, 473.
- Dessau, D. S., B. O. Wells, Z. Shen, W. E. Spicer, A. J. Arko, R. S. List, D. B. Mitzi, and A. Kapitulnik, 1991, Phys. Rev. Lett. **66**, 2160.
- Duffy, D., P. J. Hirschfeld, and D. J. Scalapino, 2001, Phys. Rev. B **64**, 224522.
- Dumoulin, L., E. Guyon, and P. Nedellec, 1975, Phys. Rev. Lett. **34**, 264.
- Dumoulin, L., E. Guyon, and P. Nedellec, 1977, Phys. Rev. B **16**, 1086.
- Edelstein, A. S., 1967, Phys. Rev. Lett. **19**, 1184.
- Emery, V. J., and S. A. Kivelson, 1995, Nature (London) **374**, 434.
- Eschrig, M., and M. R. Norman, 2000, Phys. Rev. Lett. **85**, 3261.
- Fetter, A. L., 1965, Phys. Rev. **140**, A1921.
- Fetter, A. L., and J. D. Walecka, 1971, *Quantum Theory of Many-Particle Systems* (McGraw Hill, Inc., New York).
- Fischer, O., M. Kugler, I. Maggio-Aprile, C. Berthod, and C. Renner, 2005, Rev. Mod. Phys. **XX**, ****.
- Flatté, M. E., and J. M. Byers, 1997a, Phys. Rev. Lett. **78**, 3761.
- Flatté, M. E., and J. M. Byers, 1997b, Phys. Rev. B **56**, 11213.
- Flatte, M. E., and J. M. Byers, 1998, Phys. Rev. Lett. **80**, 4546.
- Flatté, M. E., and J. M. Byers, 1999, Solid State Physics **52**, 137.
- Fogelström, M., D. Rainer, and J. A. Sauls, 1997, Phys. Rev. Lett. **79**, 281.
- Franz, M., C. Kallin, and A. J. Berlinsky, 1996, Phys. Rev. B **54**, R6897.
- Franz, M., D. E. Sheehy, and Z. Tešanović, 2002, Phys. Rev. Lett. **88**, 257005.
- Franz, M., and Z. Tešanović, 1998, Phys. Rev. Lett. **80**, 4763.
- Galitskii, V. M., and A. I. Larkin, 2002, Phys. Rev. B **66**, 064526.
- de Gennes, P. G., 1989, *Superconductivity of Metals and Alloys* (Addison-Wesley, New York).
- Ghosal, A., and H. Y. Kee, 2004, Phys. Rev. B **69**, 224513.
- Ghosal, A., M. Randeria, and N. Trivedi, 1998, Phys. Rev. Lett. **81**, 3940.
- Ginzberg, D. M., 1979, Phys. Rev. B **20**, 960.
- Glazman, L., and K. Matveev, 1989, Pisma Zh. Eksp. Teor. Phys. **49**, 570, [JETP Lett. **49**, 660 (1989)].
- Golubov, A. A., and I. I. Mazin, 1999, Phys. Rev. B **55**, 15146.
- Gong, C.-D., and J.-H. Cai, 1966, J. Phys. (China) **22**, 381.
- Gonzalez-Buxton, C., and K. Ingersent, 1998, Phys. Rev. B **57**, 15254.
- Gorkov, L. P., and P. A. Kalugin, 1985, Pis'ma ZhETF **41**, 208, [JETP Lett. **41**, 253 (1985)].
- Graf, M., A. Balatsky, and J. Sauls, 2000, Phys. Rev. B **61**, 3255.
- Graf, M. J., J. Sauls, and D. Rainer, 1995, Phys. Rev. B **52**, 10588.
- Graf, M. J., S.-K. Yip, J. A. Sauls, and D. Rainer, 1996, Phys. Rev. B **53**, 15147.
- Grimaldi, C., 1999, Europhys. Lett. **48**, 306.
- Grimaldi, C., 2002, Phys. Rev. B **65**, 094502.
- Gweon, G.-H., T. Sasagawa, S. Y. Zhou, J. Graf, H. Takagi, D.-H. Lee, and A. Lanzara, 2004, Nature (London) **430**, 187.
- Hahn, J. R., and W. Ho, 2001, Phys. Rev. Lett. **87**, 166102.
- Halperin, B. I., and M. Lax, 1966, Phys. Rev. **148**, 722.
- Hamann, D. R., 1967, Phys. Rev. **158**, 570.
- Han, Q., Z. D. Wang, X.-G. Li, and L. y. Zhang, 2002, Phys. Rev. B **66**, 104502.
- Han, Q., T. Xia, Z. D. Wang, and X.-G. Li, 2004, Phys. Rev. B **69**, 224512.
- Haran, G., and A. D. S. Nagi, 1996, Phys. Rev. B **54**, 15463.
- Haran, G., and A. D. S. Nagi, 1998, Phys. Rev. B **58**, 12441.
- Harlingen, D. J. V., 1995, Rev. Mod. Phys. **67**, 515.
- Heinrichs, J., 1968, Phys. Rev. **168**, 451.
- Hettler, M. H., and P. J. Hirschfeld, 1999, Phys. Rev. B **59**, 9606.
- Hewson, A. C., 1993, *The Kondo Problem to heavy Fermions* (Cambridge University Press).
- Hill, R. W., C. Lupien, M. Sutherland, E. Boaknin, D. G. Hawthorn, C. Proust, F. Ronning, L. Taillefer, R. Liang, D. A. Bonn, and W. N. Hardy, 2004, Phys. Rev. Lett. **92**, 027001.
- Hirschfeld, P. J., and W. A. Atkinson, 2002, J. Low Temp. Phys. **126**, 881.
- Hirschfeld, P. J., and N. Goldenfeld, 1993, Phys. Rev. B **48**, 4219.
- Hirschfeld, P. J., W. O. Putikka, and D. J. Scalapino, 1994, Phys. Rev. B **50**, 10250.
- Hirschfeld, P. J., S. M. Quinlan, and D. J. Scalapino, 1997, Phys. Rev. B **55**, 12742.
- Hirschfeld, P. J., P. Wölfle, D. Einzel, J. A. Sauls, and W. O. Putikka, 1989, Phys. Rev. B **40**, 6695.
- Hirschfeld, P. J., P. Wölfle, and D. Vollhard, 1986, Sol. State Comm **59**, 111.
- Hirschfeld, P. J., P. W. Wölfle, and D. Einzel, 1988, Phys. Rev. B **37**, 83.
- Hoffman, J. E., E. W. Hudson, K. M. Lang, V. Madhavan, H. Eisaki, S. Uchida, and J. C. Davis, 2002a, Science **295**, 466.
- Hoffman, J. E., K. McElroy, D.-H. Lee, K. M. Lang, H. Eisaki, S. Uchida, and J. C. Davis, 2002b, Science **297**, 1148.
- Hosseini, A., R. Harris, S. Kamal, P. Dosanjh, J. Preston, R. Liang, W. N. Hardy, and D. A. Bonn, 1999, Phys. Rev. B **60**, 1349.
- Hotta, T., 1993, J. Phys. Soc. Jpn **62**, 274.
- Howald, C., H. Eisaki, N. Kaneko, M. Greven, and A. Kapitulnik, 2003, Phys. Rev. B **67**, 014533.
- Howald, C., P. Fournier, and A. Kapitulnik, 2001, Phys. Rev. B **64**, 100504.
- Howell, P. C., A. Rosch, and P. J. Hirschfeld, 2004, Phys. Rev. Lett. **92**, 037003.

- Hsu, T. C., J. B. Marston, and I. Affleck, 1991, *Phys. Rev. B* **43**, 2866.
- Hu, C.-R., 1994, *Phys. Rev. Lett.* **72**, 1526.
- Hudson, E. W., K. M. Lang, V. Madhavan, S. H. Pan, H. Eisaki, S. Uchida, and J. C. Davis, 2001, *Nature* **411**, 920.
- Hudson, E. W., S. H. Pan, A. K. Gupta, K.-W. Ng, and J. C. Davis, 1999, *Science* **285**, 88.
- Hussey, N. E., 2002, *Adv. Phys.* **51**, 1685.
- Ingersent, K., 1996, *Phys. Rev. B* **54**, 11936.
- Ingersent, K., and Q. Si, 1998, eprint cond-mat/9810226.
- Ishida, K., Y. Kitaoka, N. Ogata, T. Kamino, K. Asayama, J. R. Cooper, and N. Athanassopoulou, 1993, *J. Phys. Soc. Jpn.* **63**, 2803.
- Ishida, K., Y. Kitaoka, K. Yamazoe, K. Asayama, and Y. Yamada, 1996, *Phys. Rev. Lett.* **76**, 531.
- Ishida, K., Y. Kitaoka, T. Yoshitomi, N. Ogata, T. Kamino, and K. Asayama, 1991, *Physica C* **179**, 29.
- Itoh, Y., 1993, *J. Phys. Soc. Jpn.* **62**, 2184.
- Janko, B., I. Kosztin, K. Levin, M. Norman, and D. Scalapino, 1999, *Phys. Rev. Lett.* **82**, 4304.
- Jarrell, M., 1990, *Phys. Rev. B* **41**, 4815.
- Jarrell, M., D. S. Silva, and B. Patton, 1990, *Phys. Rev. B* **42**, 4804.
- Joynt, R., 1997, *J. Low Temp. Phys.* **109**, 811.
- Kampf, A. P., and T. P. Devereaux, 1997, *Phys. Rev. B* **56**, 2360.
- Kashiwaya, S., and Y. Tanaka, 2000, *Rep. Prog. Phys.* **63**, 1641.
- Kee, H. Y., 2001, *Phys. Rev. B* **64**, 012506.
- Kee, H.-Y., S. A. Kivelson, and G. Aeppli, 2002, *Phys. Rev. Lett.* **88**, 257002.
- Ketterson, J. B., and S. N. Song, 1999, *Superconductivity* (Cambridge University Press).
- Khaykovich, B., Y. S. Lee, R. W. Erwin, S. H. Lee, S. Wakimoto, K. J. Thomas, M. A. Kastner, and R. J. Birgeneau, 2002, *Phys. Rev. B* **66**, 014528.
- Kim, H., and P. Muzikar, 1993, *Phys. Rev. B* **48**, 39332.
- Kivelson, S. A., I. P. Bindloss, E. Fradkin, V. Oganessian, J. M. Tranquada, A. Kapitulnik, and C. Howald, 2003, *Rev. Mod. Phys.* **75**, 1201.
- Koga, M., and M. Matsumoto, 2002a, *J. Phys. Soc. Jpn.* **71**, 943.
- Koga, M., and M. Matsumoto, 2002b, *Phys. Rev. B* **65**, 094434.
- Kondo, J., 1964, *Prog. Theor. Phys.* **32**, 37.
- Kosterlitz, J. M., and D. J. Thouless, 1973, *J. Phys. C* **6**, 1181.
- Kosterlitz, J. M., and D. J. Thouless, 1974, *J. Phys. C* **7**, 1046.
- Krasnov, V. M., A. Yurgens, D. Winkler, P. Delsing, and T. Claeson, 2000, *Phys. Rev. Lett.* **84**, 5860.
- Kruis, H. V., I. Martin, and A. V. Balatsky, 2001, *Phys. Rev. B* **64**, 054501.
- Kuboki, K., and M. Sgrist, 1998, *J. Phys. Soc. Jpn.* **67**, 2873.
- Kulic, M. L., and O. V. Dolgov, 1999, *Phys. Rev. B* **60**, 13062.
- Kulik, I. O., and O. Y. Itskovich, 1968, *Zh. Eksp. i Teor. Fiz.* **55**, 193, [*Sov. Phys. JETP* **28**, 102 (1969)].
- Lake, B., G. Aeppli, K. N. Clause, D. F. McMorrow, K. Lefmann, N. E. Hussey, N. Mangkorntong, M. Nohara, H. Takagi, T. E. Mason, and A. Schröder, 2001, *Science* **291**, 1759.
- Lake, B., H. M. Rønnow, N. B. Christensen, G. Aeppli, K. Lefmann, D. F. McMorrow, P. Vorderwisch, P. Smeibidl, N. Mangkorntong, T. Sasagawa, M. Nohara, *et al.*, 2002, *Nature* **415**, 299.
- Lamacraft, A., and B. D. Simons, 2000, *Phys. Rev. Lett.* **85**, 4783.
- Lamacraft, A., and B. D. Simons, 2001, *Phys. Rev. B* **64**, 014514.
- Landau, L., and E. Lifshitz, 2000, *Quantum Mechanics, vol. 3* (Butterworth-Heinemann, Oxford).
- Lang, K. M., V. Madhavan, J. E. Hoffman, E. W. Hudson, H. Eisaki, S. Uchida, and J. C. Davis, 2002, *Nature* **415**, 412.
- Lanzara, A., P. V. Bogdanov, X. J. Zhou, S. A. Kellar, D. L. Feng, E. D. Lu, T. Yoshida, H. Eisaki, A. Fujimori, K. Kishio, J.-I. Shimoyama, T. Noda, *et al.*, 2004, *Nature (London)* **430**, 187.
- Larkin, A., 1965, *JETP Lett.* **2**, 130.
- Larkin, A. I., V. I. Mel'nikov, and D. E. Khmel'nitskii, 1971, *Sov. Phys. JETP* **33**, 458.
- Larkin, A. I., and Y. N. Ovchinnikov, 1972, *Sov. Phys. JETP* **34**, 1144.
- Laughlin, R. B., 1998, *Phys. Rev. Lett.* **80**, 5188.
- Lee, P. A., 1993, *Phys. Rev. Lett.* **71**, 1887.
- Lee, P. A., and T. V. Ramakrishnan, 1985, *Rev. Mod. Phys.* **57**, 287.
- Lee, Y.-S., K. Segawa, Y. Ando, and D. N. Basov, 2004, *Phys. Rev. B* **70**, 014518.
- Li, J.-X., W.-G. Yin, and C.-D. Gong, 1998, *Phys. Rev. B* **58**, 2895.
- Liang, S. D., and T. K. Lee, 2002, *Phys. Rev. B* **65**, 214529.
- Lifshitz, I. M., 1964a, *Adv. Phys.* **13**, 483.
- Lifshitz, I. M., 1964b, *Usp. Fiz. Nauk* **83**, 617, [*Sov. Phys. Usp.* **7**, 549 (1965)].
- Lifshitz, I. M., 1967, *Zh. Eksp. i Teor. Fiz.* **53**, 743, [*Sov. Phys. JETP* **26**, 462 (1968)].
- Lifshitz, I. M., S. A. Gredeskul, and L. A. Pastur, 1988, *Introduction to the theory of disordered systems* (John Wiley & Sons, New York).
- Logan, D. E., and M. T. Glossop, 2000, *J. Phys.: Condens. Matter* **12**, 985.
- Loktev, V. M., and Y. Pogorelov, 2002, *Europhys. Lett.* **60**, 757.
- Loram, J. W., J. L. Luo, J. R. Cooper, W. Y. Liang, and J. L. Tallon, 2000, *Physica (Amsterdam) C* **341-348**, 831.
- Ma, M., and P. A. Lee, 1985, *Phys. Rev. B* **32**, 5658.
- Machida, K., and F. Shibata, 1972, *Prog. Theor. Phys.* **47**, 1817.
- Mackenzie, A. P., K. Haselwimmer, A. Tyler, G. Lonzarich, Y. Mori, S. Nishizaki, and Y. Maeno, 1998, *Phys. Rev. Lett.* **80**, 161.
- Mackenzie, A. P., and Y. Maeno, 2003, *Rev. Mod. Phys.* **75**, 657.
- Mahajan, A. V., H. Alloul, G. Collin, and J.-F. Marucco, 1994, *Phys. Rev. Lett.* **72**, 3100.
- Mahajan, A. V., H. Alloul, G. Collin, and J.-F. Marucco, 2000, *Eur. Phys. J. B* **13**, 457.
- Mahan, G. D., 2000, *Many-Particle Physics* (Kluwer Academic/Plenum Publishers, New York), 3rd edition.
- Maki, K., 1969, in *Superconductivity*, edited by R. D. Parks (Marcel Dekker, New York), p. 1035.
- Maple, M. B., 1973, in *Magnetism*, edited by H. Suhl (Academic Press, New York), volume V, p. 289.
- Marchetti, F. M., and B. D. Simons, 2002, *J. Phys. A: Math. Gen.* **35**, 4201.
- Markowitz, D., and L. P. Kadanoff, 1963, *Phys. Rev.* **131**, 563.

- Marston, J. B., and I. Affleck, 1989, Phys. Rev. B **39**, 11538.
- Martin, I., and A. V. Balatsky, 2000, Phys. Rev. B **62**.
- Martin, I., A. V. Balatsky, and J. Zaanen, 2002, Phys. Rev. Lett. **88**, 097003.
- Martnez-Samper, P., H. Suderow, S. Vieira, J. P. Brison, N. Luchier, P. Lejay, and P. C. Canfield, 2003, Phys. Rev. B **67**, 014526.
- Matsumoto, M., and M. Koga, 2002, Phys. Rev. B **65**, 024508.
- Matsuura, T., 1977, Progr. Theor. Phys. **57**, 1823.
- Matsuura, T., S. Ichinose, and Y. Nagaoka, 1977, Progr. Theor. Phys. **57**, 713.
- McElroy, K., R. W. Simmonds, J. E. Hoffman, D. H. Lee, J. Orenstein, H. Eisaki, S. Uchida, and J. C. Davis, 2003, Nature **422**, 592.
- Mendels, P., J. Bobroff, G. Collin, H. Alloul, M. Gabay, J.-F. Marucco, N. Blanchard, and B. Grenier, 1999, Europhys. Lett. **46**, 678.
- Meyer, J. S., and B. D. Simons, 2001, Phys. Rev. B **64**, 134516.
- Millis, A. J., 2003, Solid State Commun. **126**, 3.
- Misra, S., S. Oh, D. J. Hornbaker, T. DiLuccio, J. N. Eckstein, and A. Yazdani, 2002, Phys. Rev. Lett. **89**, 087002.
- Moradian, R., J. F. Annett, B. L. Gyorffy, and G. Litak, 2001, Phys. Rev. B **63**, 024501.
- Morr, D. K., 2002, Phys. Rev. Lett. **89**, 106401.
- Morr, D. K., and A. V. Balatsky, 2003, Phys. Rev. Lett. **90**, 067005.
- Morr, D. K., and R. H. Nyberg, 2003, Phys. Rev. B **68**, 060505.
- Morr, D. K., and N. A. Stavropoulos, 2002, Phys. Rev. B **66**, 140508.
- Morr, D. K., and N. A. Stavropoulos, 2003a, Phys. Rev. B **68**, 094518.
- Morr, D. K., and N. A. Stavropoulos, 2003b, Phys. Rev. B **67**, 020502.
- Movshovich, R., M. A. Hubbard, M. B. Salamon, A. V. Balatsky, R. Yoshizaki, J. L. Sarrao, and M. Jaime, 1998, Phys. Rev. Lett. **80**, 1968.
- Müller-Hartmann, E., 1973, in *Magnetism*, edited by H. Suhl (Academic Press, New York), volume V, p. 353.
- Müller-Hartmann, E., and J. Zittartz, 1971, Phys. Rev. Lett. **26**, 428.
- Nagaoka, Y., 1965, Phys. Rev. Ser. A **138**, 1112.
- Nagaoka, Y., 1967, Progr. Theor. Phys. **37**, 13.
- Neils, W. K., and D. J. V. Harlingen, 2002, Phys. Rev. Lett. **88**, 047001.
- Nersisyan, A., and A. Tsvelik, 1997, Phys. Rev. Lett. **78**, 3981.
- Nersisyan, A., A. Tsvelik, and F. Wenger, 1995, Nucl. Phys. B **438**, 561.
- Nicol, E. J., and J. P. Carbotte, 2003, Phys. Rev. B **67**, 214506.
- Norman, M. R., and H. Ding, 1998, Phys. Rev. B **57**, 11089.
- Norman, M. R., H. Ding, M. Randeria, J. C. Campuzano, T. Yokoya, T. Takeuchi, T. Takahashi, T. Mochiku, K. Kadowaki, P. Guptasarma, and D. G. Hinks, 1998, Nature (London) **392**, 157.
- Norman, M. R., M. Randeria, H. Ding, and J. C. Campuzano, 1995, Phys. Rev. B **52**, 615.
- Ogura, J., and T. Saso, 1993, J. Phys. Soc. Jpn. **62**, 4364.
- Okabe, Y., and A. D. S. Nagi, 1983, Phys. Rev. B **28**, 1320.
- Pan, S., E. W. Hudson, and J. Davis, 1998, Appl. Phys. Lett. **73**, 2992.
- Pan, S. H., E. W. Hudson, A. K. Gupta, K.-W. Ng, H. Eisaki, S. Uchida, and J. C. Davis, 2000a, Phys. Rev. Lett. **85**, 1536.
- Pan, S. H., E. W. Hudson, K. M. Lang, H. Eisaki, S. Uchida, and J. C. Davis, 2000b, Nature **403**, 746.
- Pan, S. H., J. P. O'Neal, R. L. Badzey, C. Chamon, H. Ding, J. R. Engelbrechet, Z. Wang, H. Eisaki, S. Uchida, A. K. Gupta, K.-W. Ng, E. W. Hudson, *et al.*, 2001, Nature **413**, 282.
- Pepin, C., and P. A. Lee, 1998, Phys. Rev. Lett. **81**, 2779.
- Pepin, C., and P. A. Lee, 2001, Phys. Rev. B **63**, 054502.
- Petersen, L., P. T. Sprunger, P. Hoffmann, E. Lægsgaard, B. G. Briner, M. Doering, H.-P. Rust, A. M. Bradshaw, F. Besenbacher, and E. W. Plummer, 1998, Phys. Rev. B **57**, R6858.
- Pethick, C. J., and D. Pines, 1986, Phys. Rev. Lett. **57**, 118.
- Podolsky, D., E. Demler, K. Damle, and B. I. Halperin, 2003, Phys. Rev. B **67**, 094514.
- Pogorelov, Y., 1994, Physica C **235-240**, 2279.
- Polkovnikov, A., 2002, Phys. Rev. B **65**, 064503.
- Polkovnikov, A., S. Sachdev, and M. Vojta, 2001, Phys. Rev. Lett. **86**, 296.
- Polkovnikov, A., S. Sachdev, and M. Vojta, 2003, Physica C **388-389**, 19.
- Quinlan, S. M., P. J. Hirschfeld, and D. J. Scalapino, 1996, Phys. Rev. B **53**, 8575.
- Quinlan, S. M., D. J. Scalapino, and N. Bulut, 1994, Phys. Rev. B **49**, 1470.
- Rainer, D., and M. Vuorio, 1977, J. Phys. C **10**, 3093.
- Read, N., 1985, J. Phys. C **18**, 2651.
- Read, N., and D. M. Newns, 1983a, J. Phys. C **16**, 3273.
- Read, N., and D. M. Newns, 1983b, J. Phys. C **16**, L1055.
- Renner, C., B. Revaz, J.-Y. Genoud, K. Kadowaki, and Ø. Fischer, 1998, Phys. Rev. Lett. **80**, 149.
- Rusinov, A. I., 1968, Pis'ma ZhETF **9**, 146, [JETP Lett. **9**, 85 (1969)].
- Rusinov, A. I., 1969, Zh. Eksp. i Teor. Fiz. **56**, 2047, [Sov. Phys. JETP **29**, 1101 (1969)].
- Sakai, O., Y. Shimizu, H. Shiba, and K. Satori, 1993, J. Phys. Soc. Jpn. **62**, 3181.
- Sakurai, A., 1970, Progr. Theor. Phys. **44**, 1472.
- Salkola, M. I., A. V. Balatsky, and D. J. Scalapino, 1996, Phys. Rev. Lett. **77**, 1841.
- Salkola, M. I., A. V. Balatsky, and J. R. Schrieffer, 1997, Phys. Rev. B **55**, 12648.
- Samokhin, K., and M. Walker, 2001, Phys. Rev. B **64**, 024507.
- Satori, K., H. Shiba, O. Sakai, and Y. Shimizu, 1992, J. Phys. Soc. Jpn. **61**, 3239.
- Saxena, S. S., P. Agarwal, K. Ahilan, F. M. Grosche, R. K. W. Haselwimmer, M. J. Steiner, E. Pugh, I. R. Walker, S. R. Julian, P. Monthoux, G. G. Lonzarich, A. Huxley, *et al.*, 2000, Nature. **406**, 587.
- Scalapino, D. J., P. J. Hirschfeld, and T. Nunner, 2004, proceedings of SNS-2004 (Sitges), eprint unpublished.
- Schachinger, E., 1982, Z. Phys B **47**, 217.
- Schachinger, E., and J. P. Carbotte, 1984, Phys. Rev. B **29**, 165.
- Schachinger, E., J. M. Daams, and J. P. Carbotte, 1980, Phys. Rev. B **22**, 3194.
- Schlottmann, P., 1976, Phys. Rev. B **13**, 1.
- Schmitt-Rink, S., K. Miyake, and C. M. Varma, 1986, Phys. Rev. Lett. **57**, 2575.
- Schrieffer, J. R., 1964, *The Theory of Superconductivity* (Benjamin, New York).
- Schuh, B., and E. Müller-Hartmann, 1978, Z. Phys. B **29**, 39.

- Segre, G. P., N. Gedik, J. Orenstein, D. A. Bonn, R. Liang, and W. N. Hardy, 2002, Phys. Rev. Lett. **88**, 137001.
- Senthil, T., and M. P. A. Fisher, 1999, Phys. Rev. B **60**, 6893.
- Senthil, T., and M. P. A. Fisher, 2000, Phys. Rev. B **61**, 9690.
- Senthil, T., M. P. A. Fisher, L. Balents, and C. Nayak, 1998, Phys. Rev. Lett. **81**, 4704.
- Sheehy, D. E., I. Adagideli, P. M. Goldbart, and A. Yazdani, 2001, Phys. Rev. B **64**, 224518.
- Shen, Z. X., and J. R. Schrieffer, 1997, Phys. Rev. Lett. **78**, 1991.
- Shiba, H., 1968, Prog. Theor. Phys. **40**, 435.
- Shiba, H., 1973, Prog. Theor. Phys. **50**, 50.
- Shnirman, A., I. Adagideli, P. M. Goldbart, and A. Yazdani, 1999, Phys. Rev. B **63**, 7517.
- Shytov, A. V., I. Vekhter, I. A. Gruzberg, and A. V. Balatsky, 2003, Phys. Rev. Lett. **90**, 147002.
- Shytov, A. V., I. Vekhter, I. A. Gruzberg, and A. V. Balatsky, 2004, eprint unpublished.
- Sidorov, V. A., M. Nicklas, P. G. Pagliuso, J. L. Sarrao, Y. Bang, A. V. Balatsky, and J. D. Thompson, 2002, Phys. Rev. Lett. **89**, 157004.
- Sigrist, M., and K. Ueda, 1991, Rev. Mod. Phys. **63**, 239.
- Simon, M. E., and C. M. Varma, 1999, Phys. Rev. B **60**, 9744.
- Skalski, S., O. Betbeder-Matibet, and P. R. Weiss, 1964, Phys. Rev. **136**, A1500.
- Soda, T., T. Matsuura, and Y. Nagaoka, 1967, Progr. Theor. Phys. **38**, 551.
- Spivak, B., and S. Kivelson, 1991, Phys. Rev. B **43**, 3740.
- Sprunger, P. T., L. Petersen, E. W. Plummer, E. Lægsgaard, and F. Besenbacher, 1997, Science **275**, 1764.
- Stamp, P. C. E., 1987, Journ. Magn. Magn. Materials. **63-64**, 429.
- Stipe, B., M. Rezaei, and W. Ho, 1998, Science **280**, 1732.
- Suderow, H., P. Martinez-Samper, N. Luchier, J. P. Brison, S. Vieira, and P. C. Canfield, 2001, Phys. Rev. B **64**, 020503.
- Takegahara, K., Y. Shimizu, and O. Sakai, 1992, J. Phys. Soc. Jpn. **61**, 3443.
- Takigawa, M., M. Ichioka, and K. Machida, 2003, Phys. Rev. Lett. **90**, 047001.
- Tanaka, K., and F. Marsiglio, 2000, Phys. Rev. B **62**, 5345.
- Tanuma, Y., Y. Tanaka, M. Ogata, and S. Kashiwaya, 1998, J. Phys. Soc. Jpn. **67**, 1118.
- Timusk, T., 2003, eprint cond-mat/0303383.
- Timusk, T., and B. Statt, 1999, Rep. Prog. Phys. **62**, 61.
- Tinkham, M., 1996, *Introduction to Superconductivity* (McGraw-Hill, Inc., New York), 2nd edition.
- Tsai, S.-W., and P. J. Hirschfeld, 2002, Phys. Rev. Lett. **89**, 147004.
- Tsuchiura, H., Y. Tanaka, M. Ogata, and S. Kashiwaya, 2000, Phys. Rev. Lett. **84**, 3165.
- Tsuei, C. C., and J. R. Kirtley, 2000, Rev. Mod. Phys. **72**, 969.
- Tsuneto, T., 1962, Prog. Theor. Phys. **28**, 857.
- Tu, J. J., C. C. Homes, G. D. Gu, D. N. Basov, and M. Strongin, 2002, Phys. Rev. B **66**, 144514.
- Turner, P. J., R. Harris, S. Kamal, M. E. Hayden, D. M. Broun, D. C. Morgan, A. Hosseini, P. Dosanjh, G. K. Mullins, J. S. Preston, R. Liang, D. A. Bonn, *et al.*, 2003, Phys. Rev. Lett. **90**, 237005.
- Ueda, K., and M. Rice, 1985, in *Theory of Heavy Fermions and Valence Fluctuations*, edited by T. Kasuya and T. Saso (Springer-Verlag, Berlin).
- Van Mieghem, P., 1992, Rev. Mod. Phys. **64**, 755.
- Varma, C. M., 1999, Phys. Rev. Lett. **83**, 3538.
- Vavilov, M. G., P. W. Brouwer, V. Ambegaokar, and C. W. J. Beenakker, 2001, Phys. Rev. Lett. **86**, 874.
- Vekhter, I., A. V. Shytov, I. A. Gruzberg, and A. V. Balatsky, 2003, Physica B **329-333**, 1446.
- Vekhter, I., and C. M. Varma, 2003, Phys. Rev. Lett. **90**, 237003.
- Vershinin, M., S. Misra, S. Ono, Y. Abe, Y. Ando, and A. Yazdani, 2004, Science **303**, 1995.
- Vishveshwara, S., T. Senthil, and M. P. A. Fisher, 2000, Phys. Rev. B **61**, 6966.
- Vojta, M., 2001, Phys. Rev. Lett. **85**, 097202.
- Vojta, M., and R. Bulla, 2001, **65**, 014511.
- Volovik, G. E., and L. P. Gor'kov, 1984, JETP Lett. **39**, 550.
- Walter, H., W. Prusseit, R. Semerad, H. Kinder, W. Assmann, H. Huber, H. Burkhardt, D. Rainer, and J. A. Sauls, 1998, Phys. Rev. Lett. **80**, 3598.
- Wang, Q., and C.-R. Hu, 2004, Phys. Rev. B **70**, 092505.
- Wang, Q.-H., 2002, Phys. Rev. Lett. **88**, 057002.
- Wang, Q.-H., and D.-H. Lee, 2003, Phys. Rev. B **67**, 020511.
- Wang, Q.-H., and Z. D. Wang, 2004, Phys. Rev. B **69**, 092502.
- Wiegmann, P. B., 1980, JETP Lett. **31**, 367.
- Wilson, K. G., 1975, Rev. Mod. Phys. **47**, 773.
- Withoff, D., and E. Fradkin, 1990, Phys. Rev. Lett. **64**, 1835.
- Woolf, M. A., and F. Reif, 1965, Phys. Rev. **137**, A557.
- Wu, C., T. Xiang, and Z.-B. Su, 2000, Phys. Rev. B **62**, 14427.
- Xiang, T., Y. H. Su, C. Panagopoulos, Z. B. Su, and L. Yu, 2002, Phys. Rev. B **66**, 175404.
- Xiang, T., and J. M. Wheatley, 1995, Phys. Rev. B **51**, 11721.
- Yashenkin, A. G., W. A. Atkinson, I. V. Gornyi, P. J. Hirschfeld, and D. V. Khveshchenko, 2001, Phys. Rev. Lett. **86**, 5982.
- Yazdani, A., C. M. Howald, C. P. Lutz, A. Kapitulnik, and D. M. Eigler, 1999, Phys. Rev. Lett. **83**, 176.
- Yazdani, A., B. A. Jones, C. P. Lutz, M. F. Crommie, and D. M. Eigler, 1997, Science **275**, 1767.
- Yoshioka, T., and Y. Ohashi, 1998, J. Phys. Soc. Jpn. **67**, 1332.
- Yoshioka, T., and Y. Ohashi, 2000, J. Phys. Soc. Jpn. **69**, 1812.
- Yu, L., 1965, Acta Phys. Sin. **21**, 75.
- Zhang, D., and C. S. Ting, 2003, Phys. Rev. B **67**, 100506.
- Zhang, D., and C. S. Ting, 2004, Phys. Rev. B **69**, 012501.
- Zhang, G.-M., H. Hu, and L. Yu, 2001, Phys. Rev. Lett. **86**, 704.
- Zhang, G.-M., H. Hu, and L. Yu, 2002, Phys. Rev. B **66**, 104511.
- Zhu, J.-X., and A. Balatsky, 2002, Phys. Rev. B **65**, 132502.
- Zhu, J.-X., A. V. Balatsky, T. P. Devereaux, Q. Si, J. Lee, K. McElroy, and J. C. Davis, 2005a, eprint cond-mat/0507610.
- Zhu, J.-X., W. Kim, C. S. Ting, and J. P. Carbotte, 2001, Phys. Rev. Lett. **87**, 197001.
- Zhu, J.-X., T. K. Lee, C. R. Hu, and C. S. Ting, 2000a, Phys. Rev. B **61**, 8667.
- Zhu, J.-X., I. Martin, and A. R. Bishop, 2002, Phys. Rev. Lett. **89**, 067003.
- Zhu, J.-X., K. McElroy, J. Lee, T. P. Devereaux, Q. Si, J. C. Davis, and A. V. Balatsky, 2005b, eprint cond-mat/0507621.
- Zhu, J.-X., D. N. Sheng, and C. S. Ting, 2000b, Phys. Rev. Lett. **85**, 4944.
- Zhu, J.-X., J. Sun, Q. Si, and A. V. Balatsky, 2004a, Phys. Rev. Lett. **92**, 5017002.

- Zhu, J.-X., and C. S. Ting, 2001a, Phys. Rev. B **63**, 020506.
Zhu, J.-X., and C. S. Ting, 2001b, Phys. Rev. B **64**, 060501.
Zhu, J.-X., and C. S. Ting, 2001c, Phys. Rev. Lett. **87**, 147002.
Zhu, J.-X., C. S. Ting, and C. R. Hu, 2000c, Phys. Rev. B **62**, 6027.
Zhu, L., W. A. Atkinson, and P. J. Hirschfeld, 2003, Phys. Rev. B **67**, 094508.
Zhu, L., W. A. Atkinson, and P. J. Hirschfeld, 2004b, Phys. Rev. B **69**, 060503.
Zhu, L., P. J. Hirschfeld, and D. J. Scalapino, 2004c, Phys. Rev. B **70**, 214503.
Ziegler, K., 1996, Phys. Rev. B **53**, 9653.
Ziegler, K., M. H. Hettler, and P. J. Hirschfeld, 1996, Phys. Rev. Lett. **77**, 3013.
Zittartz, J., A. Bringer, and E. Müller-Hartmann, 1972, Sol. St. Commun. **10**, 513.
Zittartz, J., and J. S. Langer, 1966, Phys. Rev. **148**, 741.
Zittartz, J., and E. Müller-Hartmann, 1970, Z. Phys. **232**, 11.